SCOUR AND SCOUR CONTROL BELOW CANTILEVERED CULVERT OUTLETS

By

George L. Smith

Prepared for
U.S. Department of Commerce
Bureau of Public Roads
under
Contract No. CPR 11-7746

Colorado State University Research Foundation
Fort Collins, Colorado

CER61GLS14

SCOUR AND SCOUR CONTROL BELOW CANTILEVERED CULVERT OUTLETS

by

George L. Smith

Prepared for
U.S. Department of Commerce
Bureau of Public Roads
under
Contract No. CPR 11-7746

Colorado State University Research Foundation
Fort Collins, Colorado

CER61GLS14

TABLE OF CONTENTS

Table of Contents - Continued

ERRATA SHEET - "Scour and Scour Control Below Cantilevered Culvert Outlets"

1. Publication Date ----- 1 May 1961

2. On page 7 ----- the beginning of the eighth line from the top of the page should read horizontal shear distribution .....

3. On page 9 ----- In the title of Fig. 2 and Fig. 3 Effects should be Effect.

4. On page 18 ----- On the graph and in the title - w_m should be W_m .

5. On page 21 ----- In the title of Fig. 6 - phase should be Phase.

6. On page 25 ----- In Fig. 8c the identification of the run should be

A 1
Run No.
1 - 1 - 50 - 2

7. On page 35 Fig. 14 ----- The dimension on the plan view for L should be L_b .

8. On page 36 ----- The second 1/8 $V_{s_{100}}$ should be 1/2 $V_{s_{100}}$ on line 17.

9. On page 40 ----- Eqs. 8, 9, and 10 as written are not right should be For

1/8 $V_{s_{100}}$ ---------- $V_{ar} = 0.106\, h^{*2}\, \epsilon$

1/4 $V_{s_{100}}$ ---------- $V_{ar} = 0.168\, h^{*2}\, \epsilon$

1/2 $V_{s_{100}}$ ---------- $V_{ar} = 0.264\, h^{*2}\, \epsilon$

10. On page 44 line 6 ----- Instead of (B = 1.0 ft) it should be (B = 10.0 ft).

11. On page 75 ----- at the end of line 7 from the top of the page delete the word size and insert nominal diameter. Also, on line 9 insert mean diameter before the symbol d_m .

12. On page 76 ----- Eq. 18 should be $W_m = 12.8\, d_n^{\,0.500}$ and Eq. 19 should be $V_b = 12.95\, d_n^{\,0.500}$

13. On page 78 ----- On the abscissa the last 10 should be 10^2 .

14. On page 95 Table 4 ----- the shape factor $\frac{c}{\sqrt{ab_s}}$ should be $\frac{c}{\sqrt{ab}}$

15. On page 96 Table 5 Column heading $\psi = \frac{h_{max}}{d_t}$ should be $\psi = \frac{h_{max}}{d_T}$

ACKNOWLEDGEMENTS

This research project was performed in the Hydraulic Laboratory of Colorado State University under the sponsorship of the Bureau of Public Roads.

The author wishes to thank Mr. Carl F. Izzard and Mr. Dasel E. Hallmark for their helpful suggestions made during the study, and to thank the Bureau of Public Roads for sponsoring the study.

Particular thanks are due Dr. Daryl B. Simons of the U.S. Geological Survey in Fort Collins for his review and criticisms of this report.

SYMBOLS

Symbol	Definition
a	Major axis of a sediment particle-mm
A	Area of freely falling jet of water at point of impingement of water surface - ft^2
A_b	Area of the bottom of the pre-shaped stilling basin - ft^2
A_r	Amount of armorplate expressed as per cent, $\% A_r = V_{ar}/V_s \times 100$
A_s	Area of the surface of a frustum of a cone - ft^2
A_t	Total surface area of the pre-shaped stilling basin - ft^2
b	Depth of tailwater - ft or intermediate axis of a sediment particle - mm
B	Width of a rectangular channel at the cantilevered culvert outlet - ft
c	Minor axis of a sediment particle - mm
C	Dimensionless parameter given by $$\frac{X - X_B}{h_t^*}$$
C_{M_F}	Momentum parameter
d	Diameter of sediment particle, and maximum diameter of sediment particle that will resist erosion - cm., in. or ft
d_B	Diameter of pre-shaped basin at depth h - ft
d_m	Geometric mean diameter of the sediment - cm or ft
d_n	Nominal diameter (diameter of a sphere having the same volume as the sediment particle)

Symbols - continued

Symbol	Definition
d_T	Diameter of pre-shaped basin at original bed level - ft
D	Maximum diameter of armorplate - in.
F	Net gravitational force on the sediment particle falling in a fluid given by $$F = \frac{\pi d_n^3}{6} g \ (\rho_s - \rho) \ -mg.$$
g	Acceleration of gravity - 980.7 cm/sec^2 or 32.2 ft/sec^2
h_{max}	Depth of pre-shaped basin or maximum depth of scour hole measured from original bed level - ft
h^*_t	Cube root of volume of the scour hole at time t, $(V_{s_t})^{1/3}$ - ft
h^*	Cube root of volume of the scour hole at time t = 100 hrs, $(V_{s_{100}})^{1/3}$ - ft
H	Height from the original bed level to the center of flow at the point of discharge - ft
L_b	Diameter of scour hole in the direction of flow at the original bed surface - ft
M_F	Momentum flux of impinging jet given by $\rho Q V$ - lb
M_P	Momemtum flux of the sediment particle mass given by $\rho_s W_m^2 d_m^2$ and $\rho_s W_m^2 \sigma_d^2$ - lb
P_n	Pipe designation as P_1, P_2 ... of experimental equipment assembly.
Q	Discharge or rate of flow - ft^3/sec
r_1	Maximum radius of a right truncated cone - ft

Symbols - continued

Symbols	Definition
r_2	Minimum radius of a right truncated cone - ft
s.f.	Corey shape factor or $c/\sqrt{ab}$
s.g.	Specific gravity of sediment particles
t	Time - sec., min., or hrs.
v	Volume of a right truncated cone given by $\frac{\pi h}{3}(r_1^2 + r_1 r_2 + r_2^2)$.
V	Velocity of freely falling jet of water at point of impingement - fps
V_{ar}	Volume of armorplate - ft^3
V_b	Is the bottom velocity in the channel - ft/sec
V_n	Valve designation as V_1, V_2 ... of experimental equipment assembly
V_{s_t}	Volume of scour hole at time t - ft^3
$V_{s_{100}}$	Volume of scour hole at time t = 100 hrs - ft^3
W	Weight of the sediment particle - mg
W_{ave}	Average fall velocity of the sediment particles, $\Sigma W_s/n$ - cm/sec or ft/sec
W_b	Diameter of the scour hole transverse to the direction of flow at the original bed surface - ft
W_m	Geometric mean fall velocity of the sediment - cm/sec or ft/sec
W_s	Fall velocity of the sediment particles - cm/sec or ft/sec
X	Distance from end of culvert outlet to maximum depth h_{max} of scour hole - ft

Symbols - continued

Symbols	Definition
X_B	Horizontal distance the freely falling jet of water travels from end of culvert outlet to point of impingement - ft
y'	The y intercept on a semi-logarithmic plot at $t = 1$
Y	Function defined by Eq. 113 of reference 7
Z	Function defined by Eq. 114 of reference 7
Z_s	The apparent true depth of scour - ft
α	Natural angle of repose of sediment - degrees
$\Delta\gamma$	Effective specific weight of the sediment - lb/ft^3
γ_s	Specific weight of sediment - lb/ft^3
γ_w	Specific weight of fluid - lb/ft^3
Δ	Symbol denoting difference between two quantities or numbers
ϵ	Hypothetical uniform thickness a given quantity of armorplate will cover the surface of a pre-shaped stilling basin - inches
θ	Angle of inclination of the freely falling jet of water at the point of impingement - degrees
μ	Dynamic viscosity of the fluid - lb sec/ft^2
π	Greek letter pi used to denote the pi-theorem and also the numerical value 3.1416
ρ	Mass density of the fluid - lb sec^2/ft^4
ρ_s	Mass density of sediment - lb sec^2/ft^4
σ_d	Standard deviation of particle size about d_m - cm or ft

Symbols - continued

Symbols	Definition
σ_w	Standard deviation of the fall velocity of the sediment particles about the mean - fall velocity - cm/sec or ft/sec
ψ	Dimensionless parameter given by h_{max}/d_T

LIST OF FIGURES

List of Figures - continued

List of Figures - continued

SCOUR AND SCOUR CONTROL AT CANTILEVERED CULVERT OUTLETS

ABSTRACT

Scour or scour control are the most difficult problems to analyze of all flow phenomena, since either is a phenomenon involving the motion of discrete particles within a fluid which is in turn moving with respect to fixed boundaries. Furthermore, with the present state of knowledge of either of the phenomenon, an approximate understanding of both phenomenon can be obtained only by isolating particular details or by so simplifying the boundary conditions that only the most significant variables be considered. Therefore, a fundamental investigation of scour and scour control must be restricted to conditions of steady, uniform flow, which in a laboratory flume can be regarded as steady only in the statistical sense.

This report is an investigation of the phenomenon of scour and scour control below a cantilevered culvert outlet under steady, uniform flow conditions. In each phase of the study primary consideration is given to the kinematics of the jet causing the scour, the boundary geometry at the outlet and the characteristics of both the bed material of the alluvial channel and the graded gravel -- armorplate -- used in scour control.

The first phase considers scour in an alluvial bed. From this basic study the geometry of a pre-shaped stilling basin is determined. The pre-shaped basin combined with graded gravel -- armorplate -- constitutes the second phase or the scour control study. Scour and scour control studies were then conducted in channels with alluvial beds but with rigid sides of varying width as well as in an alluvial channel with initial bottom width of 5 ft under various flow conditions.

In conjunction and simultaneous with the experimental investigations presented in this report, analytical studies, also under Bureau of Public Roads sponsorship, were made on the mechanics of localized sccur. These studies are reported separately in references 6 and 7 of the Bibliography.

PART I.

THE PROBLEM AND PROBLEM ANALYSIS

A. GENERAL STATEMENT

An ever present problem, which confronts the highway engineer, is erosion or gullying at the outlet end of culverts. Nature's method of keeping erosion under control on mild slopes is to spread the runoff over a wide area of the watershed so that flow depths are small and resistance to flow rather large. A highway crossing a watershed disrupts this plan of nature in that the runoff is funneled to a culvert where the flow is concentrated. This results in some erosion at the culvert entrance but the principal difficulty lies downstream since the flow cannot fan out again over a wide area after it has passed through the culvert. This concentration of flow is conducive in many instances to erosion and gullying downstream of the culvert outlet. As time goes on, erosion increases and control methods become more difficult and expensive to construct. Man is responsible for many scars on the face of the landscape and for the loss of considerable topsoil because of a heretofore generally accepted short-range viewpoint. It is no longer realistic to consider only the initial cost of a culvert and ignore the cost of future maintenance.

It is possible to alleviate gullying and degradation to some extent by constructing energy dissipators at the downstream end of culverts. Where this has been done in the past, concrete or stone structures have been employed. This type of construction can become quite an item of expense considering the number of culverts involved.

The division of Hydraulic Research of the Bureau of Public Roads and others have long recognized the need of effective measures for controlling erosion downstream from culverts. To date it has been difficult to justify the cost of such structures in light of the performance and results attained since, generally speaking, conventional types of stilling basins are expensive and seldom wholly effective at culvert outlets. Although not now available there is a very promising and inexpensive method of controlling erosion at culvert outlets.

Sufficient testing has been performed both at Colorado State University and in the field to demonstrate and verify the effectiveness of the method. In general, the method consists of simply excavating a hole downstream from the end of the culvert and lining it with a graded layer of protective material consisting of coarse sand, gravel and boulders up to a size that will resist excessive erosion at the peak flow. The utilization of a graded material as a protective blanket is of prime importance and one that has been overlooked in the past. Design of this type of energy dissipator can be determined by trial and error, but a more scientific approach can insure effective operation and minimize costs.

Information required by the designer can be stated quite simply. He needs the size, shape and position of the excavated hole, the maximum size and over-all amount of graded material required for the protective blanket, and the position in which this material should be placed in the hole for best distribution by the flow. The variables involved in determining the above dimensions and quantities, however, are numerous and for this reason cut-and-try methods of construction can be disappointing and costly.

Realizing the need for a more scientific and economical design the Bureau of Public Roads has sponsored some of the studies to develop a stilling basin for cantilevered culvert outlets. This report presents the findings of these studies. Much of the information presented can be adapted to field use in maintenance operations; however, additional studies are needed before an over-all and efficient method of design can be evolved.

B. INVESTIGATIONAL PROCEDURE

1. Review of Literature; Previous Experimental Studies

Scour in an alluvial bed caused by a jet of water flowing from a cantilevered culvert outlet is only one of the many facets of the complex phenomena of sediment transport. Therefore, as a guide in the analysis of this phenomenon the results of other investigators were used to form the framework of this experimental study. A summary of the more important studies is given in this section.

The analysis of any phenomenon of fluid motion can be achieved only by properly identifying the various factors which govern the variation of its performance. Thus, in its broader aspects, scour of an alluvial stream bed by a three-dimensional jet is primarily a function of

a. The kinetic energy of the jet at the point of impingement on the alluvial bed, and
b. The characteristics of the bed material identified as the mean fall velocity W_m and the deviation σ_w of the fall velocity W_s of the particles about this mean.

It is at once evident that for scour control it is necessary that

a. The kinetic energy of the impinging jet be effectively dissipated, or,
b. The sediment characteristics be so modified by increasing either W_m or σ_w or both (adding a gravel mixture to sand) that the bed material becomes armorplated.

All fundamental scour and scour control studies basic to this report placed greater emphasis on sediment characteristics than on kinetic energy dissipation in evaluating either phenomenon. The most important studies of scour phenomenon were made by Rouse (1), Doddiah (2) and Thomas (3). Hallmark (4) studied scour control by use of graded aggregate -- armorplate. Albertson and Smith (5) considered the various methods of energy dissipation in erosion control structures.

Rouse made systematic experiments to determine the rate of scour of a sediment bed by a vertical, deeply submerged two-dimensional jet of clear water. The following conclusions were reached:

1. The scour depth continues as an exponential function of time.
2. Two distinct regimes of flow occur: (a) the jet being deflected through nearly 180 degrees (maximum jet deflection); and (b) the jet following the scour profile to the dune crest (minimum jet deflection).

3. Greater scour may be expected with the minimum jet deflection.
4. The depth of scour in uniform bed material is dependent solely upon the size and the velocity V of the jet, the fall velocity of the sediment W_m, and the duration of the scouring action.
5. The rate of scour approaches zero as $(V/W_m - 1)$ approaches zero.
6. Due to sorting action, an increase in the effective W_m may form a relatively stable bed.

Doddiah compared the scour depth in relatively uniform gravel beds caused by vertical, three-dimensional, hollow and solid jets of water. Doddiah demonstrated that:

1. There is a critical depth of tailwater at which either an increase or decrease in tailwater causes a decrease in scour depth.
2. For a given area and velocity of jet, the scour resulting from a hollow jet as compared with a solid jet appears to indicate a single trend.

Thomas considered the case of scour resulting from a non-submerged, two-dimensional jet issuing from a free overfall and impinging on an alluvial bed covered by a pool of water having various depths. The geometric mean size of the bed material was held constant but the deviation about the mean size was varied. Significant conclusions of this experiment were:

1. An increase in the discharge causes a greater increase in depth of scour than does the same percentage increase in drop height, or change in depth of tailwater.
2. A critical depth of tailwater is reached as for three-dimensional flow, at which either an increase or decrease in tailwater causes a decrease in scour depth.

Thomas was among the first to obtain information on the use of graded gravel as armorplate in the control of scour. Specifically, his experiments provided information for choosing the proper material to prevent excessive scour at the base of a free overfall with a two-dimensional jet. This research laid the groundwork for the development of a stilling basin armor-plated with gravel for limited conditions of flow, boundary geometry and sediment characteristics.

Hallmark (3) extended the work of Thomas in the use of graded gravel as armorplating in stilling basins. Two gravels were tested. The first gravel had the same fall velocity W_m, but a different standard deviation σ_W, than the gravels tested by Thomas. The gravel was so selected as to increase σ_W by 50 per cent over the wider-size-range gravel Thomas had previously used. The second gravel tested was a natural stream sand, having nearly the same σ_W as the first gravel tested, but a different W_m. The experimental results indicated the following essential facts:

1. A relatively small amount of armorplating material will cause a relatively large decrease in the rate of scour.
2. A uniform size of aggregate slightly larger than the largest particle size of the bed material reduces the rate of scour more effectively than a larger uniform-size aggregate.
3. The rate of scour decreases with an increase in the amount of armorplate placed in the scour hole.
4. Graded armorplate material decreases the rate of scour more effectively than uniform material.
5. The effectiveness of armorplate depends not only upon its gradation but also upon its relation to the maximum size of aggregate of bed material, that is, the minimum size of the armorplate should be about the same as the maximum size of the bed material.

As previously stated effective scour control is a function of the changing of sediment characteristics and the dissipation of the kinetic energy of the jet. Albertson and Smith (5) in their analysis of energy dissipation in erosion control structures demonstrated that kinetic energy of a water jet can be most effectively dissipated by vertical diffusion in a stilling basin. The distinct advantage of vertical dissipation, according to Albertson and Smith, is that it confines the energy dissipation to a relatively small area, compared to horizontal energy dissipation as exemplified by the hydraulic jump. It is essential, however, that a minimum depth of tailwater be maintained in the stilling basin in order that the jet diffusion will be sufficient to prevent high energy waves from emanating from the stilling basin area.

The foregoing investigations, besides providing fundamental information on the phenomena of scour and scour control, were used as a basis for the study of scour and scour control in alluvial beds at cantilevered culvert outlets. Such a study represents not only a design problem to the highway engineer, but also a fluid flow problem in three-dimensions to the research engineer. Furthermore, such fluid motion, as previously stated, is not a simple phenomenon, and an understanding of its characteristics -- within limits -- can be acquired by theoretical analysis or by experimentation or by a combination of both.

This two-fold approach to the scour problem, under sponsorship of the Bureau of Public Roads and as part of the projects' over-all objective, was attempted simultaneously. The theoretical analysis was made under the direction of Dr. Yuichi Iwagaki. By use of certain basic principles and concepts mathematical expressions were obtained for scour in alluvial material by both the two-dimensional (6) and three-dimensional jet (7) acting under different boundary conditions -- submerged, non-submerged, as well as normal and inclined to the deflecting boundary. The experimental program followed the technique employed by previous investigators, that is, a dimensional analysis was first made of the problem prior to its investigation.

2. Theoretical Considerations

To evaluate the mechanics of scour by a three-dimensional jet, Iwagaki (7) first derived the equation of continuity of mass sediment transport using the polar coordinate system. The relationship between the shape of the scour hole and its variation with time was next investigated for different conditions of scour and deposition. Expressions for distribution of sediment transport along the bed were then obtained for each condition.

The impingement of a three-dimensional jet on a normal, rigid boundary was analyzed by making the assumption that the Bernoulli Equation is valid in the neighborhood of the stagnation point. Plane, potential flow was considered first, followed by flow of a fluid with viscosity. For flow with viscosity from submerged and non-submerged outlets, expressions for the horizontal and shear distribution along the boundary were obtained using Bernoulli's theorem and the boundary layer theory. In particular, results of experimental and theoretical studies by Schlichting and Truckenbrodt (8), and Truckenbrodt (9) of jet deflecting on a normal boundary; and, of experimental and theoretical studies by Albertson and others (10) on the diffusion of submerged jet were used.

The variation of the depth of scour - rate of scour - was evaluated by using the previously determined shear distributions and the continuity equation and assuming as applicable the sediment transport equation developed by Brown and Laursen (11). Also by assuming that the depth of scour is small compared with the tailwater depth in integrating the continuity equation of mass sediment transport, Iwagaki obtained for the depth of scour for the case of the inclined jet (see Fig. 1) the expression

$$\frac{Z_s}{\sqrt{A}\sin\theta} = Y\left\{\log\left(\frac{d_m}{\sqrt{A}\sin\theta}\;\frac{(V)(t)}{b}\right) + \log Z\right\} \qquad (1)$$

in which values for Y and $\log Z$ may be obtained from Figs. 2 and 3. Application of Eq. 1 to the experimental data is given in the section on analysis of experimental data.

In this theoretical treatment of the scour problem it was necessary that the problem be idealized to a certain extent; and, because of a lack of experimental evidence, it was necessary to limit the assumptions to these which were physically reasonable. Obviously, the inherent danger in making such unguided simplifications is that of obtaining physically impossible conclusions.

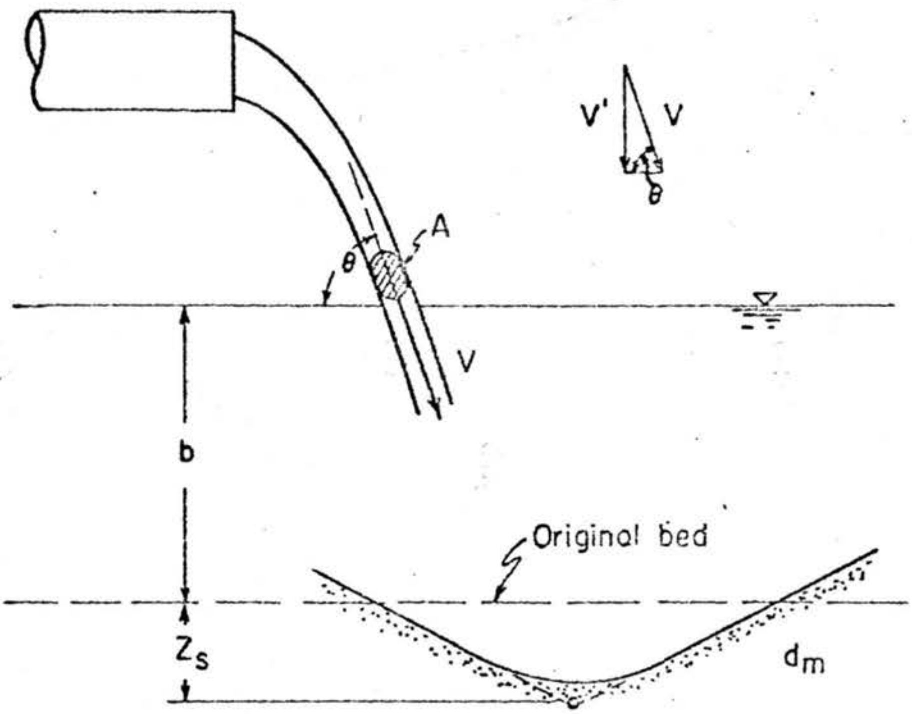

Fig. I Schematic drawing for a characteristic depth of scour in the case of the inclined jet issuing from a non-submerged outlet

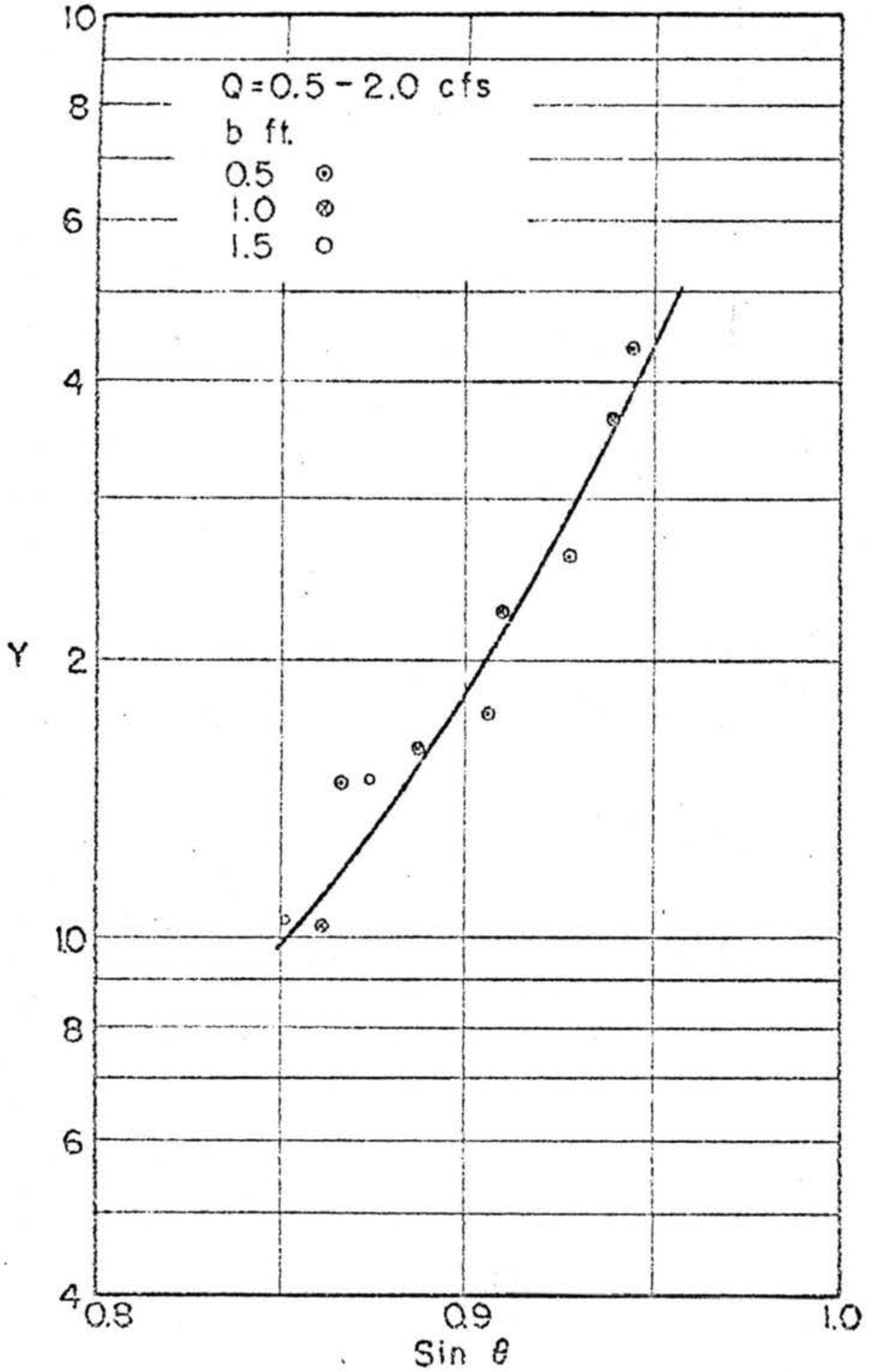

Fig. 2 Effects of the angle of jet θ on Y

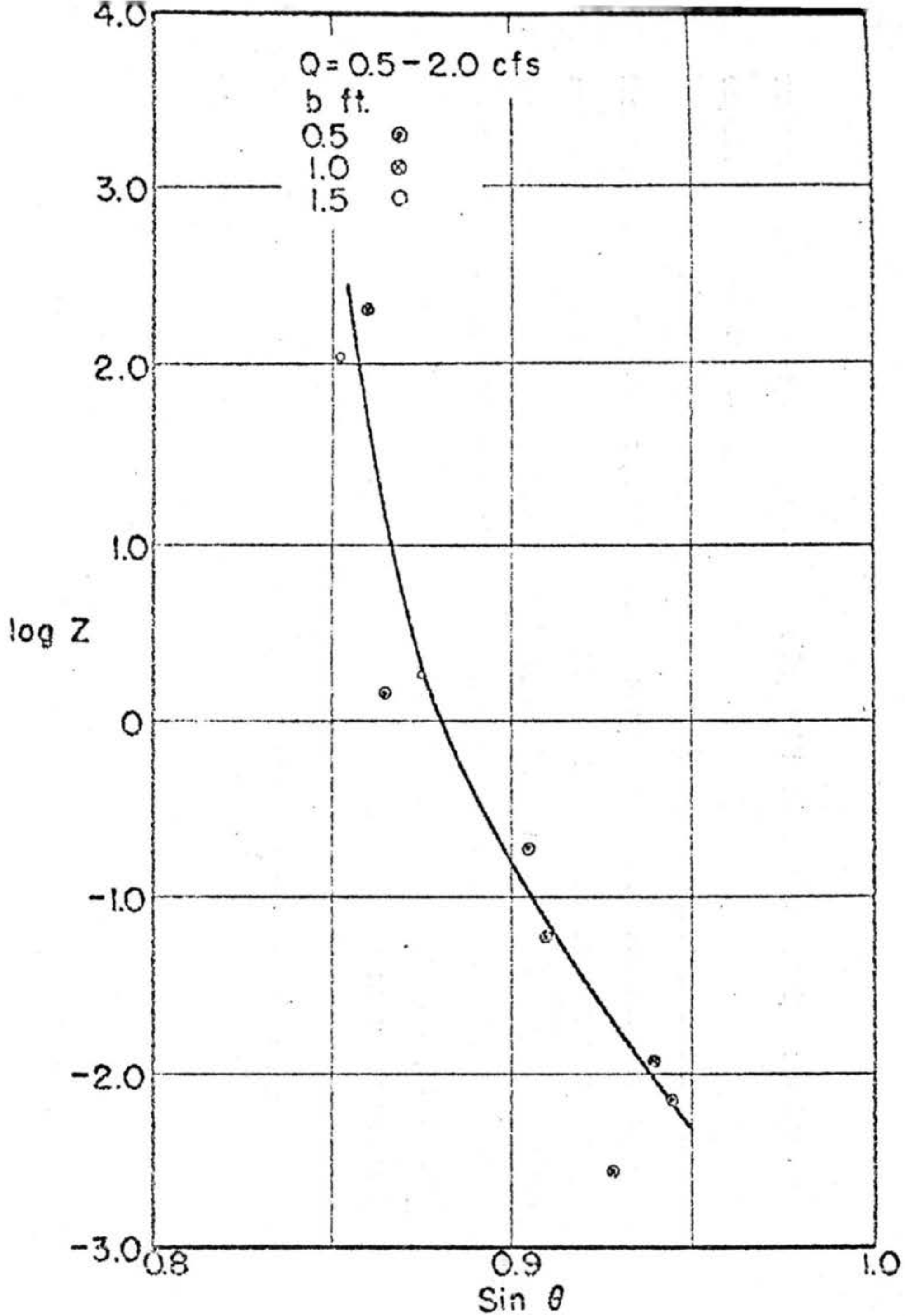

Fig. 3 Effects of the angle of jet θ on Z

Therefore, before any theory can be adopted it must ultimately be subjected to experimental verification.

In the experimental investigation of the mechanics of scour, consideration was given only to the phenomena of scour and scour control in alluvial beds resulting from cantilevered culvert outflow. Such an investigation not only would provide data for verification of the expression given by Eq. 1, but also would provide information usable to the highway design engineer.

Because of the number of variables involved in describing the actual field problem, it was necessary to simplify the problem as much as possible for the laboratory analysis. By such simplification it would be possible to increase the number of variables systematically, as well as determine the significance of each additional variable.

PART II.

EXPERIMENTAL INVESTIGATION OF THE PROBLEM

A. RESEARCH PROGRAM

In order for the initial laboratory study to begin with a minimum number of variables, it was essential that the experimental sequence begin with the simplest case possible and then progress in the direction indicated by the test results toward the more complex cases. With this criterion as a guide the general research program that evolved was as follows:

1. The investigation of scour in a rectangular channel of constant width with rigid sides and an alluvial bed.
2. The investigation of control of scour by armorplate for item 1.
3. The investigation of scour and scour control in a rectangular channel of variable width with rigid sides and alluvial bed.
4. The investigation of scour and scour control in a trapezoidal channel of alluvial sides and bed.[1]

B. PROBLEM ANALYSIS

As a thesis study Smith (12) investigated the phenomenon of scour in a channel with rigid sides and alluvial bed below a cantilevered culvert outlet. A summary of this study is presented in this section and in Phase One of the following section. Beginning with Phase Two the studies were under the Bureau of Public Roads sponsorship. The analytical approach used in the thesis study follows:

---

[1] This phase was conducted by the Engineering Research Section of Colorado State University. It is included in this report in summary form to demonstrate the use of an armorplated, pre-shaped basin in control of scour for a simulated field condition.

In investigating the phenomenon of scour, consideration was first given to those factors causing the scour. Initially, the factors considered most significant were the kinematics of the jet causing the scour, the boundary geometry at the outlet, and the sediment characteristics of the alluvial bed material. Fig. 4 shows a schematic diagram of those factors affecting scour.

In analyzing the jet consideration was given to its momentum M_F at the point of impingement upon the tailwater surface covering the bed. Other factors considered to be important were the angle of inclination θ of the jet at the point of impingement and the distance H the jet travels before it reaches the bed which is being scoured. Of the fluid properties of the jet the mass density ρ and the viscosity μ were considered.

In the initial study a rectangular channel with rigid sides and an alluvial bed was used. For this type channel only the width B of the channel and the depth b of the pool of water over the bed were considered as significant factors defining its geometry.

The characteristics of the bed sediment or discrete particles scoured by the flow first considered were a linear measure of size d_m, the standard deviation about this size σ_d, the mass density ρ_s, and the effective specific weight $\Delta\gamma$.

It was at once evident that even for the most simplified case, the number of variables to be studied would be large. Therefore, it was desirable to delimit the study still further in the following manner:

1. The jet issued from a cantilevered culvert outlet (simulated) at a height H > B and sufficiently close to the bed so that no appreciable disintegration occurred prior to striking the pool surface.
2. The depth of pool b above the original bed was varied in discrete increments.
3. The height of the cantilevered, culvert invert was approximately constant relative to the original bed level.
4. The angle of inclination θ of the jet was held constant for each test series.

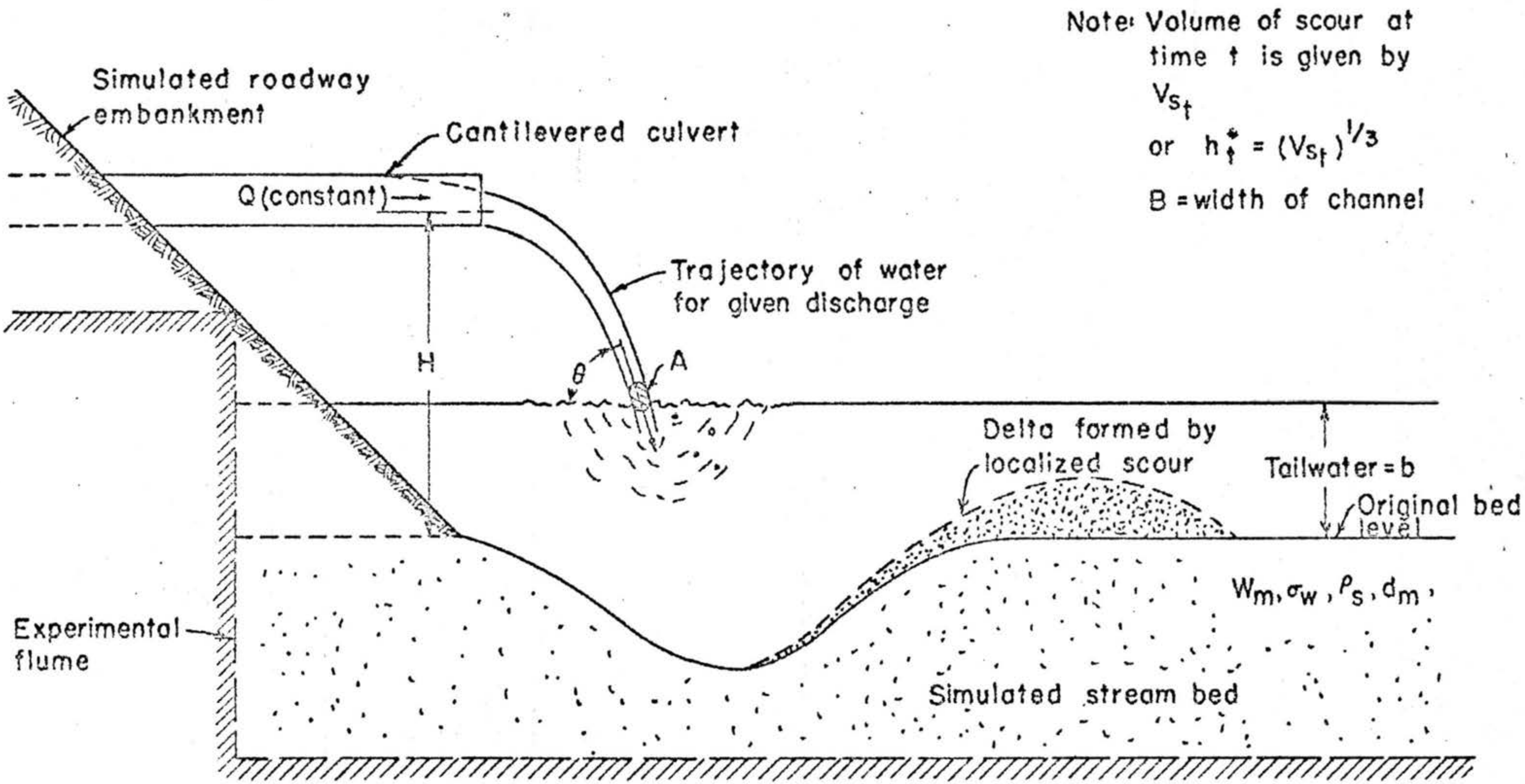

Fig. 4 Schematic diagram showing some of the variables that can affect the rate of scour caused by outflow from a cantilevered culvert into a rectangular channel with rigid sides and an alluvial bed.

5. One sand-gravel mixture was used in the simulated stream bed.
6. During any single run, the discharge was held constant and the elevation of the pool kept fixed.

With the foregoing limitations, the general relationship expressing scour phenomenon was assumed to be given by

$$\phi_1 \; (H, h_t^*, A, V, b, t, \rho, \rho_s, \mu, d_m, \sigma_d, \Delta\gamma, B, \theta) = 0 \qquad (2)$$

in which

- H is the height from the original bed level to the center of the flow at the point of discharge,
- h_t^* is the cube root of the volume of the scour hole $(V_{s_t})^{1/3}$, at time t,
- t is the time of scour, and
- A and V are the area and velocity of the jet at the point of impingement on the tailwater surface.

The remainder of the variables are as previously defined.

Although the function given by Eq. 2 with its fourteen variables was too complicated to study as a whole, it could now be simplified. As previously stated H, b, B and θ were constant for each test series. Furthermore, on the basis of scour studies by Rouse (1) it was assumed that effective scour occurs after the regime of flow has reached that of minimum jet deflection, at which time the concentration of discrete particles is relatively so low that contact among the particles can be considered as occurring very infrequently. For this flow condition, the variables d_m, ρ, μ, and $\Delta\gamma$, which together determine the fall velocity W_m of the material through the fluid, can as a first approximation be replaced by W_m. The momentum of the jet M_F can be expressed by its mass density, discharge and velocity. Thus by simplification of the variables of Eq. 2 and by means of the π-theorem, Eq. 2 may be rewritten non-dimensionally in the following manner:

$$\phi_2 \left(\frac{h_t^*}{H} ;\ C_{M_F} ;\ \frac{W_m t}{H} ;\ \frac{b}{H} ;\ \frac{d_m \ V t}{\sqrt{A}\ \sin\theta\ b} ;\ \frac{\rho}{\rho_s} \right) = 0 \qquad (3)$$

Since the last term - the ratio of the two densities - was considered as constant for the investigation, Eq. 3 becomes

$$\phi_3 \left(\frac{h_t^*}{H} ;\ C_{M_F} ;\ \frac{W_m t}{H} ;\ \frac{b}{H} ;\ \frac{d_m \ V t}{\sqrt{A}\ \sin\theta\ b} \right) = 0 \qquad (4)$$

of the various terms of Eq. 4, the second term C_{M_F} - a momentum parameter - could best be described as an example of Newton's second and third laws of motion, that is, the accelerative action of an impinging jet is countered by an inertial reaction of the alluvial bed material acted upon. Paradoxically, the parameter was recognized as one having significant importance to the testing program, and yet as one whose variables had not been established. To achieve an understanding of the variables envolved it was necessary to make an analysis of the resistance of the alluvial material to scour.

For a given bed material and tailwater depth, the accelerative force is the jet of water impinging upon the water surface, say

$$M_F = \rho\, Q\, V \text{ (momentum flux).}$$

in which

ρ is a fluid characteristic, and

Q and V are flow characteristics.

In a like manner the momentum flux M_p of the particle mass is given by

$$M_p = \rho_s\ W_m^2\ d_m^2$$

in which

ρ_s, W_m and d_m are characteristics of the bed material.

Also d_m is considered as the geometric mean diameter of the particle mass being scoured at any time t.

If, as it is generally so, the viscosity is constant, then there is a relation between W_m and d_m, at a constant shape factor

$$W_m = f_1 (d_m)$$

Thus M_p is then dependent solely upon d_m, and we have

$$M_p = \rho_s d_m^2 \left[f_1 (d_m)\right]^2$$

$$= f_2 (d_m) . \qquad (5)$$

It is obvious that the previously selected variables do not present a realistic view of the inertial ability of the alluvial material; therefore, the gradation of the alluvial material in the upper size range is the factor that determines the resistance of bed material and/or armorplate to scour. Furthermore, M_p should be a function of independent variables. Using the effect of gradation as a basis M_p can now be expressed by

$$M_p = \rho_s W_m^2 \sigma_d^2 \qquad (6)$$

in which

σ_d is a characteristic length which is both a function of gradation and the mean diameter of the sediment mass.

The momentum coefficient C_{M_F} is now given by

$$C_{M_{F_1}} = \frac{\rho Q V}{\rho_s W_m^2 \sigma_d^2}$$

Because other researchers (2), (3), (4), demonstrated that a critical depth of tailwater is reached at which either an increase or decrease in tailwater causes a decrease in scour depth, the momentum coefficient can also be be given by

$$C_{M_{F_2}} = \frac{\rho Q V}{\rho_s W_m^{2} \sigma_d b}$$

When the bed material is uniform, σ_d approaches zero, and C_{M_F} becomes very large, or the rate of scour is very high. Conversely as the mean fall velocity W_m increases, both C_{M_F} and the rate of scour decreases, that is, with ρ/ρ_s constant and b less than critical, as QV increases W_m must be increased by increasing σ_d. In short, the control of scour is evidently a function of both size of armorplate and its gradation.

With the variables of C_{M_F} identified, it was then necessary to investigate each of the parameters, $C_{M_{F_1}}$ and $C_{M_{F_2}}$. To do this Eq. 4 was written as

$$\frac{h_t^*}{H} = \phi_3 \left(C_{M_{F_N}} ; \frac{W_m t}{H} ; \frac{b}{H} ; \frac{d_m V t}{\sqrt{A} \sin \theta \, b} \right) \qquad (7)$$

A relationship of the form as expressed by Eq. 7 was used to conduct the experimental investigations of both the thesis study and the studies of this report. Application of Eq. 7 to experimental results of the thesis study is illustrated in Fig. 5, which shows the variation of h_t^*/H with $W_m t/H$ for $b/H = 0.375$ and different values of $C_{M_{F_1}}$. In this report only the relationship between the parameters h_t^*/H, $C_{M_{F_2}}$ and $d_m Vt/\sqrt{A} \sin \theta \, b$ are presented.

Although the parameter $C_{M_{F_1}}$, a function of the sediment characteristics σ_{d_2}, and $C_{M_{F_2}}$, a function of tailwater depth b, may be used in the analysis of experimental data; there is still need for a better understanding of the mechanics of scour to establish either as a sufficient and complete parameter.

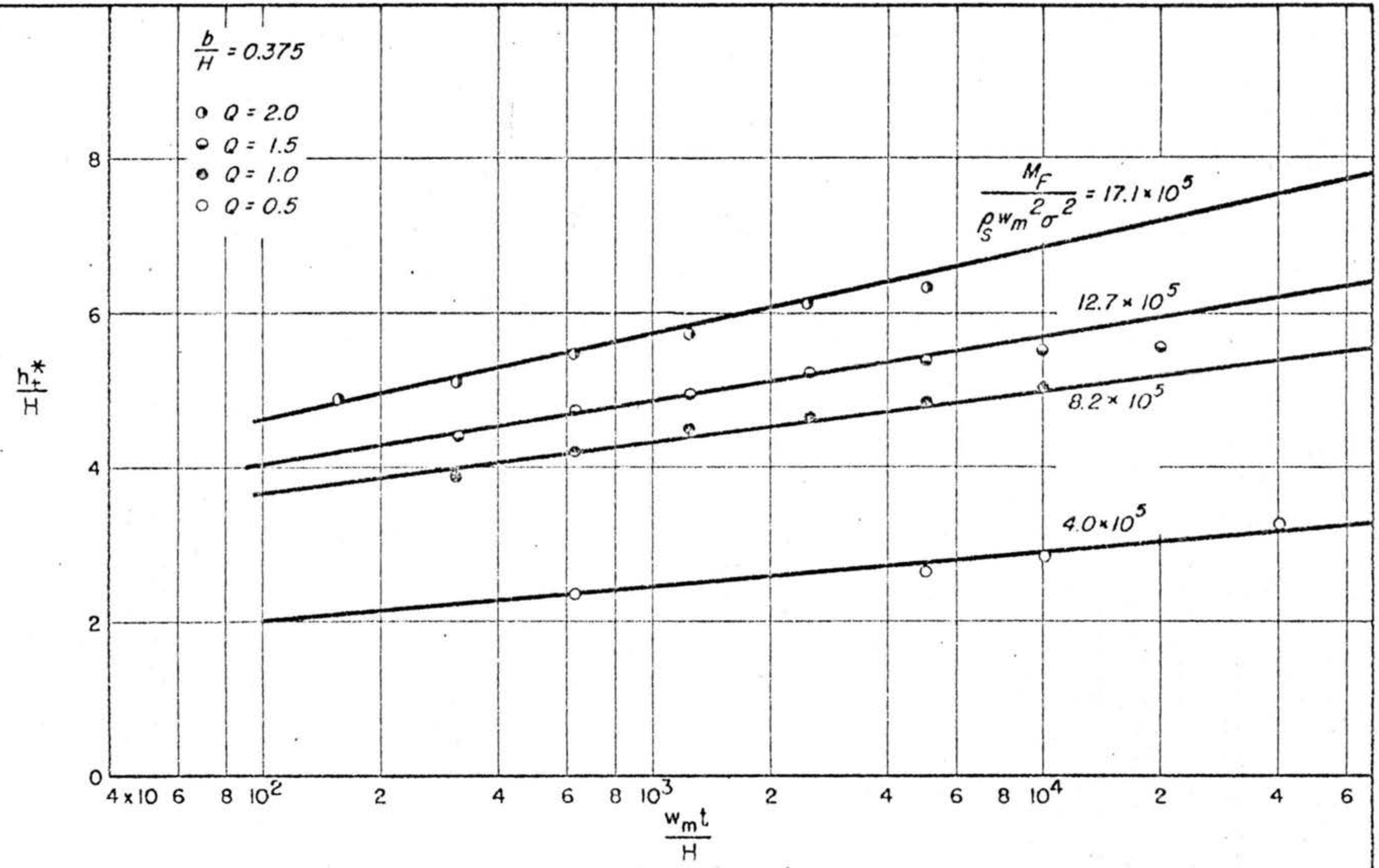

Fig. 5 Variation of $\frac{h^*}{H}$ with $\frac{w_m t}{H}$ for $\frac{b}{H}$ = 0.375

C. EXPERIMENTAL EQUIPMENT AND PROCEDURE

The analysis of scour and scour control demonstrated that limitations must be imposed on the scope of either phenomenon to make a laboratory investigation practicable. By establishing certain limitations the number of variables was reduced so that adequate information could be obtained on the remainder . Only the most simple case was considered first to be followed by the more complex cases. To achieve this objective the experimental program was divided into two phases, - each phase utilizing different experimental equipment, but the same range in the various variables such as

$H \approx$ 4 ft,
Q = 0.5, 1.0 and 2.0 cfs,
b = 0.5, 1.0 and 2.0 ft,
B = 10 ft in Phase 1.
B = 5, 10, and 20 ft in Phase 2.
T = 0.25, 0.5, 1.0, 2.0 ... 238 hrs in Phase 1.
T = 0.25, 0.5, 1.0, 2.0 ... 8 hrs in Phase 2.

The alluvial material used for both phases had essentially the same characteristics. Also, each phase consisted of several parts as follows:

1. Phase One.
   a. The collection of experimental data on scour phenomenon in a rectangular channel of constant width and rigid sides and an alluvial bed, and
   b. The collection of experimental data on the control of scour in the channel of item (a) by use of a pre-shaped, armorplated stilling basin.

2. Phase Two.
   a. The collection of experimental data on scour phenomenon in rectangular channels with rigid sides but of different widths, and an alluvial bed .

b. The collection of experimental data on the control of scour in the largest width channel of (a) by use of a pre-shaped, armorplated stilling basin, and

c. The collection of experimental data (qualitative only) on scour control by use of armorplate including the investigation of an armorplated basin installed in an entirely alluvial channel with an initial bottom width of 5 ft at the culvert outlet.

The laboratory equipment employed in both phases of the experimental studies consisted essentially of a simulated cantilevered pipe outlet, a simulated stream bed of a sand and gravel mixture, a water supply system with means of regulating the discharge, and a flume or basin to accomodate the bed material and discharge.

1. Phase One: Equipment Assembly and Recirculating System

Figure 6 shows the equipment assembly. Clear water was pumped from an underground sump to an 8-in. pipe line (P_1, P_2, P_3, P_4 and P_5) by a 60-horsepower Fairbanks-Morse No. 14 propeller-type pump. The discharge through the supply line was regulated by the value V_1 located in pipe P_3. The flow was measured by an orifice meter installed in pipe P_2 downstream from the pump.

Guide vanes were used in the 90-degree bends connecting pipes P_3, P_4, and P_5, to prevent zones of separation from developing and to help establish uniform flow conditions in pipe P_5. The installation of the water supply line was such that the pipe P_5 was exactly centered over the upstream end of the flume, and the invert of the discharge pipe was at a fixed height of 4 ft above the alluvial bed. Pipe P_5 was also level.

Flume -- The flume, of dimensions given in Fig. 6, was filled to a depth of 2 ft with a sand and gravel mixture. The 2-ft bed terminated in a 3-ft wide sediment trap at the downstream end of the flume. At one end of the trap was a 1-ft square orifice through which the water flowed before spilling

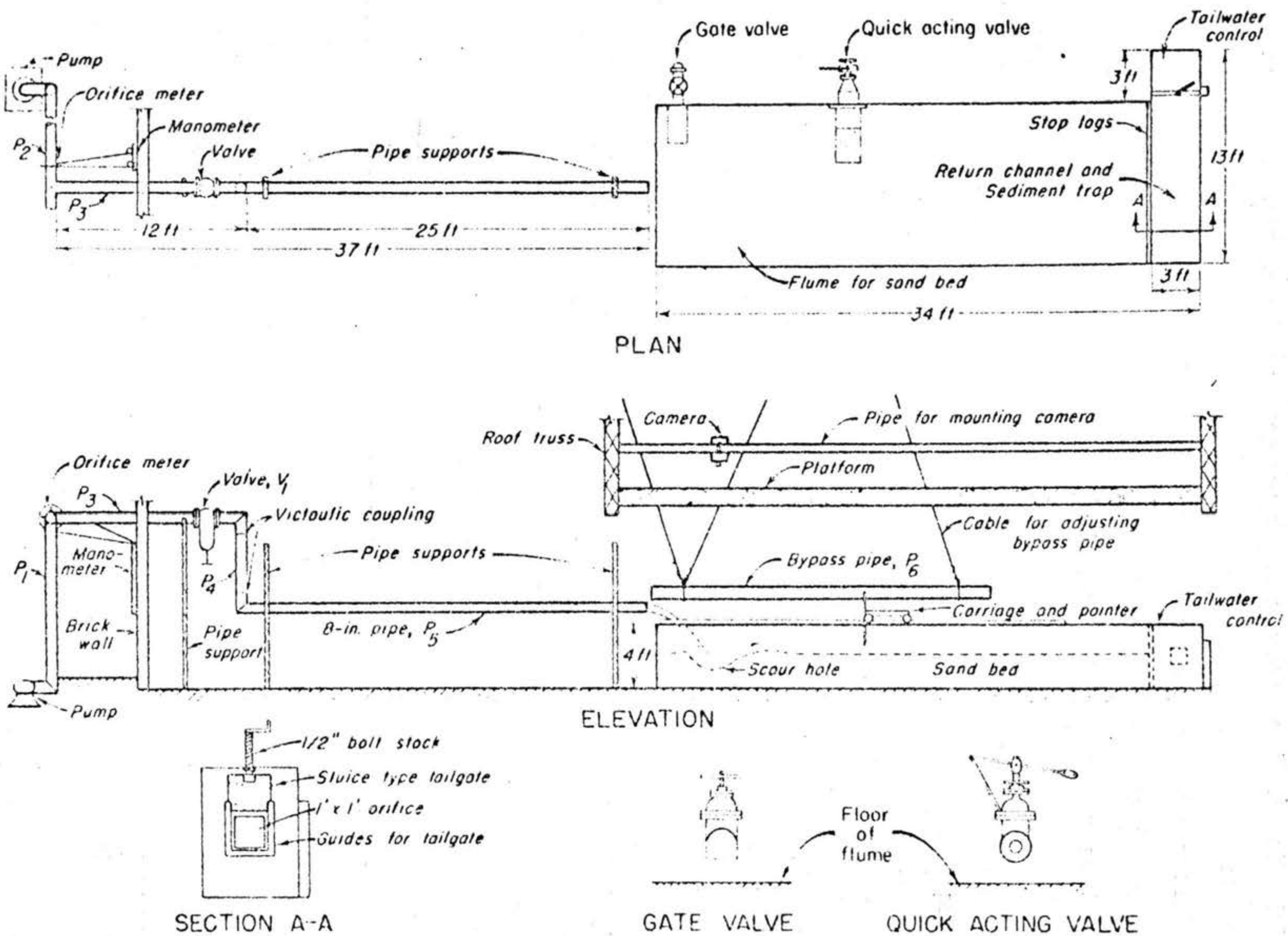

Fig. 6. Laboratory layout for study of scour below a culvert outlet--phase one.

into the return channel to the sump.

Tailwater control -- To vary the depth of water over the alluvial bed, a sluice-type tailgate was used to regulate the size of opening of the orifice outlet. The tailgate was operated by means of a 1/2-in. screw which permitted a sensitive adjustment in the tailwater depth. A point gage was used to measure tailwater depth. It was located at the inside corner of the flume near the point of jet impingement.

Since it was necessary to establish a constant depth of tailwater over the alluvial bed before the jet was allowed to impinge upon the pool, a pipe P_6 was used to divert the jet downstream beyond the extent of the test area until equilibrium discharge and tailwater depth were established.

Since time was a significant variable, a quick change in the volume of water in the flume was found to be desirable. It was noted that a rapid change in the tailwater depth, if properly controlled, could represent a saving of several hours for each experimental run.

Outlet control valves -- An installation that proved satisfactory in controlling tailwater consisted of two 4-in. outlet pipes with valves placed on the flume floor. One pipe with a gate valve was located at the side wall of the flume near the test area; the other pipe with a quick-acting valve was located near the mid-point of the flume. The pipes projected one foot into the flume. To prevent undesirable flow conditions near the scour hole as well as to prevent sand entering the sump, closed cylinders of heavy brass plate were attached to the inlet of each pipe. The cylinders, three-feet long and one foot in diameter were perforated with 1/4-in. holes on 2-in. centers. Each cylinder was wrapped with a double thickness of 1/8-in. hardware cloth to prevent undesirable entry of sand into the sump. The pipe with the quick acting valve permitted rapid adjustment of tailwater depth; the other unit permitted rapid control of the water surface in the scour hole.

Photographic layout -- A photographic record was made of both the scour phenomenon, as illustrated in Fig. 7, and the effect of armorplate in

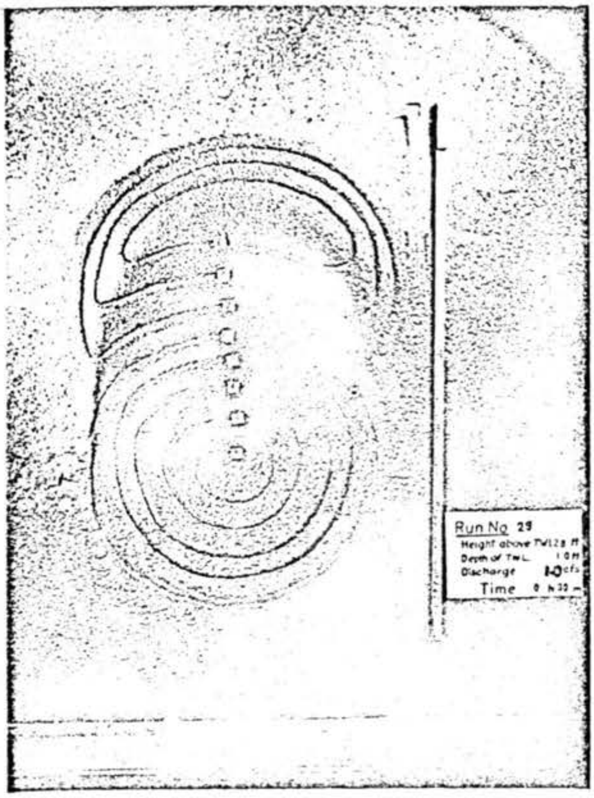

(a) Point 1 on graph — Time = 0 h. 30 min.

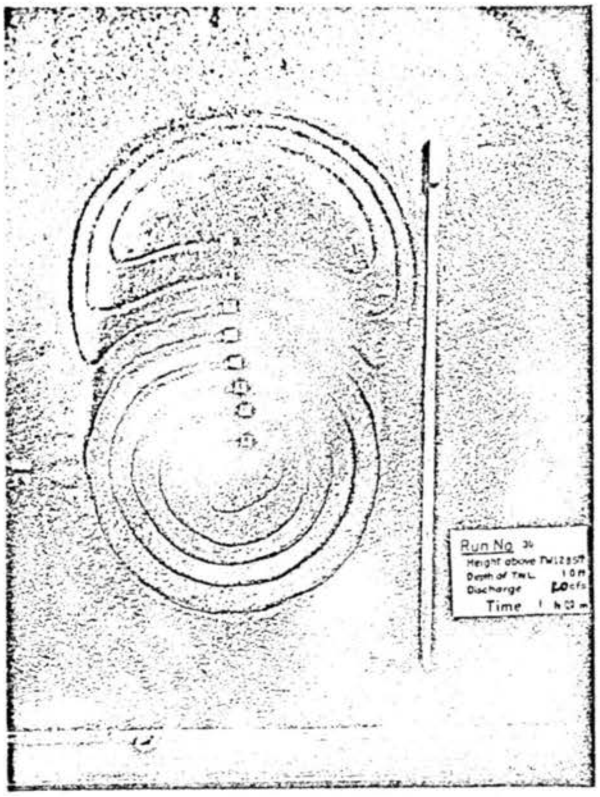

(b) Point 2 on graph — Time = 1 h. 0 min.

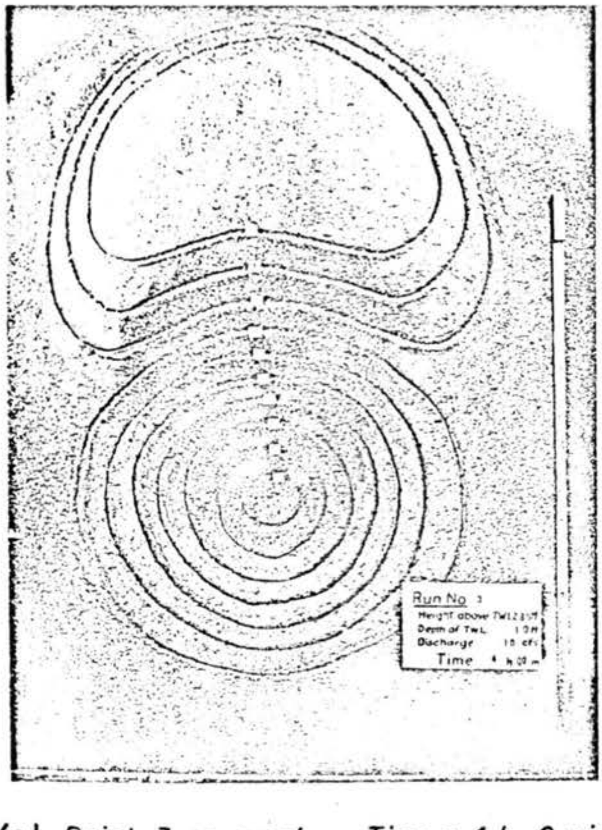

(c) Point 3 on graph — Time = 4 h. 0 min.

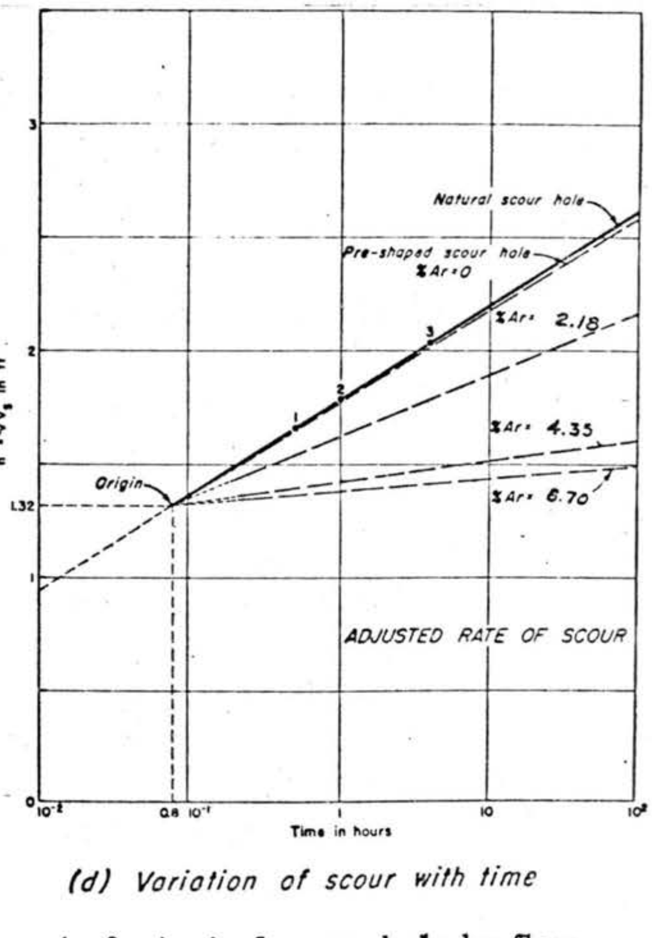

(d) Variation of scour with time

Fig. 7 - Photographic record of the development of a typical scour hole by flow from a cantilevered culvert.

$Q = 1.0$ cfs $\qquad b = 1.0$ ft $\qquad H = 4.0$ ft scour control, as illustrated in Fig. 8. To obtain a plan view of the scour hole or armorplated basin it was necessary to construct a platform above the flume. A 2-ft by 14-ft platform securely bolted to the roof trusses was used. Two cameras, a Speedgraphic 4 by 5 and a Rolleiflex f 3.5, were used for taking pictures. Portable photo-flood lamps with 1000-watt photo bulbs were used on both sides of the flume for the proper lighting effect. A bank of four 150-watt spotlights mounted directly above the outlet of the pipe P_5 were used for auxiliary light.

Miscellaneous equipment -- A carriage was essential for making measurements of both the scour hole and the armorplated, pre-shaped basin as the water surface receded after termination of a particular run. The carriage used was a 2-in. by 12-in. wooden plank with 3-in. brass wheels. Rails for the carriage wheels were 1/8-in. by 2-in. steel angles bolted to the top of the sides of the flume. Two 1/8-in. by 2-in. angles with cross braces were bolted to the carriage and to a 1-in. by 4-in. by 10-ft wooden plank, which was used as a bed leveler.

The angle of jet impingement was measured by means of a 1-ft protractor, which was held in position on a slotted 1/8-in. by 1-in. steel strap by a wing nut. Measurements made by this method gave results within 1 percent of the computed value. A metal arrow attached to the protractor by a wing nut was used in marking the angle. The slotted steel strap in the form of a T-section permitted vertical and horizontal movement of the protractor.

A mercury thermometer, graduated to 1.0 degree centigrade was used to measure the temperature of the water in the flume.

Sediment -- Sediment of the sand and gravel classes only was used. For local scour studies a sand-gravel mixture ranging in diameter from 0.125 mm to 4 mm was used. The armorplate for scour control consisted of graded gravel and had a size range from 4 mm to 30 mm.

The sand-gravel mixture was obtained from a gravel pit located near the Big Thompson River at Evans, Colorado. The mixture was washed once

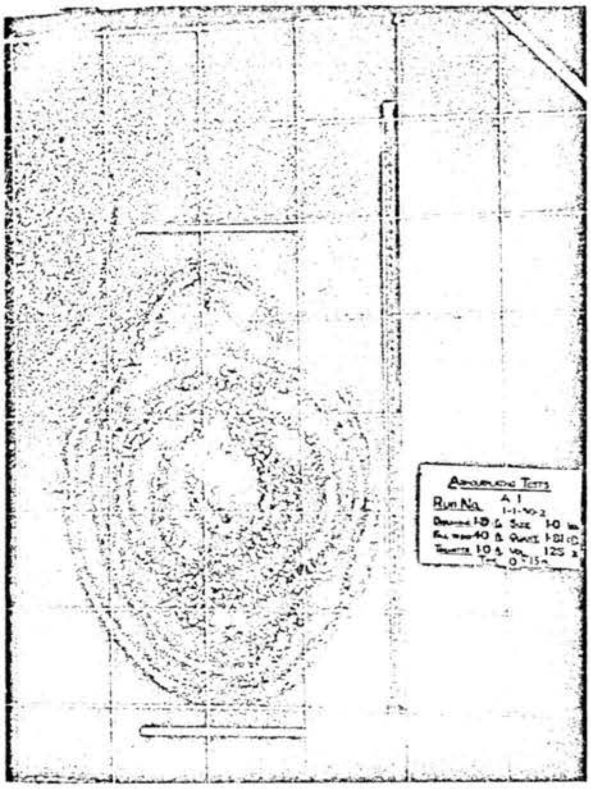

(a) Point 1 on graph — Time = 0 h. 15 min.

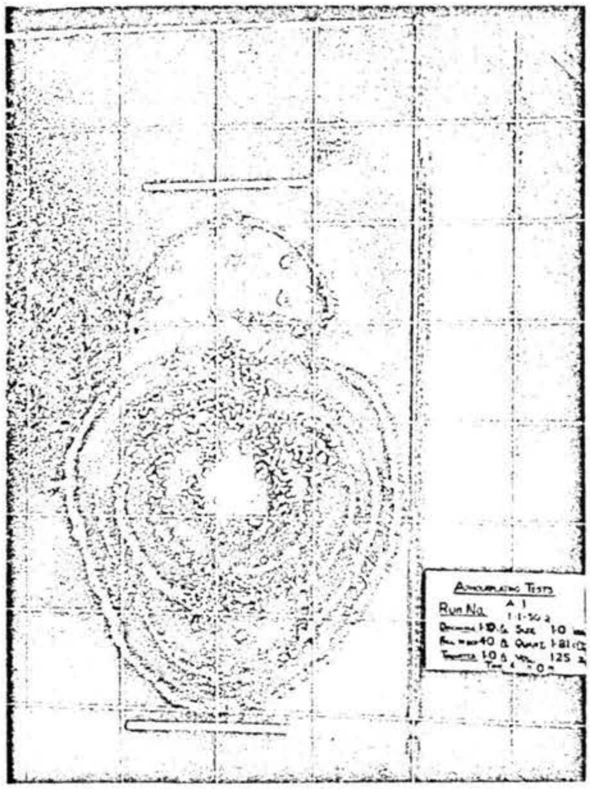

(b) Point 2 on graph — Time = 4 h. 0 min.

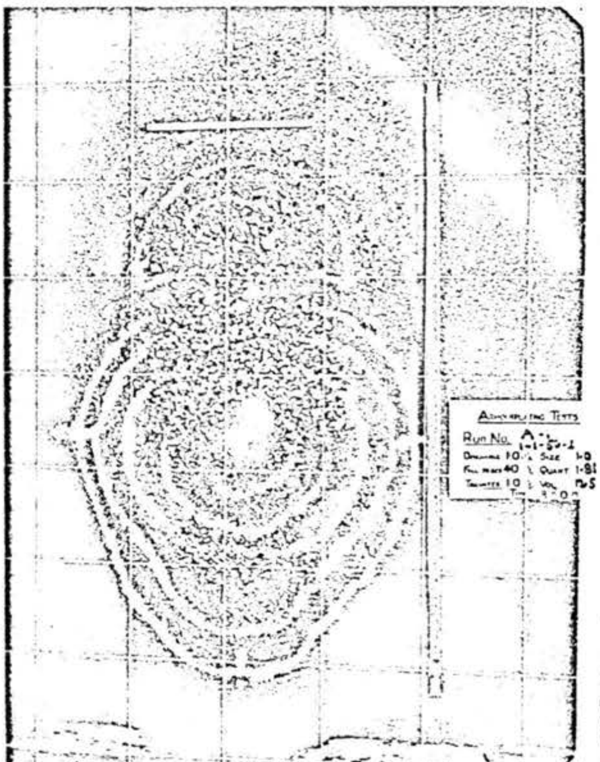

(c) Point 3 on graph — Time = 8h. 0 min.

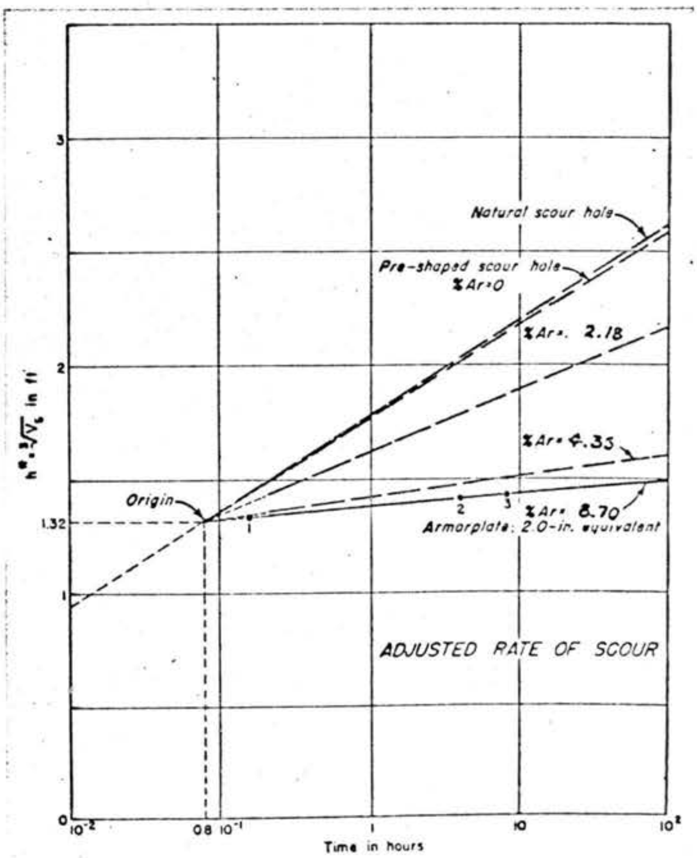

(d) Variation of scour with time

Fig. 8 - Photographic record of influence of armorplate in controlling rate of scour.

(V /V = 8.70 %) Q = 1.0 cfs b = 1.0 ft H = 4.0 ft at the site before it was transported and placed in the flume. The armorplate was obtained from a commerical gravel pit located near the Cache La Poudre River at Fort Collins, Colorado. Pit-run material was used instead of an artifically graded material since it would be the kind of material most likely available to field engineers.

The properties of the sediment were determined by various methods as outlined in Appendix A.

2. Phase Two: Equipment Assembly and Recirculating System

Figure 9 shows the equipment assembly. Clear water was pumped from an underground sump to an 8-in. pipe line, P_1, by a 20-horsepower Fairbanks-Morse propeller-type pump. The discharge through the supply line was regulated by the valve V_1 located in pipe P_1. The flow was measured by an orifice meter installed in pipe P_1 downstream of the pump and upstream of valve V_1.

Guide vanes were used in all 90-degree bends of the supply line P_1 to prevent zones of separation from developing and to help establish uniform flow conditions at the point of discharge. The installation of the point of discharge was such that it was exactly centered over the mid point of the upstream end of the scour basin. The invert of the discharge pipe was at a fixed height of 4 ft above the original bed level during the test runs.

Scour basin -- The 20-ft by 20-ft scour basin was filled to a depth of 2 ft with a sand and gravel mixture. The sediment bed terminated in a 5-ft wide sediment trap at the downstream end of the flume. The tailwater control box (see Fig. 10b) was opposite of the discharge control box, shown in Fig. 10a. The tailwater control box consisted of a 1-ft square orifice, a sluice-type tailgate and a by-pass control pipe P_4 with a butterfly valve. The flow returned to the supply sump through the orifice and a return channel.

Tailwater control -- As in the flume the depth of water over the alluvial bed was controlled by a sluice-type tailgate. The tailgate was operated by means

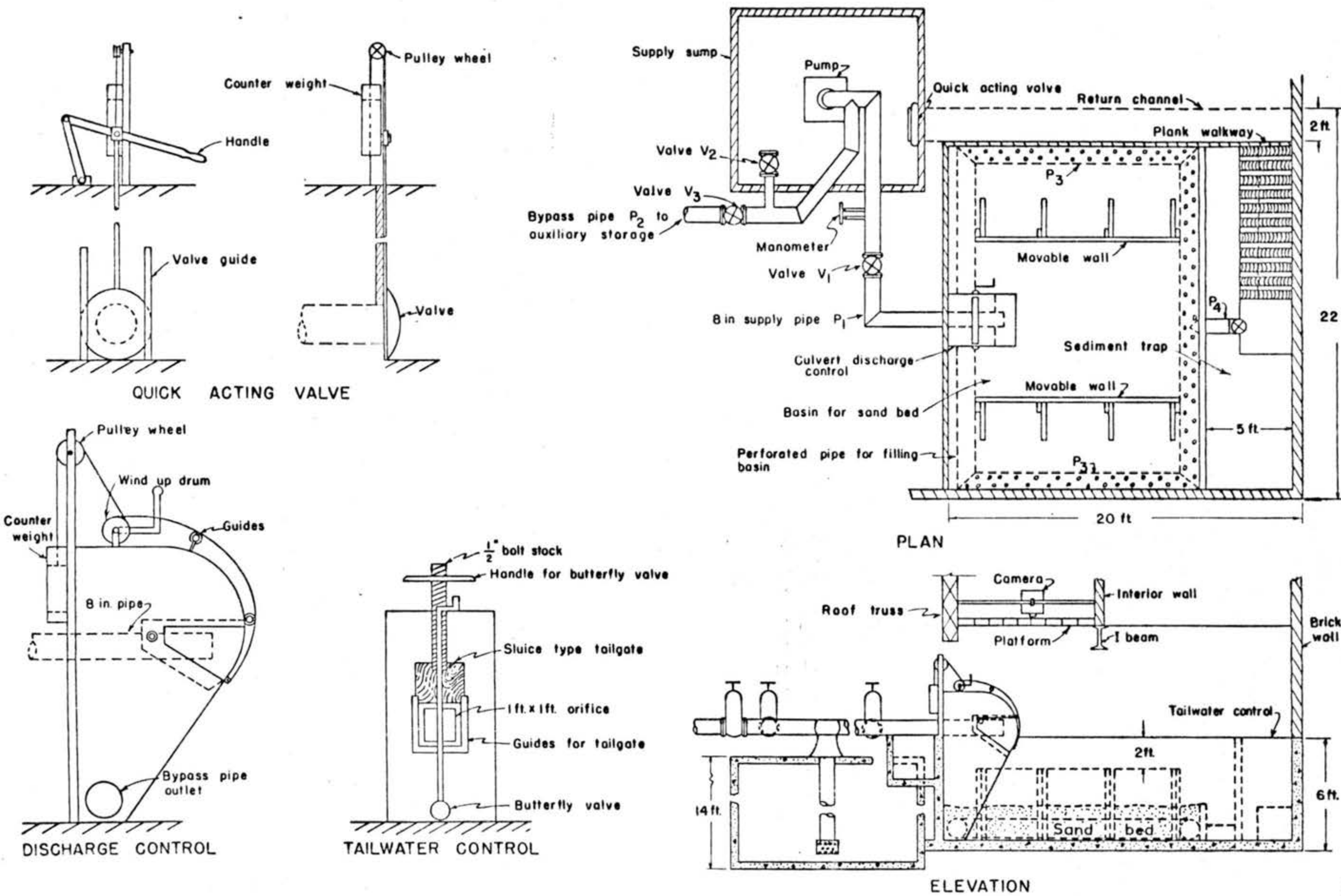

Fig. 9 Laboratory layout for study of scour and scour control below a culvert outlet — — Phase Two

a. Discharge control showing discharge from culvert. Note: Valve V_1 and water manometer for orifice meter.

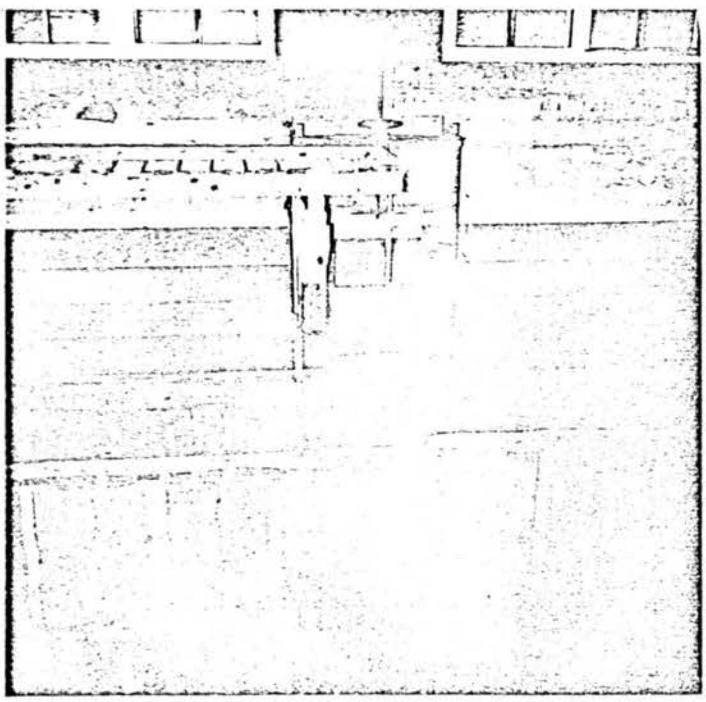

b. Tailwater control directly opposite discharge control in basin

Fig. 10 - Discharge and tailwater control used in basin

of a 1/2-in. screw which permitted a sensitive adjustment in the tailwater depth. A point gage was used to measure tailwater depth. It was located at the upstream corner of the discharge control box.

Since it was necessary to establish a constant depth of tailwater over the alluvial bed before the jet was allowed to impinge upon the pool, the discharge was first introduced into the alluvial bed by outflow from the discharge box through the perforated pipe, P_3. To prevent undesirable piping by outflow from the perforations a 1-ft layer of crushed gravel of 2-in. maximum diameter was placed above the pipe. With the rise of tailwater above the alluvial bed, the valve in P_4 was closed, the tailgate gradually opened until equilibrium between discharge and the desired tailwater depth was achieved.

From the experience gained in operating the flume, it was known that a rapid change in the tailwater depth, if properly controlled, could represent a saving of several hours for each experimental run.

<u>Outlet control valve</u> -- An installation that proved satisfactory in controlling tailwater was a quick acting valve located in the supply sump at the exit end of the return channel. Additional control of ground-water flow was provided by the butterfly valve in pipe P_4, which controlled the return ground-water flow into the perforated pipes.

<u>Photographic layout</u> -- As in the flume a photographic record was made of each overhead platform with either a Speedgraphic 4 by 5 or a Rolleiflex f 3.5 camera. Suspended photo-flood lamps with 1000-watt bulbs were used for lighting.

<u>Miscellaneous equipment</u> -- Contouring the scour hole as the water receded after completion of a run was accomplished by the use of a point gage mounted on a swinging truss and a pointed marker stick as shown in Fig. 11a. The contoured scour hole is illustrated in Fig. 11b.

Because of the width and depth of basin, it was not possible to measure the angle of jet impingement for each test; therefore, a relationship between discharge and angle of impingement for different tailwater depths was determined and is given in Table 5 of Appendix C.

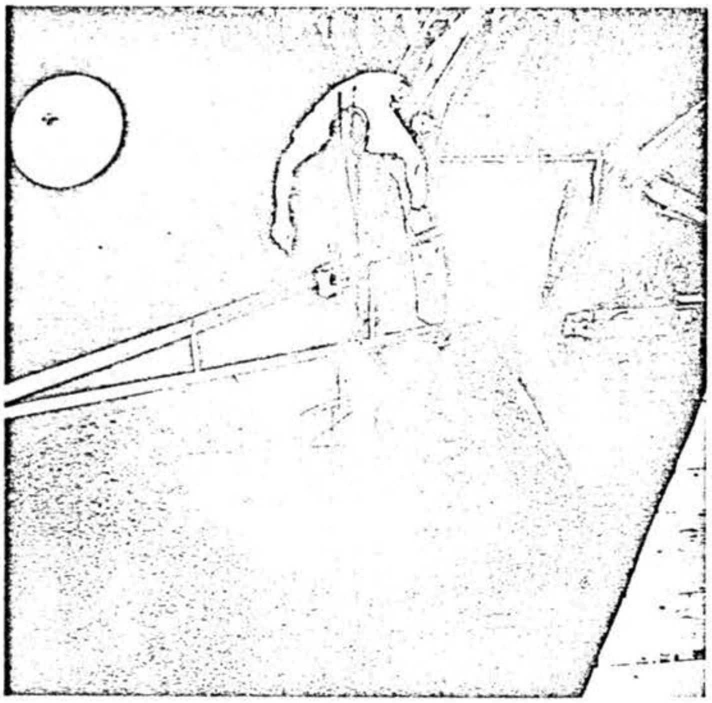

a. Contouring the scour hole at a given depth below the original bed level

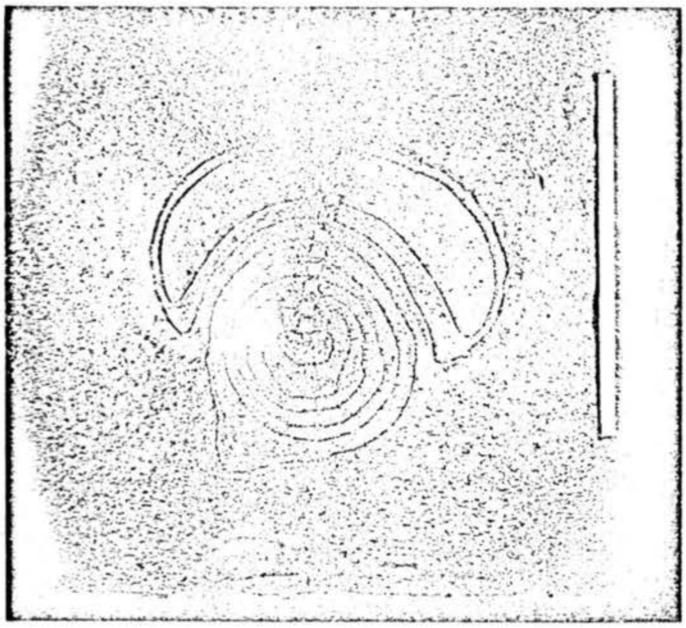

b. Typical photograph record of contoured scour hole

Fig. 11 - Illustration of techniques employed in obtaining experimental data of scour phenomenon in basin

To vary the width of the channel, vertical walls consisting of 1/2-in. plywood were used. The sides were braced by 2" x 4" ribs bolted to 2" x 4" supports, making a 45 degree angle with the side and floor. These 2" x 4" supports were in turn bolted at the floor to a horizontal 2" x 4" bolted to the bottom of the vertical rib. (See Fig. 9.)

Sediment and armorplate -- See sections on sediment and armorplate given in Phase One and Appendices A and B.

Alluvial channel at culvert outlet -- The experimental program in Phase Two of scour and control of scour by armorplate included a qualitative investigation of the case of an alluvial channel of a 5-ft bottom width at a culvert outlet. (See Fig. 12.) In conducting the investigation for a comparative basis of test results it was first necessary, a) to determine the natural angle of repose of the sediment under the submerged conditions, and b) to determine a method of providing for uniformity of compactness of the sediment for each test.

The angle of repose under submerged conditions was found by first filling the basin with water and then depositing the sediment into a number of piles in the basin. After a period of submergence of several hours the water was drained and the angle of repose of the various piles measured. The mean angle of repose was found to be 30°, which was about the same as the mean angle of repose of the sediment under conditions of localized scour.

Uniformity of compaction was achieved by the following procedure:

a. Maintaining, as near as possible, homogeneity of sediment by thorough remixing of the sediment after each scour test, and screening and remixing of the sediment after each control of scour test;

b. Shaping the remixed sediment to the desired trapezoidal cross section and then submerging the alluvial channel for a period of several hours;

c. Raising and lowering the tailwater as rapidly as possible from

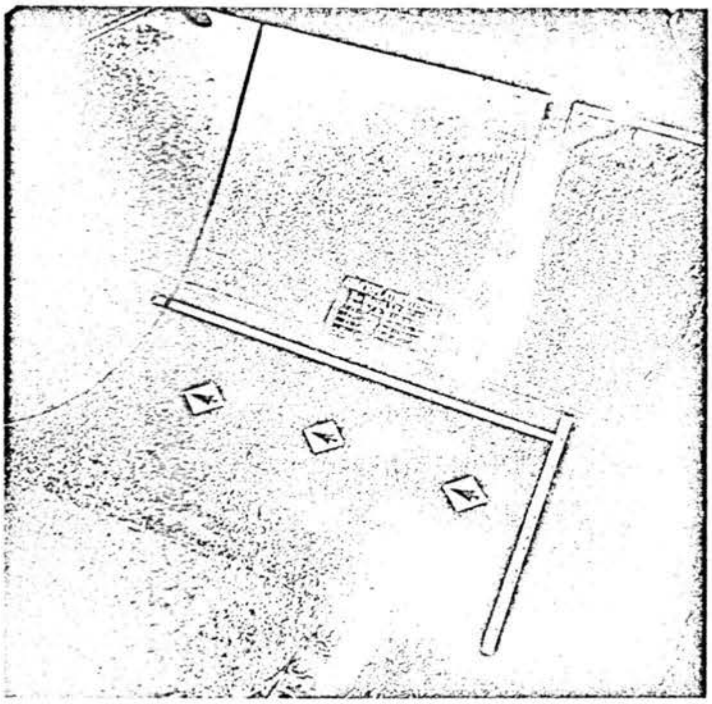

a. Without armorplating

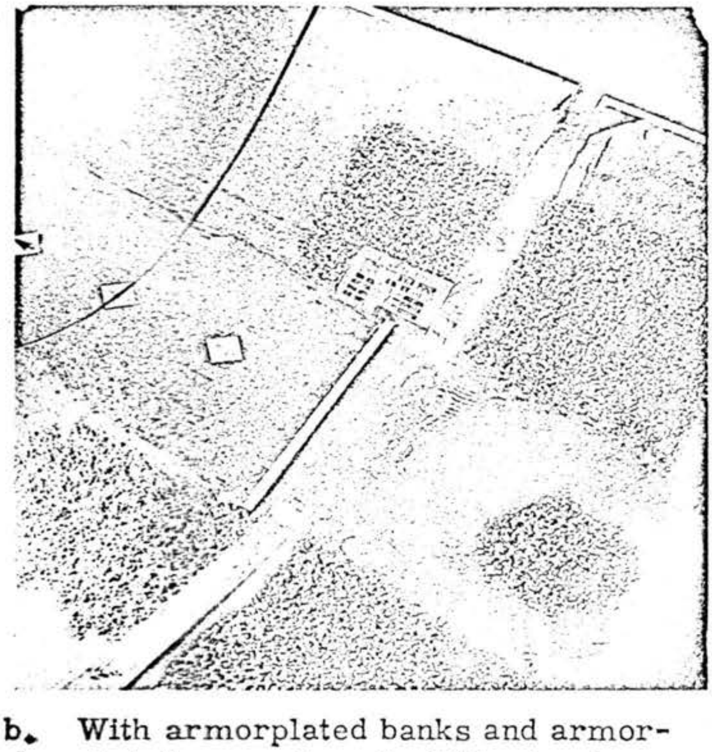

b. With armorplated banks and armor-plated, pre-shaped stilling basin

Fig. 12 - Simulated alluvial channel at culvert outlet used for qualitative investigation of scour and control of scour by armorplate. Arrows indicate direction of flow.

bankfull to bed level after the initial period of submergence until there was little or no sloughing of the banks; and

d. Reshaping and varying the tailwater depth until the channel sides were stable.

For the scour control tests it was necessary to maintain uniformity of depth of the armorplate on the channel banks. The variation in the depth of armorplate was based on a multiple of the maximum diameter of the armorplate that is, nD in which n is 1, 2, 3 ... and D is the diameter in inches. The initial depth of armorplate was equal to D with D = 1 in. The height of the armorplate on the channel side was maintained approximately 6 inches above the tailwater for each test run.

The quantity of armorplate needed for a given tailwater depth per foot of channel length was computed and that amount was then dumped from the top of the bank and permitted to assume its natural angle of repose along the channel side. (See Fig. 12b.) This procedure simulated dumping of armorplate riprap in the field along the channel by dump trucks.

The last experiments of Phase Two were concerned with the effect of the angle of slope of the channel bank on scour control. That is, would flattening the channel side slopes increase or decrease the effectiveness of the armorplate in scour control? Procedure in preparation of the channel was the same as previously described except that a different template was used. The tests were qualitative. Results of these tests are not given in this report.

3. Scour Control by Use of Armorplate

The general experimental procedure to determine the effect of armorplate on the rate of scour was the same as was used for the investigation of the scour phenomenon; that is, the flow and tailwater were established before jet impingement; and, the scoured hole was contoured and photographed, and its geometry measured for each increment of time. However, in addition to the general procedure, it was necessary to investigate:

a. The use of an excavated hole of given geometry shown in Fig. 13 (hereinafter called the pre-shaped stilling basin) at the culvert outlet as a depository for the armorplate;

b. The effect of size of the pre-shaped stilling basin in combination with armorplate on the rate of scour;

c. The method of placement of the armorplate in the pre-shaped stilling basin, that is, to determine if spreading of the armorplate over the surface of the basin was more effective in scour control than dumping of the armorplate as a mound in the basin;

d. The effect of the quantity of armorplate on the rate of scour; and

e. The most effective point of placement of the minimum amount of armorplate, as determined by d, relative to the point of impingement of the jet at the original bed level.

In order that scour control by armorplate could be systematically tested, it was first necessary to provide a means of containing the armorplate relative to the point of jet impingement. It was obvious that a pre-shaped stilling basin located downstream of the culvert outlet would meet this need.

From an analysis of the thesis data the geometry of a pre-shaped basin was developed in terms of the cube root of the volume of a scour hole, which would be created by a given discharge in a given period of time with a given depth of tailwater. The performance of the pre-shaped basin was then tested by comparing its rate of scour to that of the natural basin (See graphs on Figs. 7 and 8) and found to compare favorably. The design criteria for the pre-shaped basin, in terms of the cube root of the volume of scour hole at time t, $(V_{st})^{1/3}$, are as follows:

$d_T = 2.38\, h_t^*$ (Diameter of pre-shaped basin at original bed level.)

$d_B = 0.65\, h_t^*$ (Diameter of pre-shaped basin at depth h.)

$h = 0.50\, h_t^*$ (Depth of pre-shaped basin measured from original bed level.)

However, these design criteria for a pre-shaped basin do not provide for a sufficient test of the effectiveness of armorplate in the control of scour.

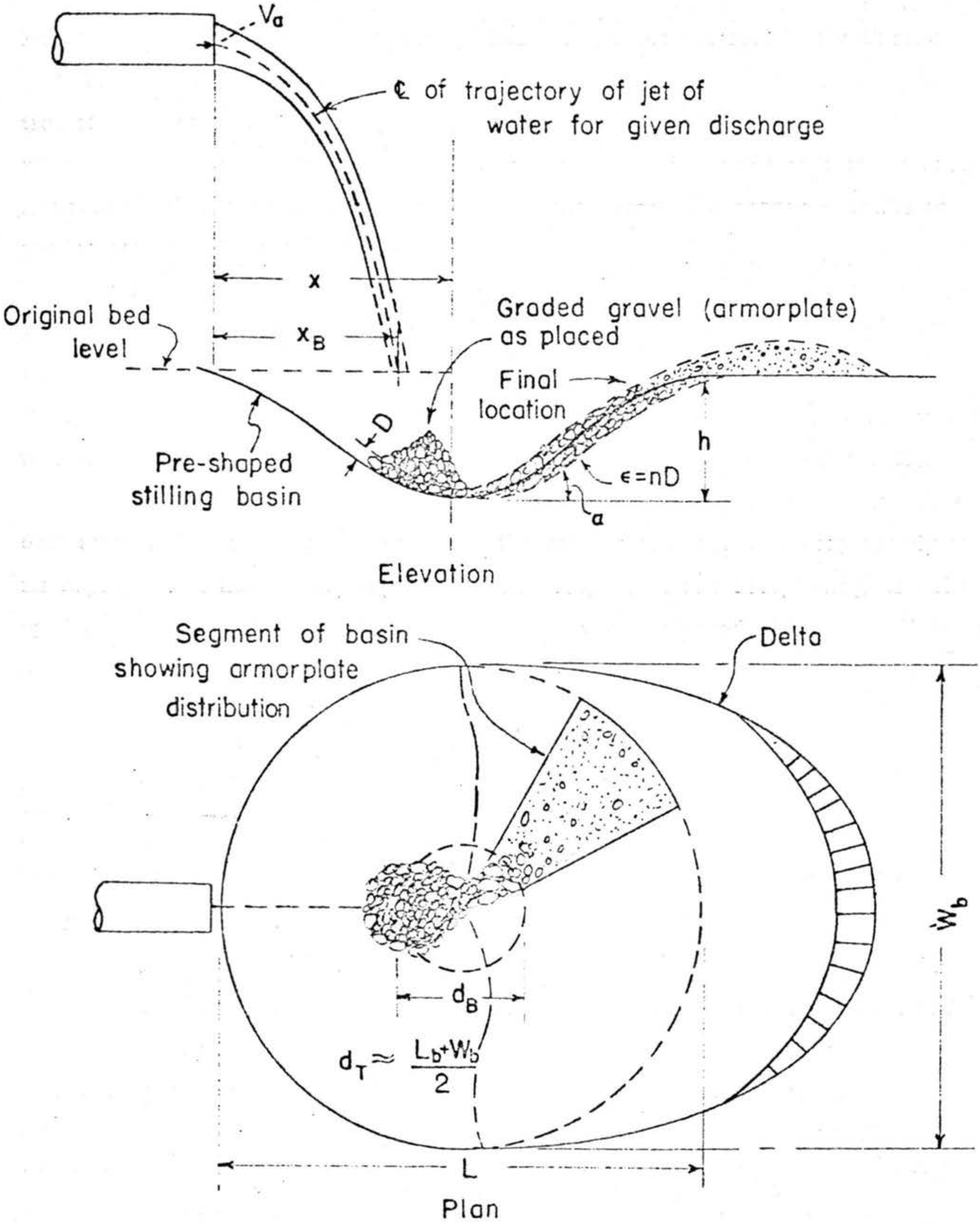

Fig. 13 Schematic drawing of experimental pre-shaped stilling basin used for study of control of scour by armorplate showing pertinent geometric dimensions.

For example, consider the size of the basin only. As the size of the basin is increased the control of scour is less a function of basin size and more a function of the dissipation of energy through the turbulence created by jet diffusion within the stilling pool of the basin. On the other hand, as the size of the basin is reduced the control of scour depends the more upon the characteristics and properties of the armorplate.

Thus, the next step in determining the effectiveness of armorplate in scour control was to adopt a maximum (design) size of pre-shaped basin. With such a pre-determined size a given quantity of armorplate placed in various fractional sizes of the maximum size could be systematically studied for effective control of scour. This is considered in the next section in more detail.

From an analysis of experimental data on scour phenomenon it was evident after 100 hours of scouring action the volume of scour was very nearly at its asymptotic limit. Adopting this as the design size and designating its volume by $V_{s_{100}}$, three fractional sizes of $V_{s_{100}}$ were selected to test the effectiveness of armorplate in control of scour, namely: 1/8 $V_{s_{100}}$, 1/4 $V_{s_{100}}$ and 1/8 $V_{s_{100}}$. It was also noted that the size of each fractional basin would vary for each change in flow conditions, that is, $V_{s_{100}}$ would be larger for increased discharges and a given tailwater depth.

Using the design criterion (see Appendix B) for the pre-shaped stilling basin, the following studies were then made of the use of armorplate control scour.

a. Method of placement,

b. Location of armorplate relative to the center of scour hole, and

c. Effect of quantity of armorplate on rate of scour.

In each of these tests the median size basin 1/4 $V_{s_{100}}$ was used. The basis for its selection is given in the following section on experimental results. Likewise, for each of these tests a discharge of 1.0 cfs and a tailwater depth of 1.0 ft was used. The discharge and tailwater depth were selected on the basis of being representative of average flow and tailwater conditions of previous tests made in the same experimental equipment. In regard to armorplate, it was assumed that any given quantity of armorplate would blanket the entire surface of the basin to a depth $\epsilon = nD$ (See Fig. 33), in which n is equal to 0, 1/4, 1/2, 1, or 2, and D is the maximum size of armorplate used. For all tests D was equal to 1 in. To determine the best method of placement the armorplate was handled as follows:

1. The armorplate was carefully tamped into place over the entire surface of the pre-shaped basin.
2. The armorplate was spread in a loose condition over the entire surface of the pre-shaped basin.
3. The armorplate was dumped into a pile in the basin at the point where the jet would normally strike the original bed surface.

Because the interaction of the impinging jet upon the armorplate resulted in the eventual concentration of the armorplate at the bottom of the basin for all three methods, the method of dumping was selected as the most effective method of placement.

For the test of the variation in the rate of scour as influenced by location of armorplate, the quantity of riprap used was for $\epsilon = 1/2\ D$; that is, the maximum diameter of armorplate was still 1 in. but the amount of armorplate would cover the entire surface of the basin to a depth equal to 1/2 D. In the test series the armorplate for each run was dumped at different points along the center line of the basin in the direction of flow relative to the center point of the basin.

The test series for the influence of quantity of armorplate on the rate of scour made use of the three sizes of basins: $1/8\ V_{s_{100}}$, $1/4\ V_{s_{100}}$ and $1/2\ V_{s_{100}}$ for Q = 1.0 cfs and b = 1.0 ft. The essential factor in conducting these tests was to maintain uniformity of the sediment characteristics of the bed material for each run. This was achieved by screening out the armorplate after each run, and then thoroughly remixing the sieved sediment with bed material taken from the downstream end of the flume. The remixed material was then leveled and its height from the pipe invert measured. From a sieve analysis of several random samples of the remixed bed material it was evident that the changes in the sediment characteristics were insignificant.

D. EXPERIMENTAL RESULTS

Localized scour at culvert outlets can be controlled by armorplated, pre-shaped stilling basins. Presented in this section, for limited hydraulic conditions of discharge, tailwater depth, and time of scour, are criteria for armorplating a pre-shaped basin. The criteria are based on an analyses of: (a) the scour profile developed in an alluvial bed of a rectangular channel of width B = 10 ft; (b) the location of armorplate in the basin relative to the culvert outlet, and (c) the increase of the quantity of armorplate in the basin. Results of the effect of boundary geometry on rate of scour follow. Two types of boundary geometry are investigated: (a) the variation of the channel width for the case of the rectangular channel with alluvial bed, and (b) the trapezoidal channel with alluvial bed and sides and an initial bottom width of 5 ft. The section concludes with a description of scour control that can be provided to an alluvial channel by use of armorplate on its sides and an armorplated pre-shaped basin.

1. Experimental Analysis of Armorplate

To armorplate a pre-shaped stilling basin, it is essential to know:

a. The quantity of armorplate needed,

b. The location or point of placement of the armorplate,

c. The minimum size of armorplate that will resist erosion at peak design flow, and

d. The size of pre-shaped basin that would provide the most severe test on control of scour by the armorplate.

It was obvious that the design volume - volume of scour hole developed after 100 hours of scouring action for a given discharge and tailwater depth - would be of excessive size for use as a test volume. It was necessary, therefore, to select a smaller size basin that could be adopted to use in the experimental flume. It was also apparent that several smaller size basins would be desirable in order that the armorplate be properly tested.

Three pre-shaped basins were selected on the following basis:

1. It was assumed that the volume of a scour hole increases uniformly with time, that is, exponentially between $t = 0.5$ hr and $t = 100$ hr.
2. The design volume would be given the symbol $V_{s_{100}}$.
3. The size of a pre-shaped basin would be increased by a factor of two, that is, the largest size would be four times the smallest size.
4. Each pre-shaped basin would be made a fractional size of the design volume, that is, $1/8\ V_{s_{100}}$, $1/4\ V_{s_{100}}$ and $1/2\ V_{s_{100}}$.

Although volume defines the amount of scour for the three-dimensional case, it was desirable for convenience in plotting data to have a length measure representative of the extent of scour. The cube root of the volume of scour would give the desired length parameter, or

$$h_t^* = (V_{s_t})^{1/3}$$

This compares with the maximum depth h_{max} used to define extent of scour in the two-dimensional studies (3), (4). If we let $h^* = (V_{s_{100}})^{1/3}$, then for the previously mentioned fractional volumes $1/8\ V_{s_{100}}$, $1/4\ V_{s_{100}}$ and $1/2\ V_{s_{100}}$ write

$$h_t^* = (1/8)^{1/3} (V_{s100})^{1/3} = 0.50\ h^*$$

$$= (1/4)^{1/3} (V_{s100})^{1/3} = 0.63\ h^*$$

$$= (1/2)^{1/3} (V_{s100})^{1/3} = 0.79\ h^*$$

The criteria for quantity of armorplate V_{ar} as developed in Appendix B , in terms of h^* and ϵ is given by

$$1/8\ V_{s100}/V_{ar} = 0.106\ h^{*2}\ \epsilon \tag{8}$$

$$1/4\ V_{s100}/V_{ar} = 0.168\ h^{*2}\ \epsilon \tag{9}$$

$$1/2\ V_{s100}/V_{ar} = 0.264\ h^{*2}\ \epsilon \tag{10}$$

If $\%\ A_r = \dfrac{V_{ar}}{V_{s100}} \times 100$

then for

$1/8\ V_{s100}$

$$\%\ A_r = \frac{0.106\ h^{*2}\ \epsilon}{h^{*3}} \times 100 = \frac{10.6\ \epsilon}{h^*} \tag{11}$$

$1/4\ V_{s100}$

$$\%\ A_r = \frac{0.168\ h^{*2}\ \epsilon}{h^{*3}} \times 100 = \frac{16.8\ \epsilon}{h^*} \tag{12}$$

$1/2\ V_{s100}$

$$\%\ A_r = \frac{0.264\ h^{*2}\ \epsilon}{h^{*3}} \times 100 = \frac{26.4\ \epsilon}{h^*} \tag{13}$$

To determine if the three fractional sizes of V_{s100} would be suitable for testing the efficiency of armorplate in control of scour, it was first necessary to investigate their similarity of performance. Specifically, it was desirable to know if the rate of scour could be kept constant by decreasing the quantity of armorplate at the same percentage rate as the size of basin increase, that is, would the rate of scour be constant if the quantity of armorplate was reduced 50 per cent when the size of basin was increased 50 per cent. This is demonstrated by plotting experimental results given in Table 6, Appendix C in Fig. 14. The general equation for the curves is

$$h_t^* = 0.14 \log_{10} t + y' \qquad (14)$$

in which the value 0.14 is the slope of each curve and y' is equal to the y intercept at $t = 1$.

Having demonstrated the similarity of performance between the different size pre-shaped basins, it was desirable to know their performance when each basin contained the same quantity of armorplate. Again on the basis of experimental data of Table 6, Fig. 15 shows that the larger size basins with a quantity of armorplate based on $\epsilon = 1.0$ performs more efficiently than the smallest basin. Observation of the basins during the test revealed that the $1/4\ V_{s100}$ basin performed in the most acceptable manner. There was a negligible amount of scour and the dissipation of the impinging jet was largely confined to the basin.

The $1/8\ V_{s100}$ basin was undesirable because it deflected a major portion of the impinging jet rather than dissipating the energy within the basin. Under certain field conditions this would probably result in the formation of a hydraulic jump and associated energy waves downstream of the basin area. On the other hand, the $1/2\ V_{s100}$ basin was of such a size as to cause almost complete diffusion of the jet before it reached the armorplate material. This was evidenced by the relatively small amount of disturbance in the original quantity of armorplate as placed in the pre-shaped basin. Therefore, on the basis of the observed performance of these basins, the $1/4\ V_{s100}$ basin was

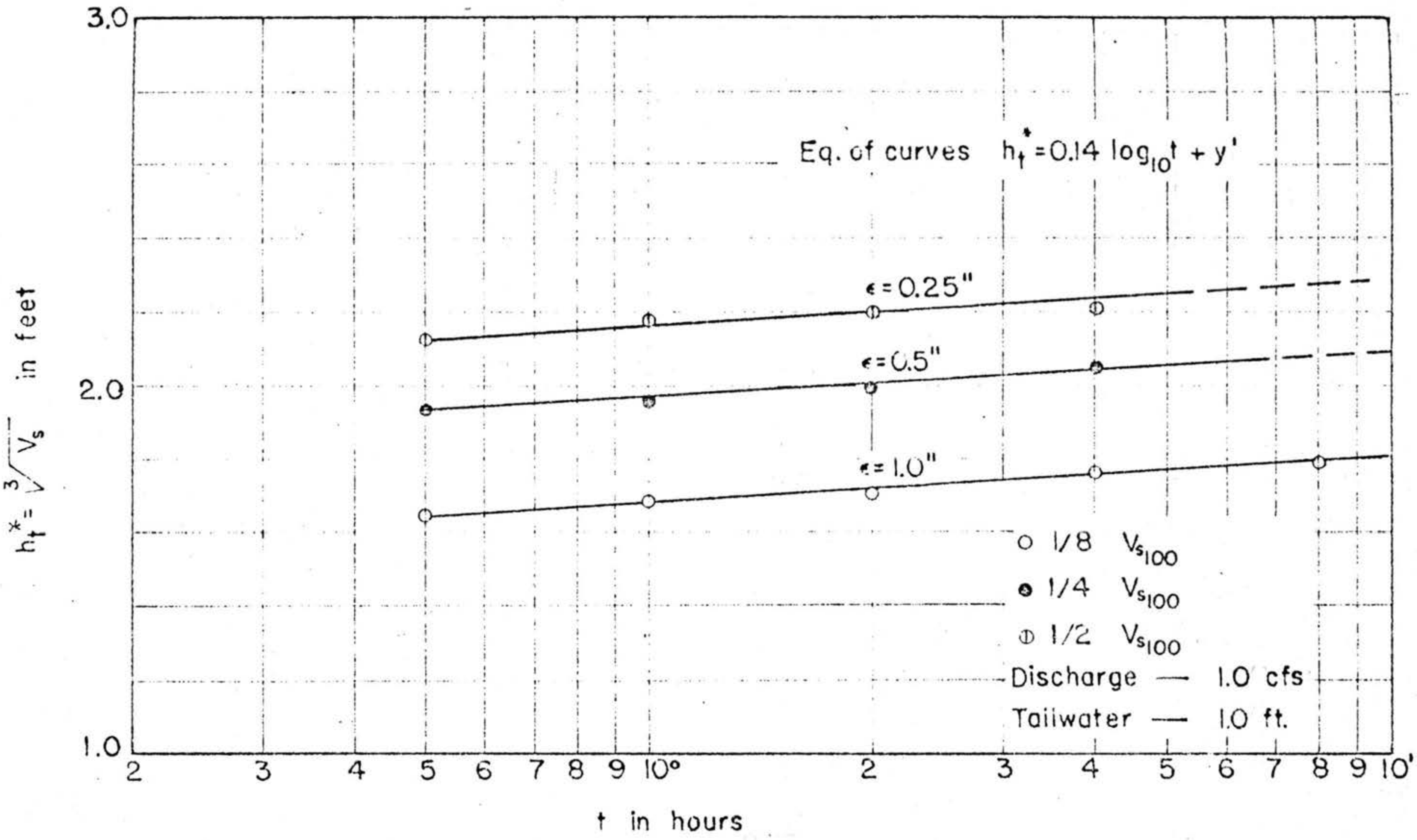

Fig. 14 Rate of scour when the quantity of armorplate is decreased by the same percentage as the increase in size of pre-shaped basin.

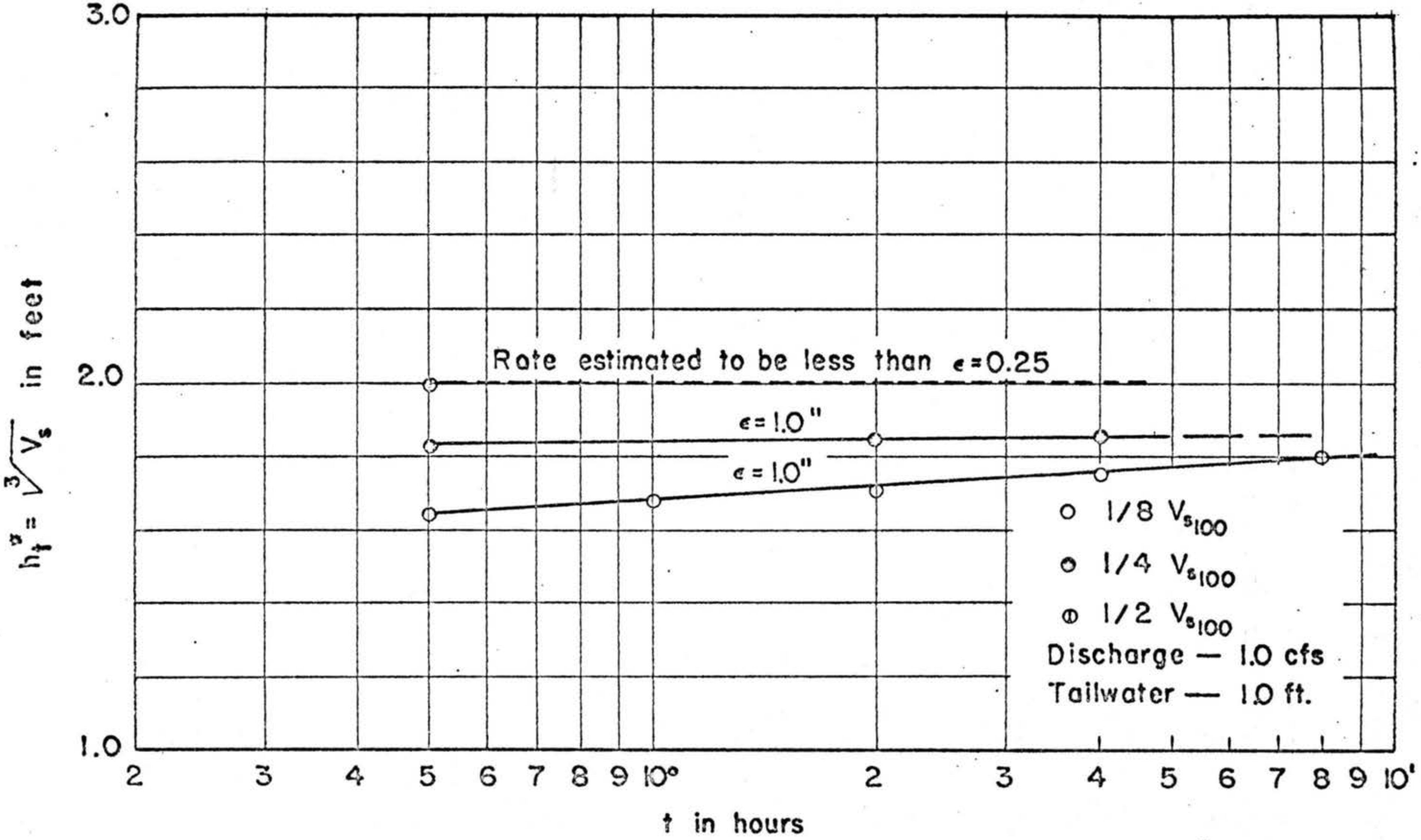

Fig. 15 Rate of scour as a function of an equal quanity of armorplate in the three different size pre-shaped stilling basins.

used as the pre-shaped basin for determining the effect of point of placement and quantity of armorplate on scour.

Before Eq. 9 or Eq. 12 could be used to compute the amount of armorplate in the aforementioned tests, it was necessary to determine h^*_t for $Q = 1.0$ cfs and $b = 1.0$ ft. Since the armorplate tests were to be conducted in the flume ($B = 1.0$ ft) use was made of the results of the analysis of data of reference 12, given in Table 8, to determine h^* herein defined as $(V_{s100})^{1/3}$. From the analysis of data an expression for h^* in terms of t was found to be

$$h^* = \frac{t}{0.25 + 0.41\,t} \tag{15}$$

Thus, when $t = 100$ hours h^* equals 2.43 ft.

For the variation in the rate of scour as influenced by location of armorplate use was made of Eq. 12, or

$$\%\,A_r = \frac{16.8\,\epsilon}{h^*}\,.$$

For a discharge of 1 cfs and a tailwater depth of 1 ft, h^* is equal to 2.43 ft. Since $\epsilon = nD$ then for $n = 1/2$ and $D = 1.0$ in. Eq. 12 gives

$$\%\,A_r = \frac{(16.8)(0.5)(1)}{2.43} = 3.42$$

Results of the tests are plotted in Fig. 16 which shows that the most effective point of placement is slightly downstream of the junction the impinging jet makes with the original bed level.

Following the point of placement tests, a series of tests were made to evaluate the effect of quantity of armorplate on the rate of scour. Again using the same hydraulic conditions and Eqs. 12 and 15 to determine quantity of armorplate it was found that the rate of scour decreased as the amount of armorplate material was increased. Results of the tests given in Table 8 of Appendix C

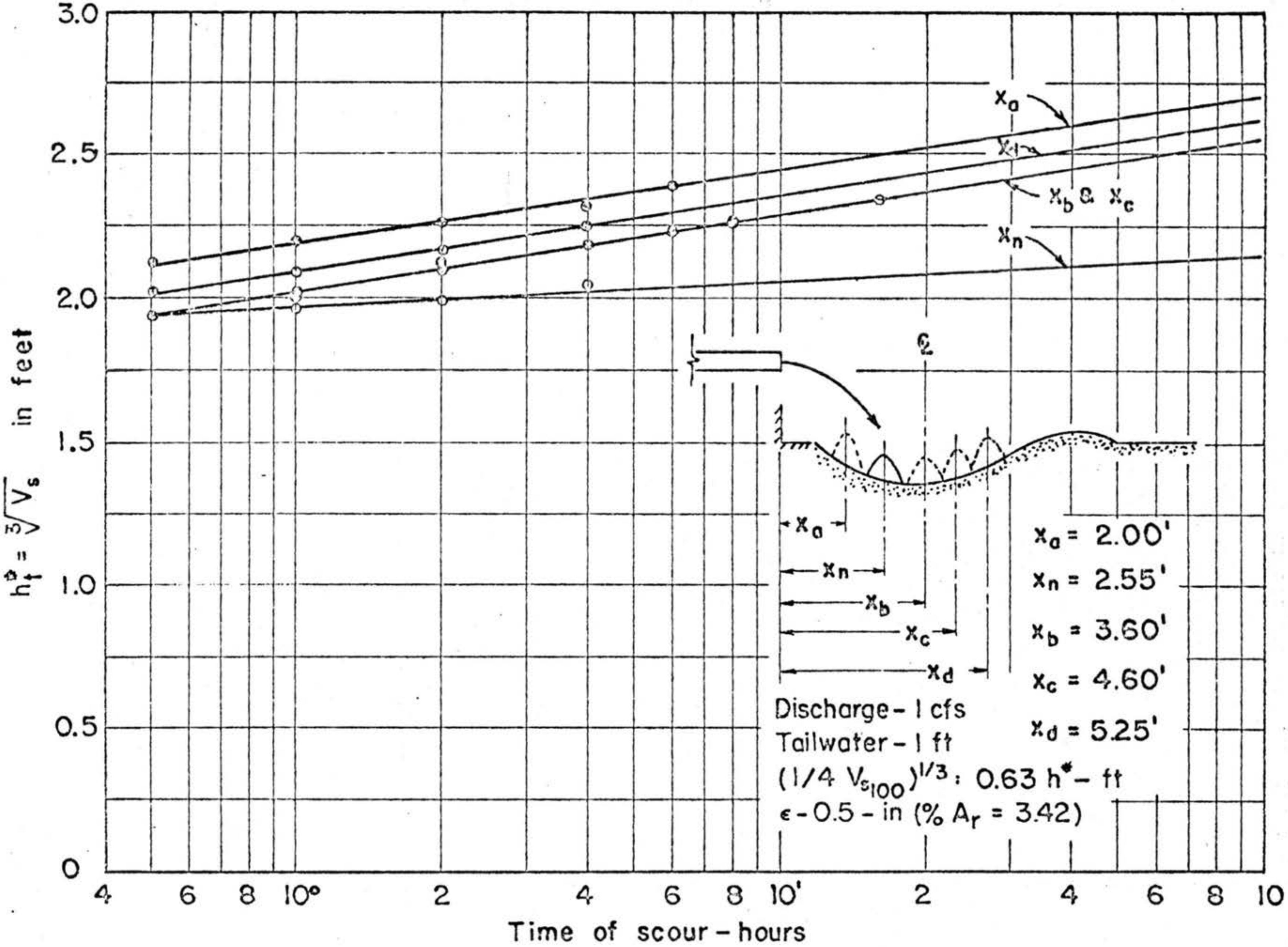

Fig. 16 Rate of scour as influenced by location of armorplating

are plotted in Figs. 17, 18, 19 for $Q = 1.0$ cfs and $b = 1.0$. Fig. 20 shows the rate of scour as a function of quantity of armorplate and for $Q = 2.0$ cfs with $b = 1.0$. The dashed line on Fig. 20 compares the rate of scour for $Q = 1$ cfs and $b = 1.0$ ft for the same quantity of armorplate ($\% A_r = 2.72$) and size of pre-shaped basin (0.79 h*).

As demonstrated by Hallmark (4), Fig. 17, for example, shows that there is an apparent optimum in the amount of armorplate needed for control of scour. More explicitly, doubling the amount of armorplate from 6.92 % to 13.84 % did not significantly decrease the rate of scour. Furthermore, the rate of scour was not measurable for $\% A_r = 13.84$. Thus, <u>for the conditions tested</u>, the amount of armorplate needed to control scour should not exceed 10 % of the volume of the pre-shaped basin. However, it is to be emphasized that a very low rate of scour can be obtained with a relatively small amount of armorplate if it has the proper size and size gradation.

To stabilize the pre-shaped basin it is necessary to use not only armorplate of uniform gradation, but also to know the criteria for selecting its minimum and maximum diameter. As demonstrated in these and other studies on armorplate (4) the minimum diameter should be equal to the maximum diameter of the bed material in which the pre-shaped basin is formed. By definition the maximum diameter should be of sufficient size to resist erosion at the peak flow. No quantitative studies have been made on determining criteria for maximum diameter. Peterka (14) in his study of armorplate performance in a stilling basin reports that the maximum diameter can be estimated from the formula

$$V_b = 2.57 \sqrt{d} \qquad (16)$$

in which V_b is the bottom velocity of flow in the channel, and d is the maximum diameter of the sediment particle in inches that will resist erosion. In this equation the specific gravity of the particle is 2.65 and shape factor 0.73.

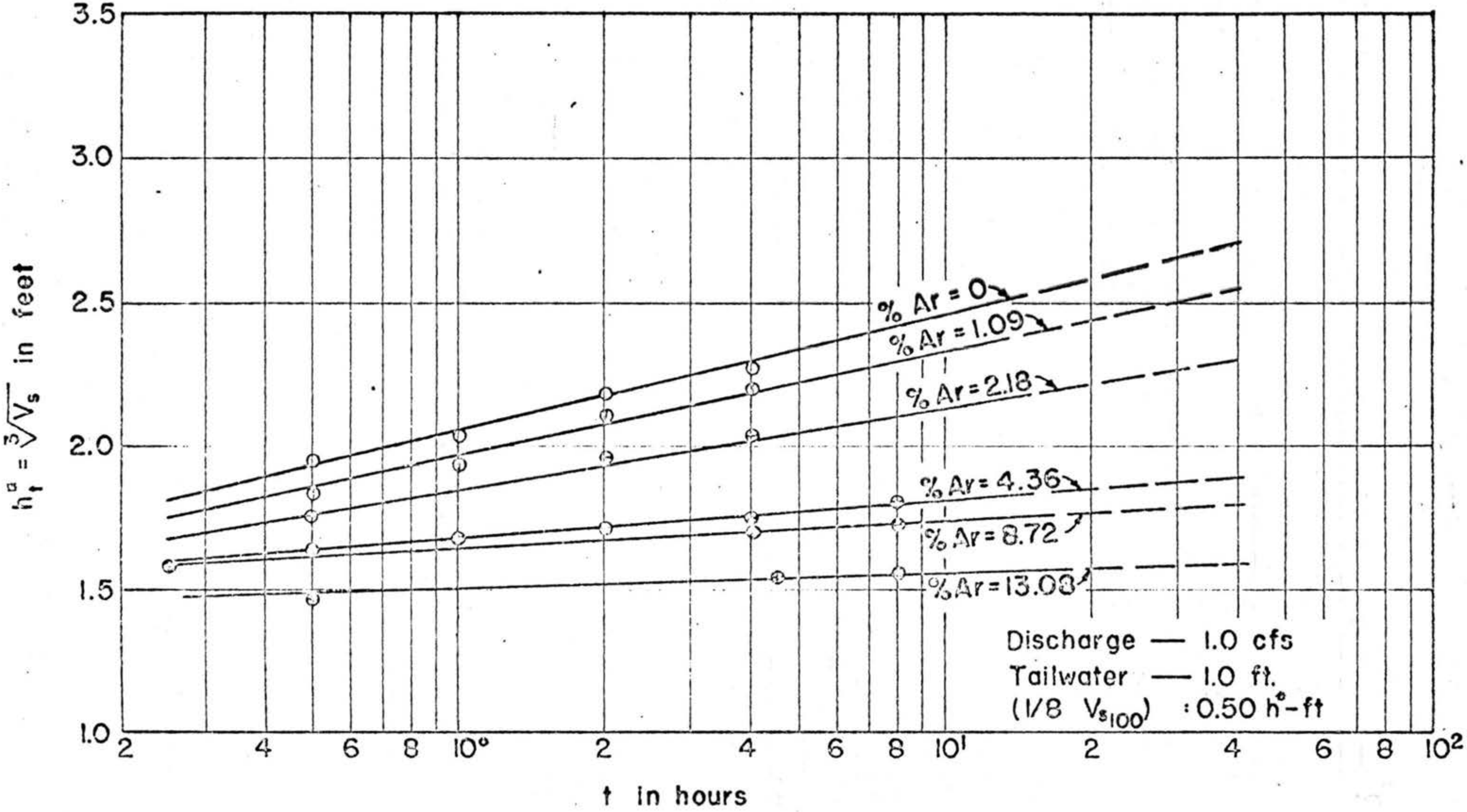

Fig. 17 Rate of scour as a function of quantity of armorplate for pre-shaped stilling basin of given size

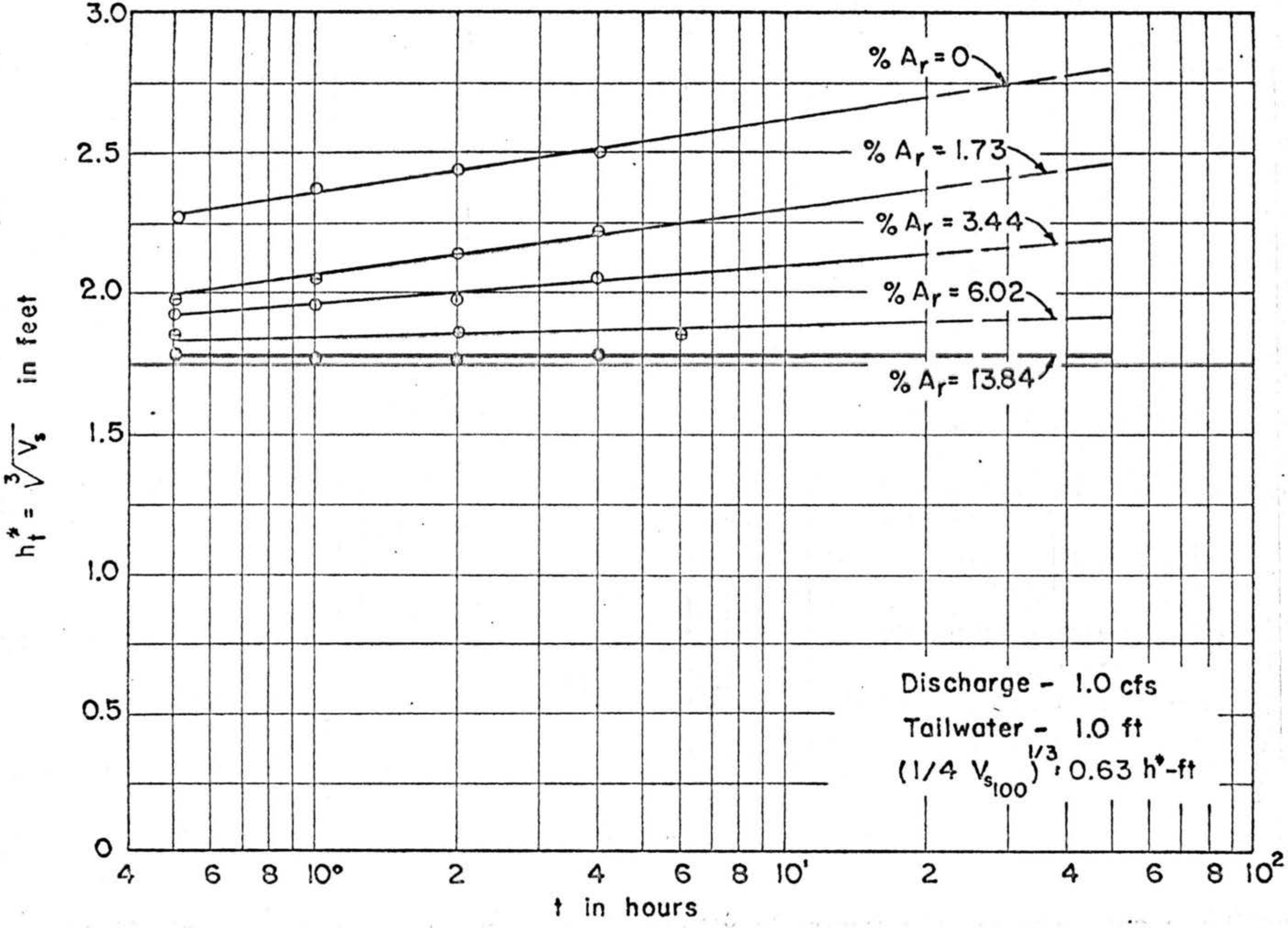

Fig. 18 Rate of scour as a function of quantity of armorplate for pre-shaped stilling basin of given size.

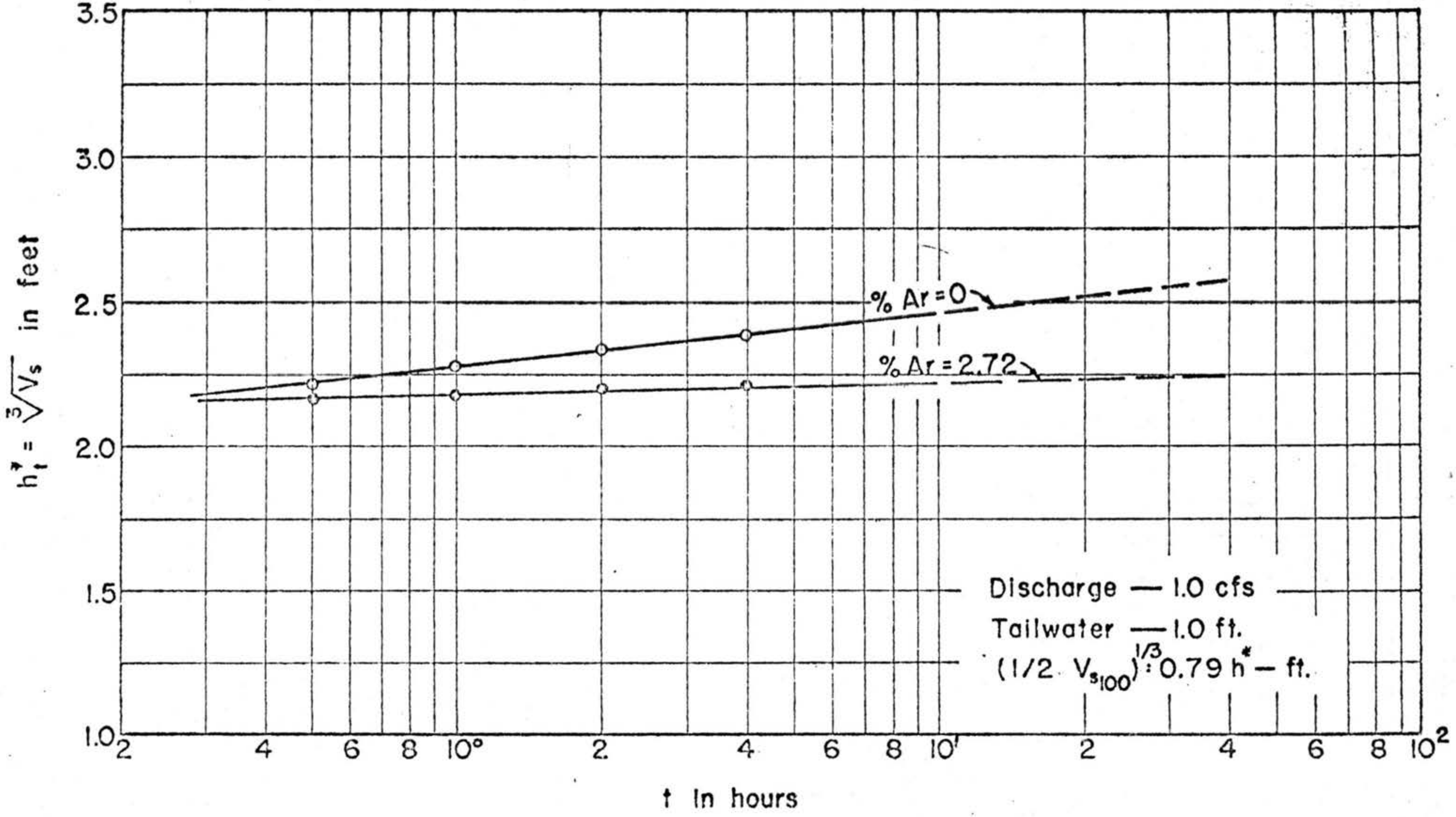

Fig. 19 Rate of scour as a function of quantity of armorplate for pre-shaped stilling basin of given size

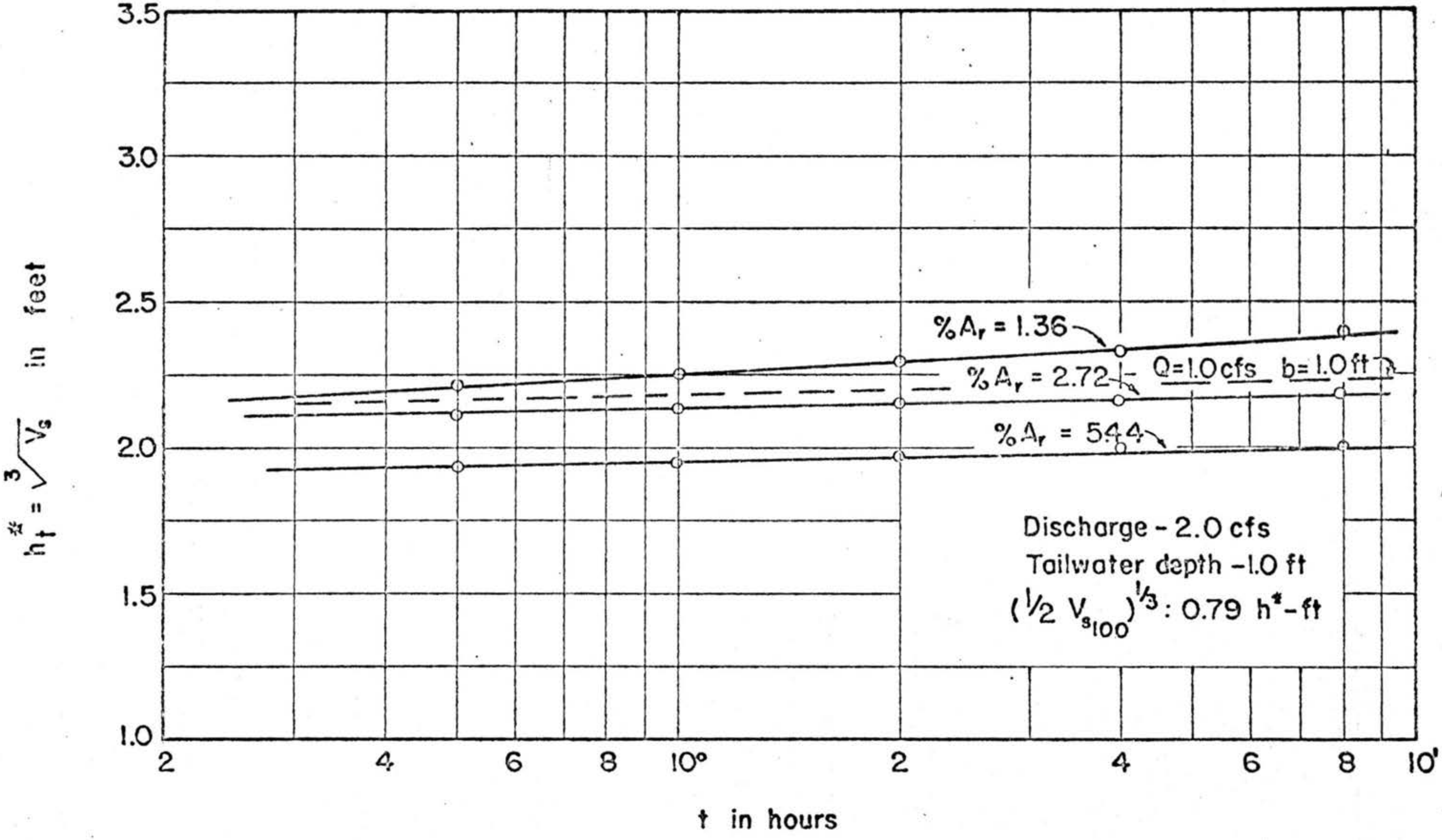

Fig. 20 Rate of scour as a function of quantity of armorplate for pre-shaped stilling basin of given size.

The use of Eq. 16 to calculate the maximum diameter of armorplate depends upon establishing a relationship between the maximum velocity of that portion of the diffused jet moving along the surface of the armorplated basin and V_b. Such a relationship has not been as yet established, but is currently under experimental investigation (15).

2. Influence of Boundary Geometry on Scour

Any consideration of the effects of geometry on scour in the pre-shaped basin must start with the simplest boundary form. A channel that is rectangular in cross section is of this type. A further simplification was to keep the sides rigid. The study of effect of channel width B on the rate of scour was the next logical step in the analysis of the various aspects of the scour phenomena. This study concluded with a qualitative investigation of scour and scour control in an alluvial channel of trapezoidal cross-section and an initial bottom width of 5 ft.

From an analysis of experimental data given in Table 8, in Appendix C, the effect of the variation in channel width B on the rate of scour is determined. For example, for a discharge of 1.0 cfs and a tailwater depth of 1.0 ft, Fig. 21 shows that scour increases with an increase in channel width. Fig. 22 shows that, as expected, as the discharge is increased the rate of scour is increased and that the effect of channel width is as shown in Fig. 21. Fig. 23 shows that the effect of channel width is still the same for an increase of tailwater depth only.

The protective effect of armorplate in alluvial channels is illustrated in Figs. 24 and 25. The plan view of the channel in Fig. 24a shows the flow pattern and action of the water on the alluvial banks. Fig. 24b shows the extent of scour on the right bank at time $t = 4$ hrs. A comparison of Fig. 24 with Fig. 12a illustrates the extent of scour in the unprotected channel. The alluvial channel with armorplated channel and banks prior to testing is illustrated by Fig. 12a. The degree of protection provided by the armorplate is shown in Fig. 25 for the same discharge ($Q = 1$ cfs) and tailwater depth ($b = 1.0$ ft) as for Fig. 24. The time of scour for Fig. 25 is twice that of Fig. 24 or, in other words, $t = 8$ hrs.

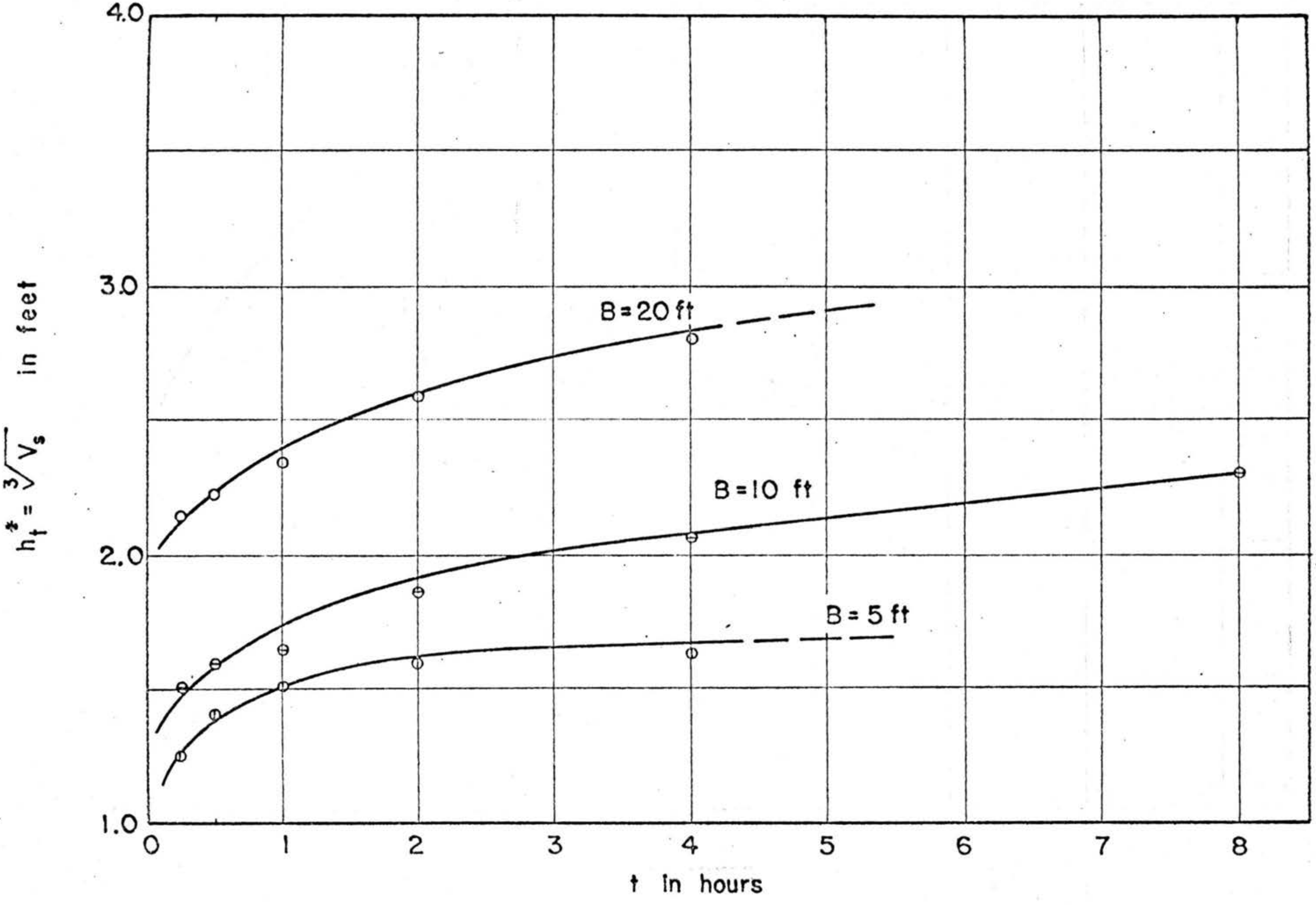

Fig. 21 Rate of change of scour volume with time for a discharge of 1.0 cfs and a tailwater depth of 1.0 ft.

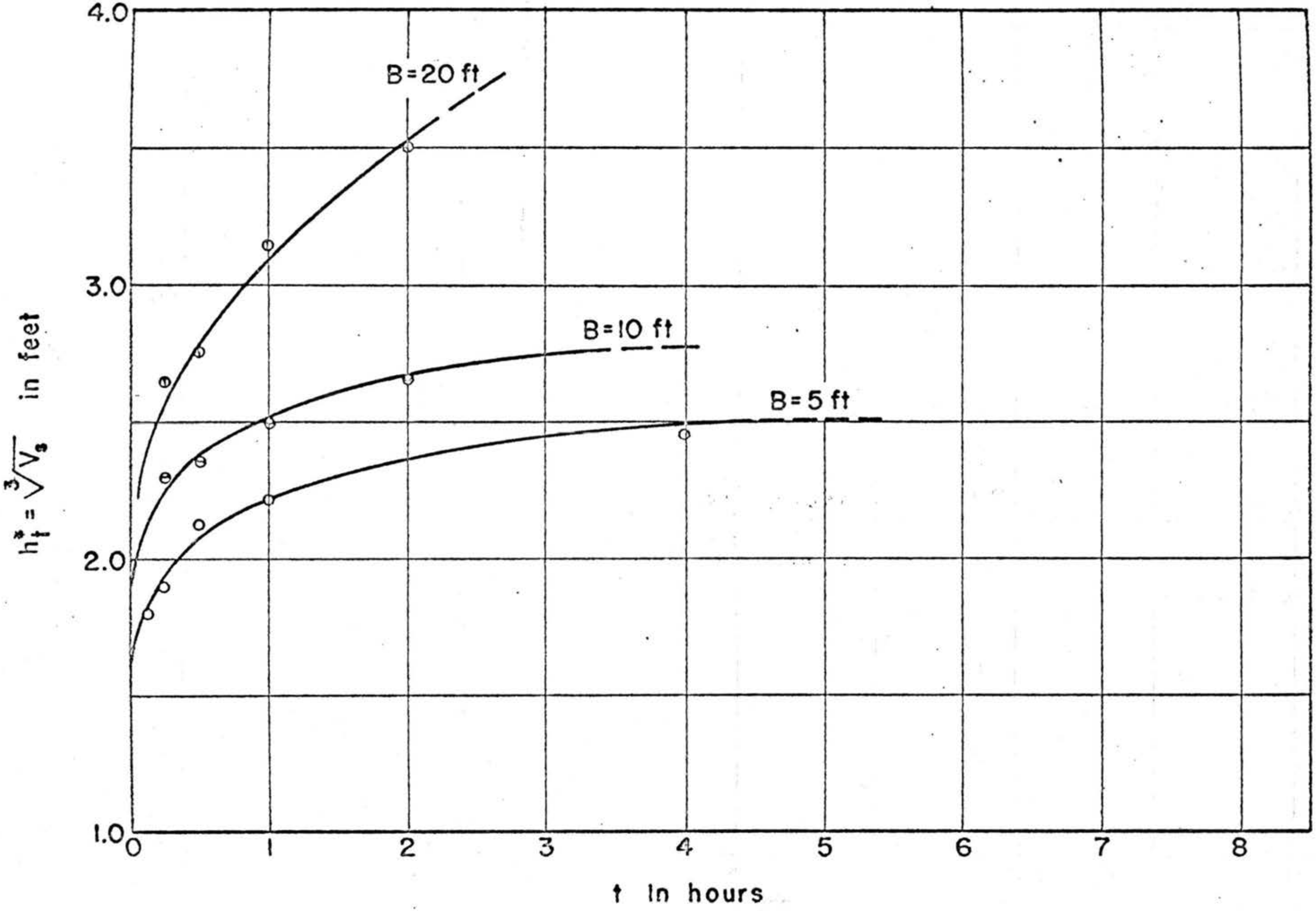

Fig. 22 Rate of change of scour volume with time for a discharge of 2.0 cfs and a tailwater depth of 1.0 ft.

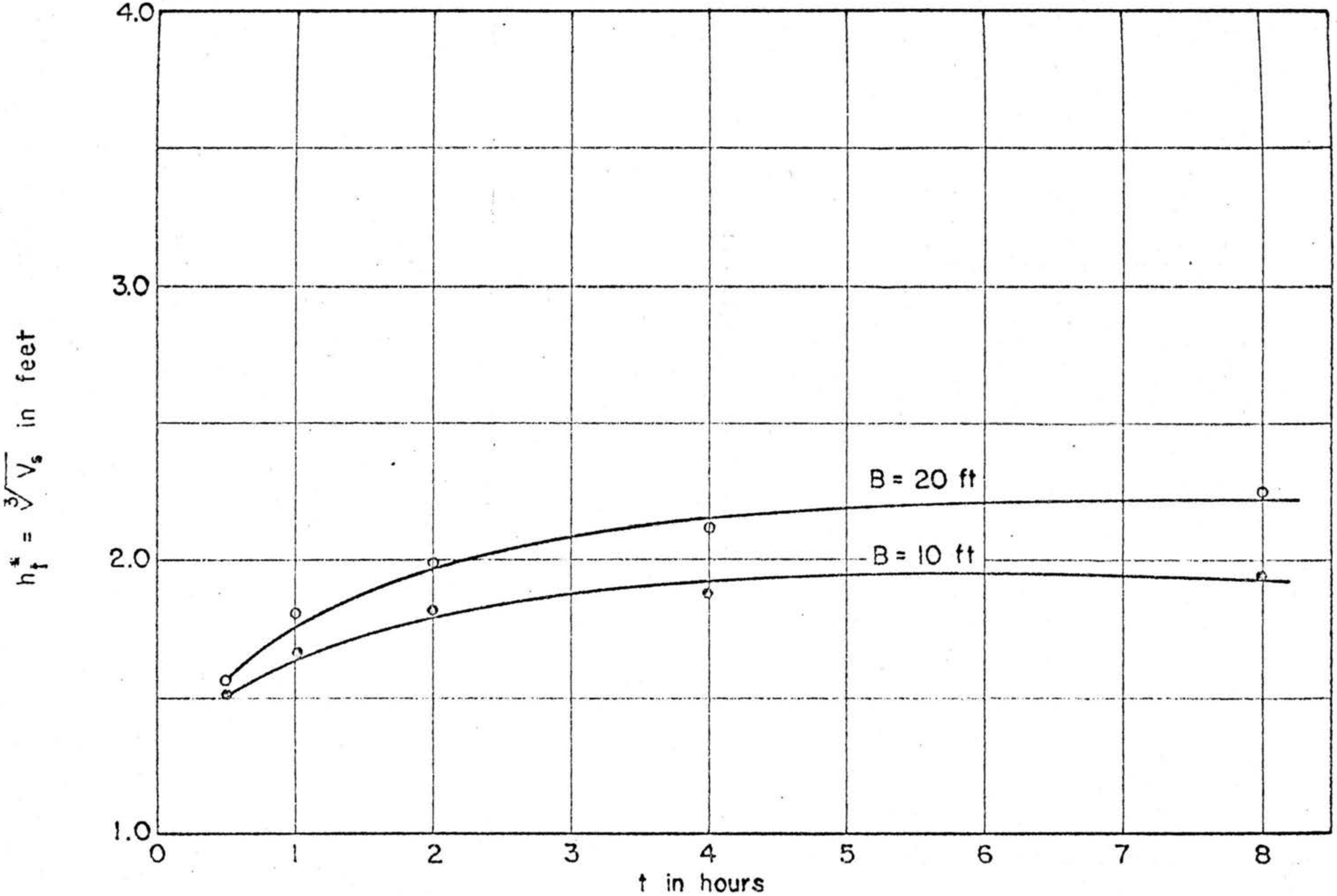

Fig. 23 Rate of change of scour volume with time for a discharge of 1.0 cfs and a tailwater depth of 1.5 ft

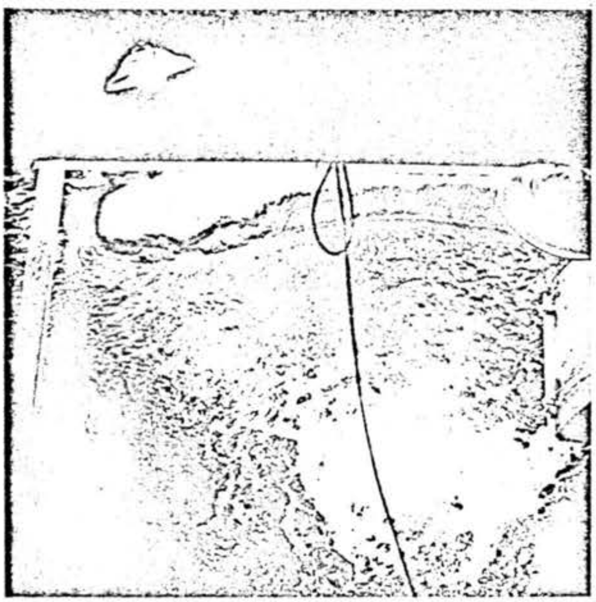

a. Unprotected alluvial banks subjected to localized scour

b. Plan view of eroded channel bed and banks

Fig. 24 - Effect of localized scour on an unprotected alluvial channel for a discharge of 1 cfs and a tailwater depth of 1.0 ft

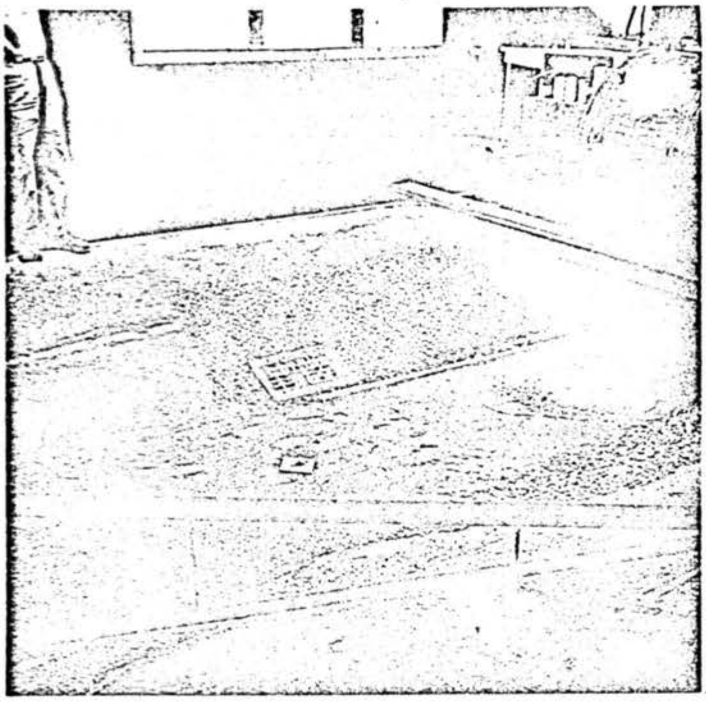

a. View from left bank of extent of scour of an armorplated, alluvial channel

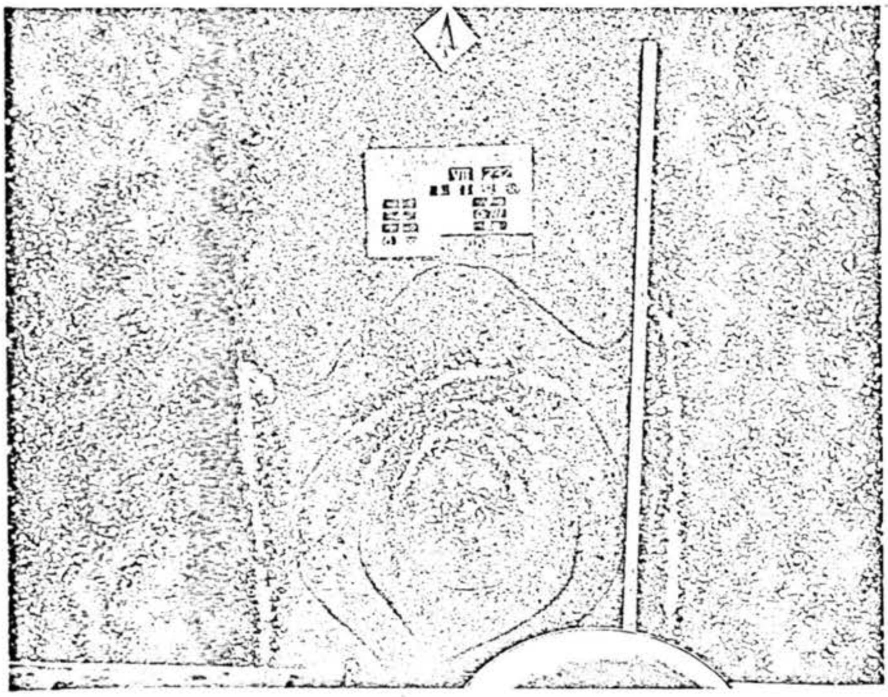

b. Plan view of extent of scour of an armor-plated, alluvial channel

Fig. 25 - Scour control in an alluvial channel by use of an armorplated basin and armorplating of banks for discharge of 1.0 cfs and tailwater depth of 1.0 ft

PART III.
IMPLICATION OF THE EXPERIMENTAL RESULTS

A. SCOUR PHENOMENON

An evaluation of the phenomenon of localized scour involving flow from a cantilevered culvert can best be made by application of Eqs. 1 and 7 to the experimental data. Eq. 1 was developed by Iwagaki (7) in his theoretical analysis of the mechanics of scour by a three-dimensional jet for the case of the inclined jet issuing from a non-submerged outlet. Dimensional reasoning was applied to the selected primary variables to obtain Eq. 7. Inferences obtained by the application of these equations will now be discussed.

Figure 26 illustrates the application of Eq. 1 to scour data (See Table 9, Appendix C) obtained in the ten-foot flume. Because of the apparent generality in the scour pattern developed in the bed of each of the rectangular flumes, this figure is representative of similar data obtained in either of the other flumes.

The figure, in dimensionless terms, shows that there are apparently three regimes of the scour development. These regimes are associated with (a) maximum jet deflection, (b) minimum jet deflection, which are identified by Rouse (1), and (c) a final condition of scour.

Significantly, the regimes shift from maximum jet deflection (curves with flatter slopes) to minimum jet deflection at approximately the same time as determined by Rouse (1) for the two-dimensional case.

Scour data besides indicating several regimes of flow, also indicated that there was an apparent effect of change in channel width on the rate of scour. Such effect is illustrated by Fig. 27, which is based on a relationship of the form expressed by Eq. 7. Data for Fig. 27 is given in Table 10, Appendix C.

The inference made from Fig. 27 is that the increase in scour with an increase in channel width is due in part to the standing eddy which develops

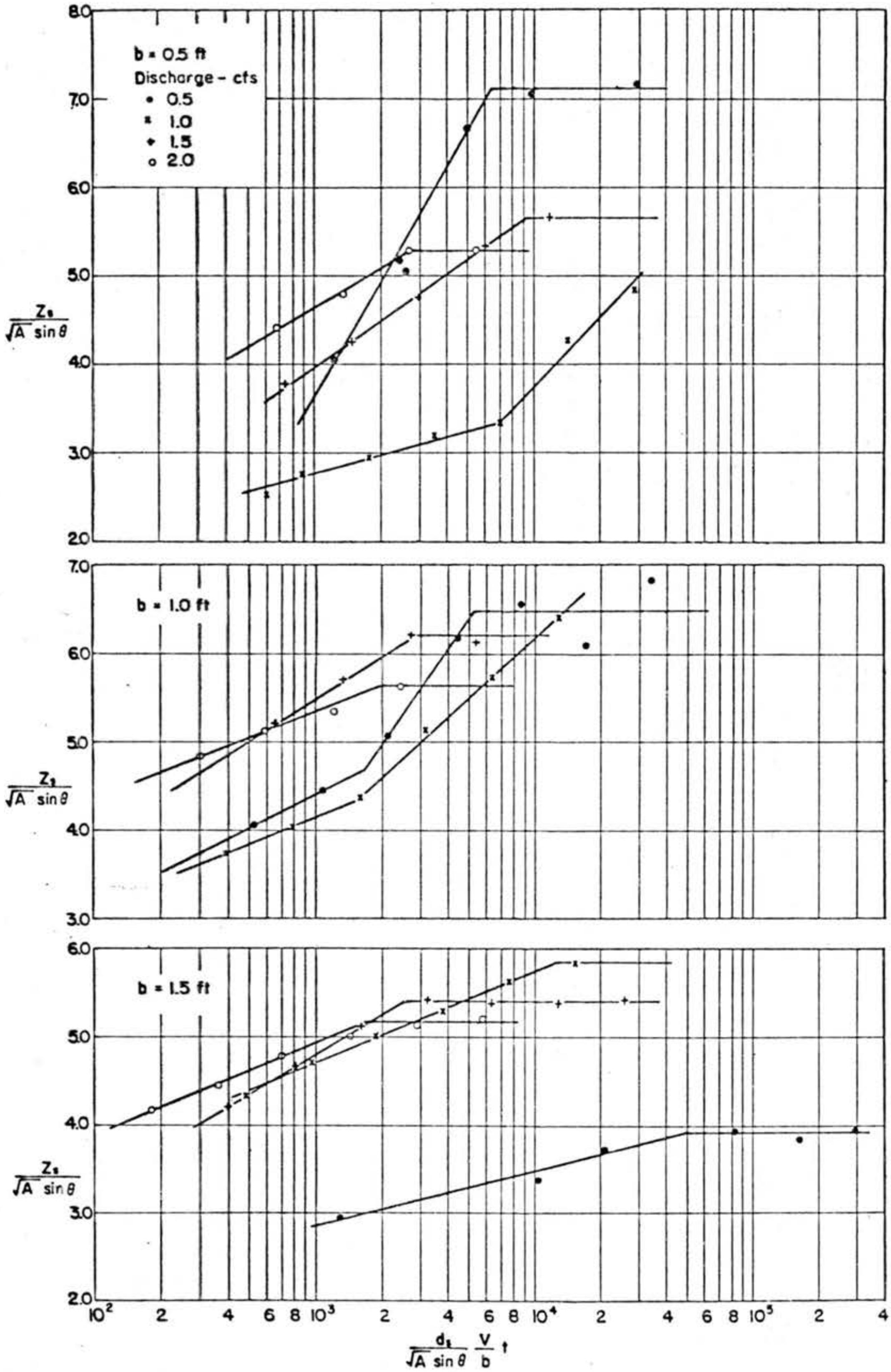

Fig. 26 Variations of $\frac{Z_s}{\sqrt{A}\sin\theta}$ with $\frac{d_s}{\sqrt{A}\sin\theta}\frac{V}{b}t$ for the inclined jet issuing from a non-submerged outlet

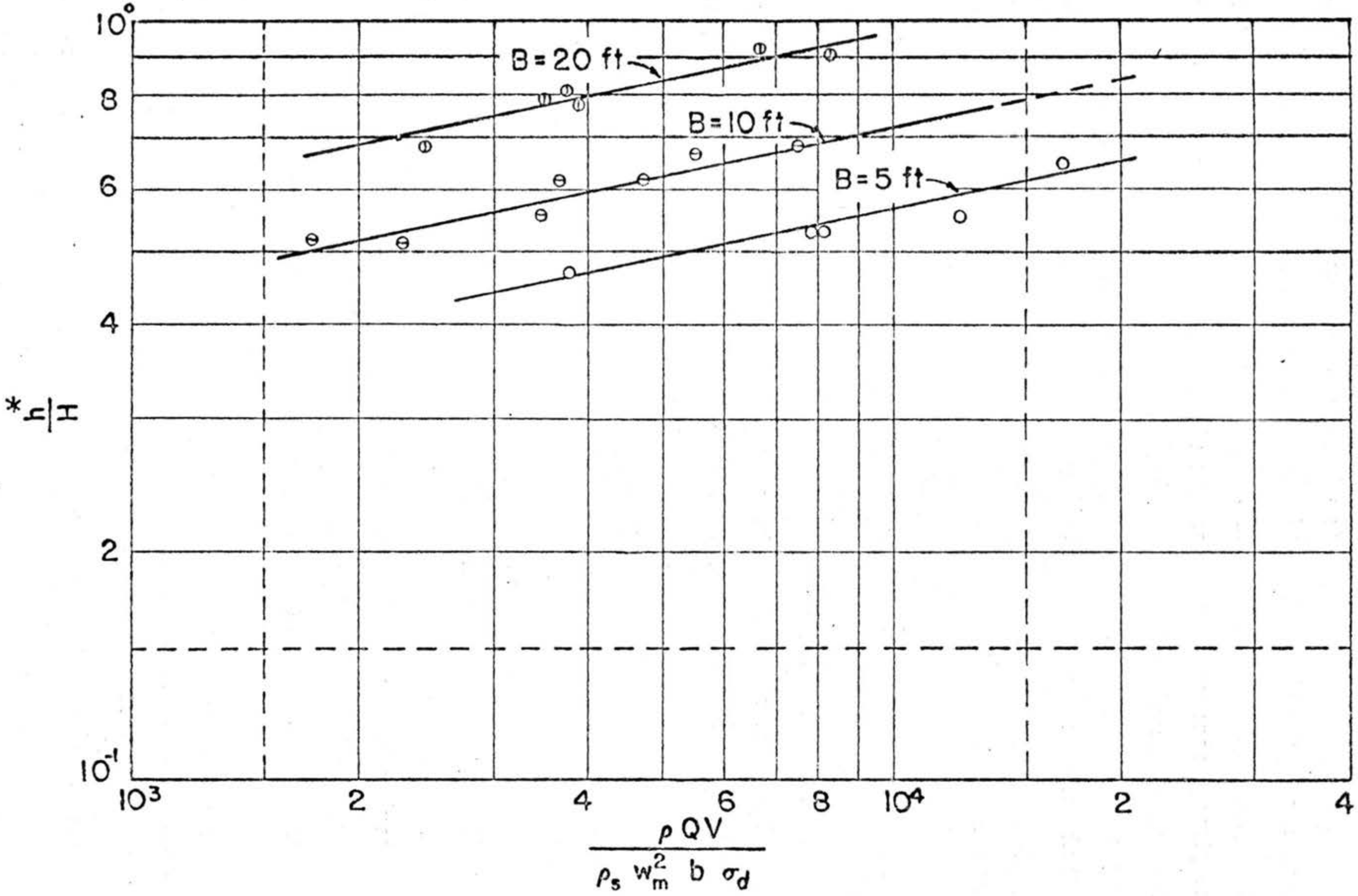

Fig. 27 Generalized plot showing variation of scour parameter with momentum parameter for different widths of channel.

between the impinging jet and the channel sides. As the channel becomes wider, the eddy increases in both magnitude and stability.

Exerting a shear force along the bed surface and with a decreasing pressure gradient normal to the bed, the standing eddy lifts into suspension the dislodged fine sediment particles. As it rotates, the suspended particles are carried into the jet flow and eventually to a point of deposition downstream.

The effect of the stabilized or rigid channel sides is to destroy the energy of the eddy by providing frictional resistance to the rotating fluid. As the channel width is decreased and the sides approach the impinging jet, there is an increase in the energy transfer to small scale turbulence. This small scale turbulence is then dissipated in the form of heat.

Another fundamental factor in the effect of boundary geometry on scour is the slope of the channel bank, which changes the cross section from a rectangular shape to a trapezoidal one. Furthermore, in practical hydraulics, rigid boundaries are seldom, if ever, encountered at culvert outlets, and kinetic energy in one form or another is constantly attacking the channel banks.

B. ARMORPLATE PHENOMENON

In the analysis of scour control by armorplate, consideration is given first to the phenomenon of sediment movement in the vicinity of the impinging jet. The controls of sediment transport by armorplate is discussed. The effect of armorplate on alluvial channel banks concludes this section.

In its broadest sense localized scour caused by cantilevered culvert outflow is a function of jet diffusion before impingement on the alluvial bed and the sediment characteristics of the alluvial bed. For this analysis it is assumed that initially the depth of tailwater is not sufficient to cause appreciable jet diffusion before the jet impinges upon the bed. Since the bed surface represents a boundary through which the jet cannot pass, it must be considered.

At the onset of jet impingement, the sediment particles on the bed surface will move under the shearing action of the deflected jet. The movement of sediment requires the transfer of energy to the sediment particles.

To stabilize an alluvial bank, it is necessary that those flow characteristics causing its erosion be determined. Keeping the channel width constant, a study was made of the flow phenomenon causing disintegration of an alluvial bank.

After flow conditions had been established, it was noted that bank disintegration was due almost entirely to the constant attack on the bank by the waves emanating from the stilling pool area. The impact of the wave on the bank dislodges the fine soil particles, which are carried away by the receding or reflected wave as suspended material. This suspended material is carried into the main stream flow by the action of the standing eddy between the bank and the center of the stilling pool. As the soil particles are removed, sloughing of the banks occurs under the action of gravity and wave forces, and the exposed raw bank provides a fresh source of the fine soil particles. As the banks erode, the stilling area increases in diameter. There is a decrease in the amplitude of the waves reaching the bank, and an increase in size of the standing eddy. The velocity of the flow immediately adjacent to the bed surface is now analyzed to determine the effect of sediment particles in the dissipation of energy of flow.

Each sediment particle acts as an element of form resistance to the surrounding flow. The flow striking a given particle is divided and accelerated around the particle. For example, consider a large sediment particle resting on a bed of fine material. In this condition the accelerated flow around the particle scours away the fine material supporting it, while at the same time the drag force pushes the particle into the scoured area. Eventually such a particle is buried in the bed of the finer material surrounding it. Thus, where there is a gradation of sediment particles, selective sorting of particles occur and the bottom of the scour hole becomes lined with a progressively coarser material.

In armorplating, the significant factor is that each sediment particle is protected by the smaller particles underneath so that it does not become undermined. More specifically, for the portion of flow entering the alluvial bed through the interstices of the particles, the fluid-filaments are continuously diverted and divided by the supporting sediment particles. As the flow is diffused its energy is dissipated by viscous shear. The diffused flow eventually enters the alluvial bed as seepage flow at a low velocity and an appreciable pressure gradient.

The interstices between the larger particles permit flow entry, but prevent or retard the passage of smaller particles outward into the higher-velocity flow. The support and counter-support and eddy generation in the mean flow with resulting small-scale turbulence is designated as "Armorplating", by graded gravel.

In alluvial channels protection of the bank against scour is of prime importance in the design of a stable bank. Since wave action is the significant factor causing erosion, armorplate not only must be of uniform gradation, but also must be of sufficient size to withstand the impact force of the wave. The quantity needed is also important.

Hallmark (4) observed that the effect of selective sorting action on the bed material would cause it to develop an armorplate of coarse particles at the bottom and along the basin surface downstream of the point of jet impingement. The thickness of the sorted material was approximately three times the largest size of particle at a given point. It was also observed that the effect of selective sorting action on armorplate material of a given maximum size added to the scoured basin, was to redistribute the material over the surface of the basin to a depth equal the maximum size of the armorplate.

For the qualitative tests, armorplating of the alluvial channel banks so that there was an effective control of scour was achieved as follows:

a. By using armorplate material having a uniform gradation from the maximum size of the bank sediment to particles one inch in diameter,

b. By artificially paving the slope of the bank from channel bottom to the top of the freeboard to a depth approximately equal to three times the maximum diameter of material used, that is, to a depth of three inches, and

c. By using a freeboard of armorplate equal to twice the anticipated maximum wave height.

C. SUMMARY

Erosion below cantilevered culvert outlet structures often occurs when runoff from wide areas is concentrated in a single culvert. Erosion control at culvert outlets depends upon dissipation of kinetic energy in the horizontal direction, vertical direction, or combination of both directions. Dissipation of kinetic energy may be accomplished to a great extent in the vertical direction by use of a pre-shaped armorplated stilling basin.

Systematic experiments upon the rate of scour and scour control in an alluvial bed by a jet of freely falling clear water have indicated the following essential facts:

a. There are apparently three regimes of scour development: (1) a maximum jet deflection, (2) minimum jet deflection, and (3) a final condition of scour.

b. A graded gravel has proven to be extremely effective as protection against erosion from high-velocity flow and waves. It is important, however, that the gravel be graded so that the larger size material is protected from undermining by the smaller size material underneath. The maximum size of the gravel material must be sufficient to resist movement from the stilling basin.

c. Wave action and standing eddies at culvert outlets are two factors causing erosion of alluvial banks. An increase in channel width near the culvert outlet causes an increase in the rate of scour.

d. Armorplate protection must be provided to the channel banks within the vicinity of the stilling basin to provide protection from waves and eddies.

Under laboratory test conditions -- limited boundary geometry, flow, fluid and sediment characteristics -- the design criteria for armorplated, pre-shaped stilling basin in terms of h_t^* are given by

$$d_T = 2.38\, h_t^*$$

$$h = 0.5\, h_t^*$$

$$d_B = 0.65\, h_t^*$$

$$X = X_B + 0.61\, h_t^*$$

$$V_{ar} = 0.423\, h_t^{*2}\, \epsilon$$ [1/]

in which

h_t^* is the cube root of the volume of scour $(V_{s_t})^{1/3}$ developed by a jet of clear water in t hours of scouring action,

X_B is the horizontal distance from the end of the culvert to the point of impingement of the jet on the tailwater surface, and

ϵ is the equivalent uniform thickness of the layer of graded gravel having this volume which would cover the surface of the pre-shaped basin.

D. ADDITIONAL STUDY REQUIRED

Practical results of importance to highway engineers will result from fundamental research investigations regarding the dynamics of the kinetic energy of a jet of fluid and its proper control. In general, in order to obtain improved design criteria for stilling basins at culvert outlets, it will be necessary to study and understand the mechanics of scour and energy dissipation

---

1/ Eq. 31 of Appendix B.

more thoroughly. Furthermore, in conjunction with the analytical studies certain experimental investigations should be conducted to evaluate the basic aspects of scour phenomenon. The experimental studies should be guided by the present knowledge of fundamental fluid mechanics.

Although research advances made in the last few years have been very fruitful, there is still need for investigations such as: (1) rate of scour of various types of natural bed materials -- cohesive and non-cohesive -- under different hydraulic conditions, and (2) effect on the rate of scour of the degree of overlap of material size between armorplate and bed material. These and other scour phenomena could be studied by means of several small scale, inexpensive models. Other significant studies applicable to small scale models include:

a. The determination of the maximum size of armorplate for varied flow conditions that would resist erosion.

b. The effect of height of fall of the jet on the scour phenomenon.

Also, a research study is needed using results previously obtained on low cost armorplating scour control for culverts laid on the natural grade of the stream bed.

Another study of interest to the design engineer would be the influence of the rising and falling flood hydrograph -- unsteady flow -- on the armorplated, pre-shaped stilling basin. Preliminary studies have indicated that slight modifications would be needed in the given design criteria. This can be accomplished by a systematic study using a large-scale, three-dimensional model.

In keeping with these fundamental studies it is axiomatic that control of erosion of highway embankments along right-of-ways should be considered also. Recent studies indicate that, by combining the tractive force concepts and Blench's (21) regime theory it may be possible to develop a theoretical procedure for controlling scour in open channels. Such a theory should be verified by experiment.

REFERENCES

1. Rouse, Hunter. Criteria for similarity in the transportation of sediment. Proc. Hyd. Conf., Univ. of Iowa Studies in Engineering, Bulletin 20, 1940. pp. 33-49.

2. Doddiah, Doddiah. Comparison of scour caused by hollow and solid jets of water. Master's thesis, Colorado A and M College, 1950.

3. Thomas, Robert K. Scour in a gravel bed. Master's thesis, Colorado A and M College, 1953.

4. Hallmark, Dasel E. Scour at the base of a free overfall. Master's thesis, Colorado A and M College, 1955.

5. Albertson, Maurice L., and Smith, George L. Principles of energy dissipation in erosion-control structures. Dept. of Civil Eng. Prepared for joint ARS-SCS Irrigation-Drainage Conf., Colorado Springs, Colo., Jan. 14-17, 1957.

6. Duckstein, Lucien; Iwagaki, Yuichi; Smith, George L., and Albertson, Maurice L. Analytical study of the mechanics of scour for two-dimensional jet. Colorado State University Research Foundation, Report No. CER60GLS12.

7. Iwagaki, Yuichi, Smith, George L., and Albertson, Maurice L. Analytical study of the mechanics of scour for three-dimensional jet. Colorado State University Research Foundation, Report No. CER60GLS9.

8. Schlichting, H., and Truckenbrodt, E. Die Strömung an einer angelbasenen rotierenden scheibe. ZAMM, Band 32. Heft 4/5. April/Mai. 1952. S. 97-111.

9. Truckenbrodt, E. Die trubulent Strömung an einer angelblasenen rotierenden scheibe. ZAMM, Band 34. Heft 4/5. April/Mai. 1954. S. 150-162.

10. Albertson, M. L.; Dia, Y.B.; Jensen, R. A., and Rouse, H. Diffusion of submerged jets. Trans. ASCE. Vol. 115, 1950. pp. 639-697.

11. Brown, C. B., and Laursen, E. M. Sediment transportation (In Hyd. Conf., Fourth, 1949, Iowa City, Iowa. Proc. Ed. by Hunter Rouse, New York, John Wiley and Sons, 1950, p. 769-857).

12. Smith, George L. An analysis of scour below culvert outlets. Master's thesis, Colorado State University, 1957.

13. Peterka, A. J. Stilling basin performance studies an aid in determining riprap sizes. Hyd. Lab. Report No. HYD 409, Bureau of Reclamation, February 23, 1956.

14. Poreh, M. Flow characteristics of a circular submerged jet impinging normally on a smooth boundary. Master's thesis, Colorado State University, 1959.

15. Poreh, M., and Cermak, J. E. Flow characteristics of a circular submerged jet impinging normally on a smooth boundary. Paper prepared for Sixth Annual Conference on Fluid Mechanics, held at the University of Texas, Austin, Texas, September, 1959.

16. Krumbein, W. C., and Pettijohn, F. J. Manual of sedimentary petrography, D. Appleton - Century Co., 1958.

17. Corey, A. T. Influence of shape on the fall velocity of sand grains. Master's thesis, Colorado A and M College, 1949.

18. Cooperative Federal Inter-Agency Project. Methods of analyzing sediment samples. Report No. 4. St. Paul. U.S. Eng. Dist. Sub-office, Hyd. Lab., University of Iowa, 1941. p. 41.

19. Wilde, R. H. Effect of shape on the fall-velocity of gravel-sized particles. Master's thesis, Colorado A and M College, 1952.

20. Schulz, E. F. Effect of shape on the fall velocity of sand particles. Master's thesis, Colorado A and M College, 1954.

21. Blench, T. Regime behavior of canals and rivers. Butterworth's Scientific Publications, London and Toronto, 1957.

APPENDICES

INDEX TO APPENDICES

APPENDIX

A. SEDIMENT PROPERTIES

In the mechanism of localized scour Rouse (1) has demonstrated that the primary characteristic of sediment is the mean fall velocity W_m. Furthermore, the terminal velocity of fall W_s of the sediment particle depends primarily upon the size, shape and specific gravity of the sediment particle and the viscosity of the fluid. Thus, in localized scour the significant sediment properties are specific gravity, size and shape; the primary sediment characteristic is the geometric mean fall velocity W_m. These were determined as follows:

Specific gravity - A study of a representative sample of the sediment under a microscope revealed that about 55 per cent of the sand particles were quartz grains, 45 per cent feldspar, and 5 per cent biotite. Since the average published value for specific gravity of quartz and feldspar is 2.65, this value was adopted as representative of the sediment.

To determine the mean diameter of the alluvial material and armorplate a mechanical analysis was first made of several sediment samples selected at random from the flume, basin or stockpile. From a graphical plot of the particle distribution determined by the mechanical analysis the mean diameter of sediment was obtained.

More specifically, mechanical analysis is the placing of a sediment sample of a given size in a nest of sieves following the Wentworth grade scale and the subsequent shaking of the sieves in a mechanical shaker for five or more minutes. The Wentworth scale is based on a square-root-of-two geometric progression, which is convenient for statistical analysis of sediment particle distribution. For the 250 gram sample of the alluvial material a nest of Tyler sieves - No's 4, 5, 6, 8, 10, 14, 20, 28, 35, 48 , and 65 were used. For the 750 gram sample of the armorplate additional Tyler sieves to those used for the alluvial material included No. 3 and sieves with sieve openings of

13.33 mm (0.525 in.), 18.85 mm (0.742 in.), and 26.67 mm (1.05 in.). Results of the sieve analysis are given in Tables IA, IB, IC, and ID.

By plotting the sieve analysis data of Tables IA, IB, IC, and ID on arithmetic - probability graph paper (Figs. 28, 29, and 30) the mean diameter d_m and the standard deviation σ_d of the particle sizes about the mean diameter was determined. The magnitude of the mean diameter is given by the 50 per cent intercept; the magnitude of the standard deviation is given by the difference between the value of the 84.1 per cent intercept and the value of the 50 per cent intercept, $\sigma_d = d_{84.1} - d_{50} = d_{84.1} - d_m$.

Shape factor -- In sediment analysis the most pertinent shape parameter is sphericity, which Krumbein (16) defines as the ratio of the surface area of a sphere having the same volume as the particle to the surface area of the particle. The primary role of sphericity lies in its effect upon the relative motion between the particle and the fluid. Sphericity tends to decrease with decreasing size of particle. Because of the practical difficulty of measuring sphericity, the particle is usually represented by an ellipsoid of the same proportions, that is, by a ratio of the three principle axes of the particle comparable to the three principle axes of the ellipsoid. Corey (17) defines the ratio of axes as the shape factor sf of the sediment particle, and expresses it as

$$sf = \frac{c}{\sqrt{ab}} \qquad (17)$$

in which

- a is the longest or major axis of the sediment particle,
- b is the intermediate axis of the sediment particle, and
- c is the shortest or minor axis of the sediment particle.

To determine a representative shape factor sf of the bed material, the axes of each of the particles used in determining W_m were measured by means of an ocular micrometer. For the bed material the average shape factor was found to be 0.643 (See Table 2), it being the average of the average values given for each sieve fraction size.

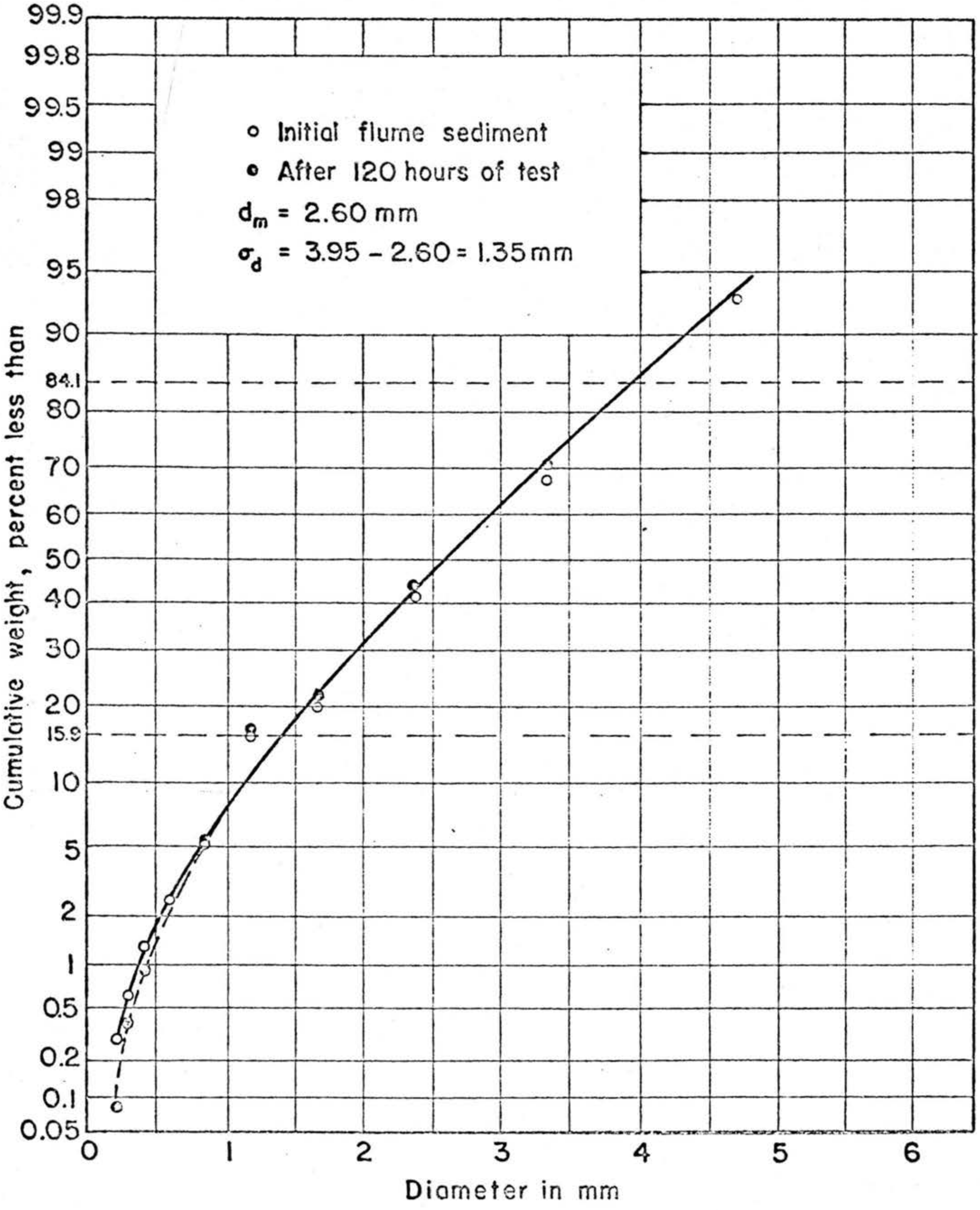

Fig. 28 Probability plot of cumulative frequency of the sieve analysis of the flume sediment.

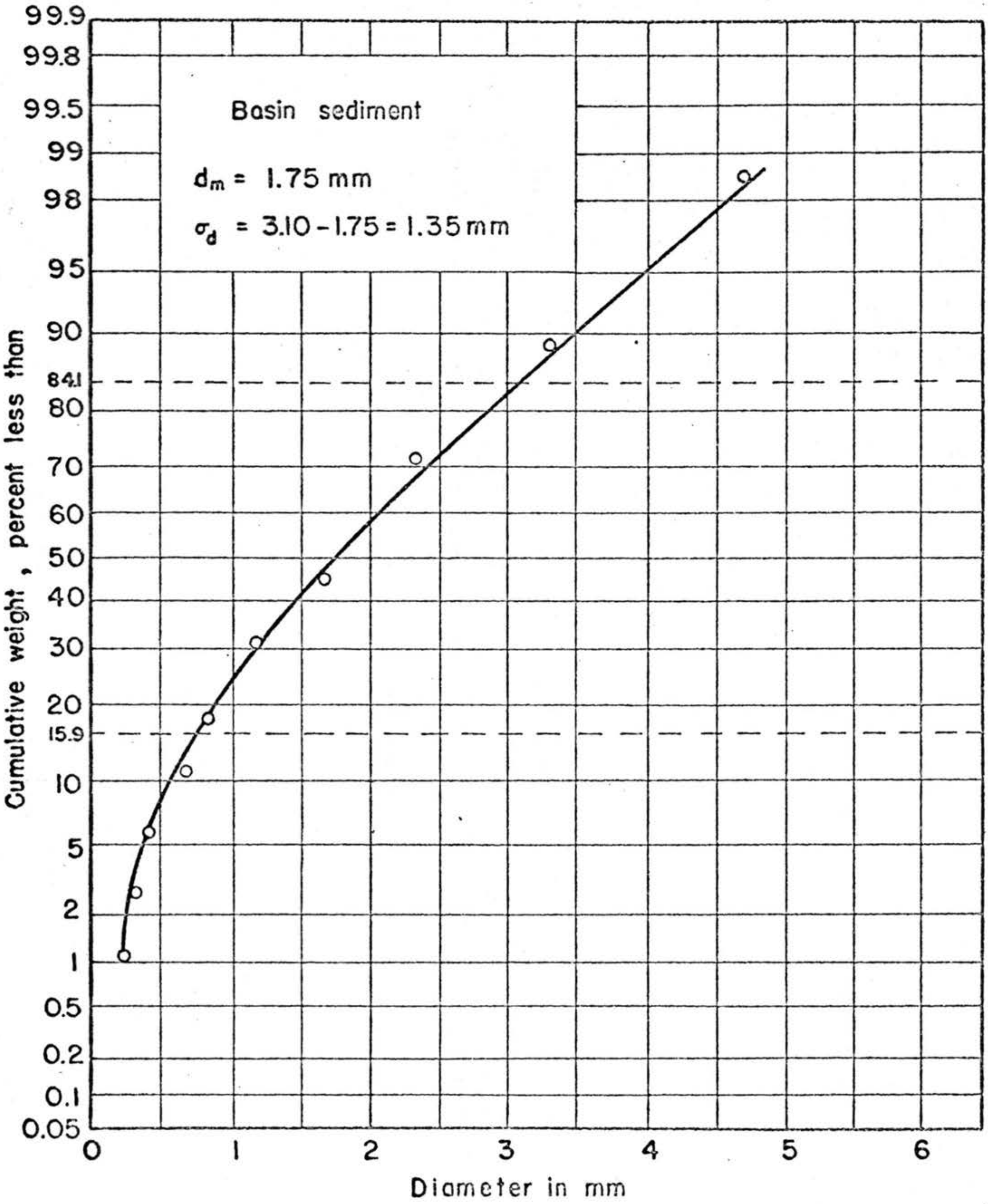

Fig. 29 Probability plot of cumulative frequency of the sieve analysis of the basin sediment.

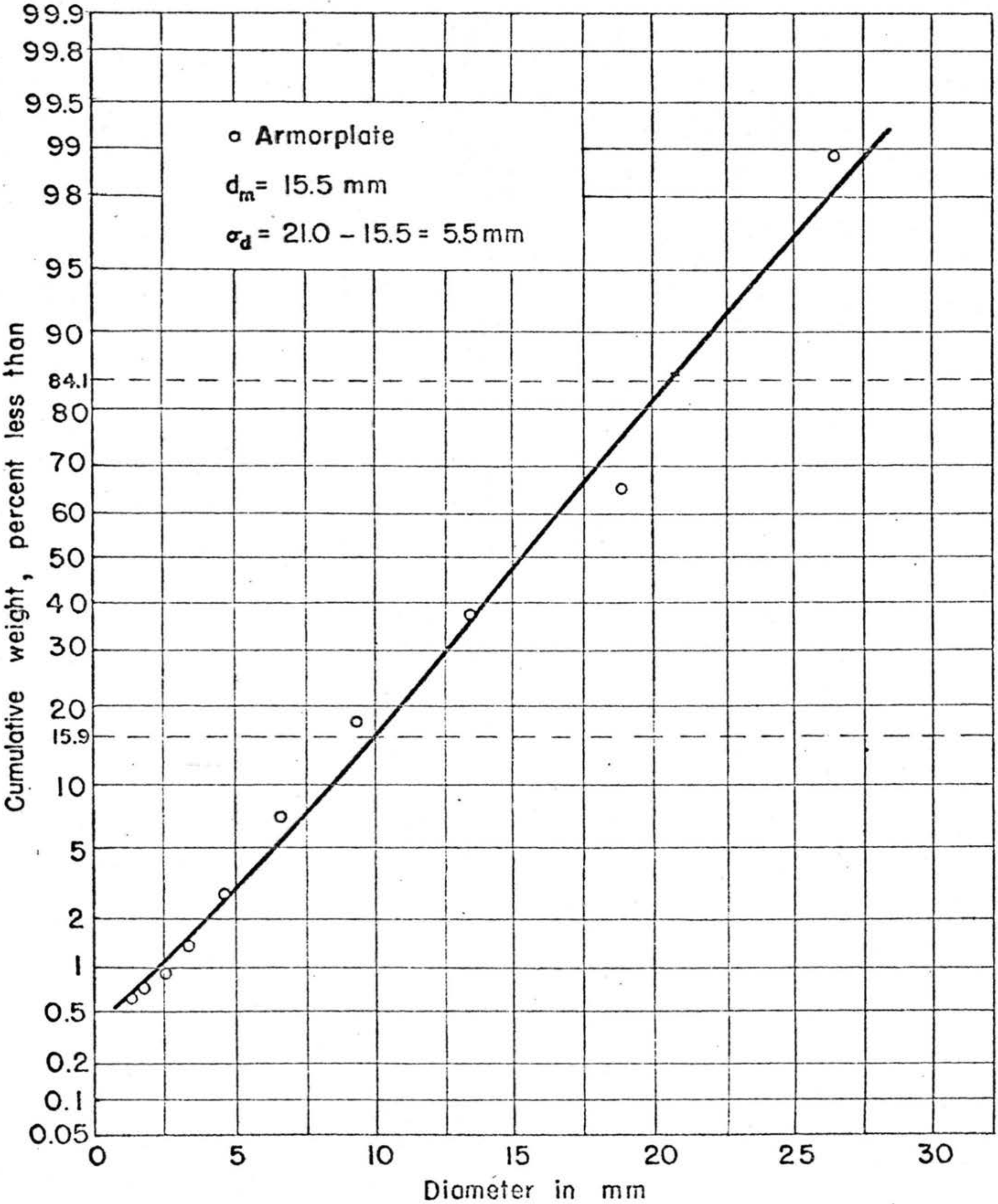

Fig. 30 Probability plot of cumulative frequency of the sieve analysis of the armorplate.

Geometric mean fall velocity -- Although Rouse (1) first established the importance of W_m through a dimensionless relationship showing depth of scour as a function of size and velocity of jet, time and fall velocity of sediment, his study provided no usable information for determining W_m for a given sediment. However, later studies on the effect of shape on the fall velocity of sedimentary particles by Rouse (18), Corey (17), Wilde (19), and Schulz (20) provided both a technique for determining W_m and a relationship between size d_n and W_m. The technique is primarily applicable to sediment less than 4 mm in diameter; establishing a relationship between d_m and W_m is applicable to armorplate.

For the bed material (sand-gravel mixture) W_m was determined by two methods. In the first method ten representative sediment particles were obtained in a random fashion, that is, a representative sample of 250 grams was passed through a mechanical divider until only ten particles remained in each of a pair of divider pans. Each particle was then weighed to the nearest 0.1 milligram. After determining its weight, the terminal rate of fall of each particle was measured in a glass cylinder 10 in. in diameter and 10 ft long.

Acceleration to terminal velocity was found to be established in a distance of 1 ft for the largest size particles. A distance of 18 in. below the water surface was marked on the tank as the starting point for determination of all fall velocities. The fall velocity of each representative particle for each of the sieve sizes was timed independently by two observers over its distance of fall of three feet. The fall velocity W_s of each particle was the average of two or more runs and is given in Table 2. The geometric mean fall velocity of the bed material was found to be 21.30 cm/sec, (See Table 3).

During each test the average temperature of the water over the test section was measured to the nearest 0.1°C. The temperature range was found to be from 18.9°C to 20.0°C.

In the second method, a arithmetic-probability graph (Fig. 31) was drawn with the average fall velocity for each sieve size being plotted against "per cent finer", (Table 3). From this plot for the 50 per cent intercept of the curve the value for W_m was found to be 23.30 cm/sec. The graphical method gives a value of W_m that is approximately nine per cent greater than the measured mean. The measured value of W_m was used in the analysis of experimental data.

W_m in cm/sec for armorplate is obtained from the empirical expression (See Fig. 32).

$$(\text{cm/sec})\ W_m = 12.8\ d_n^{\ 0.500} \tag{18}$$

which is based on the experimental results of Corey, Wilde, Schulz, Smith and Peterka given in Table 4. In general, the investigators, except for Peterka, sought an empirical relationship between W_m and d_n for sediment having different shape factors.

From an examination of Fig. 32 it is noted that V_b approximates W_m, and d approximates d_n for sediment particles having a shape factor of 0.73. This is evident, since Eq. 16 with d in mm may be written as

$$\left(V_b = 12.95\ d_n^{\ 0.5} \right) \tag{19}$$

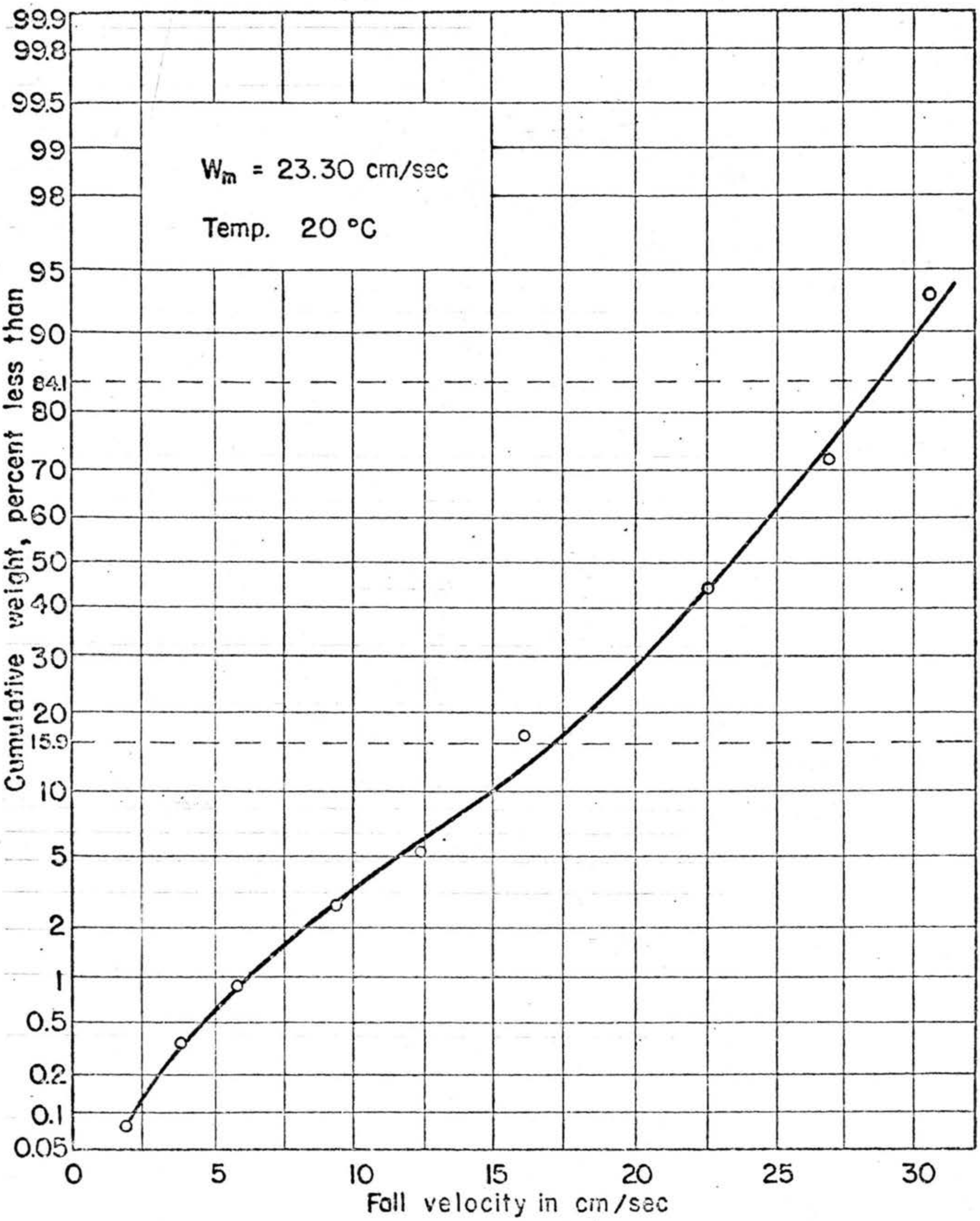

Fig. 31 Probability plot of cumulative frequency of fall velocity of sediment particles representative of alluvial material.

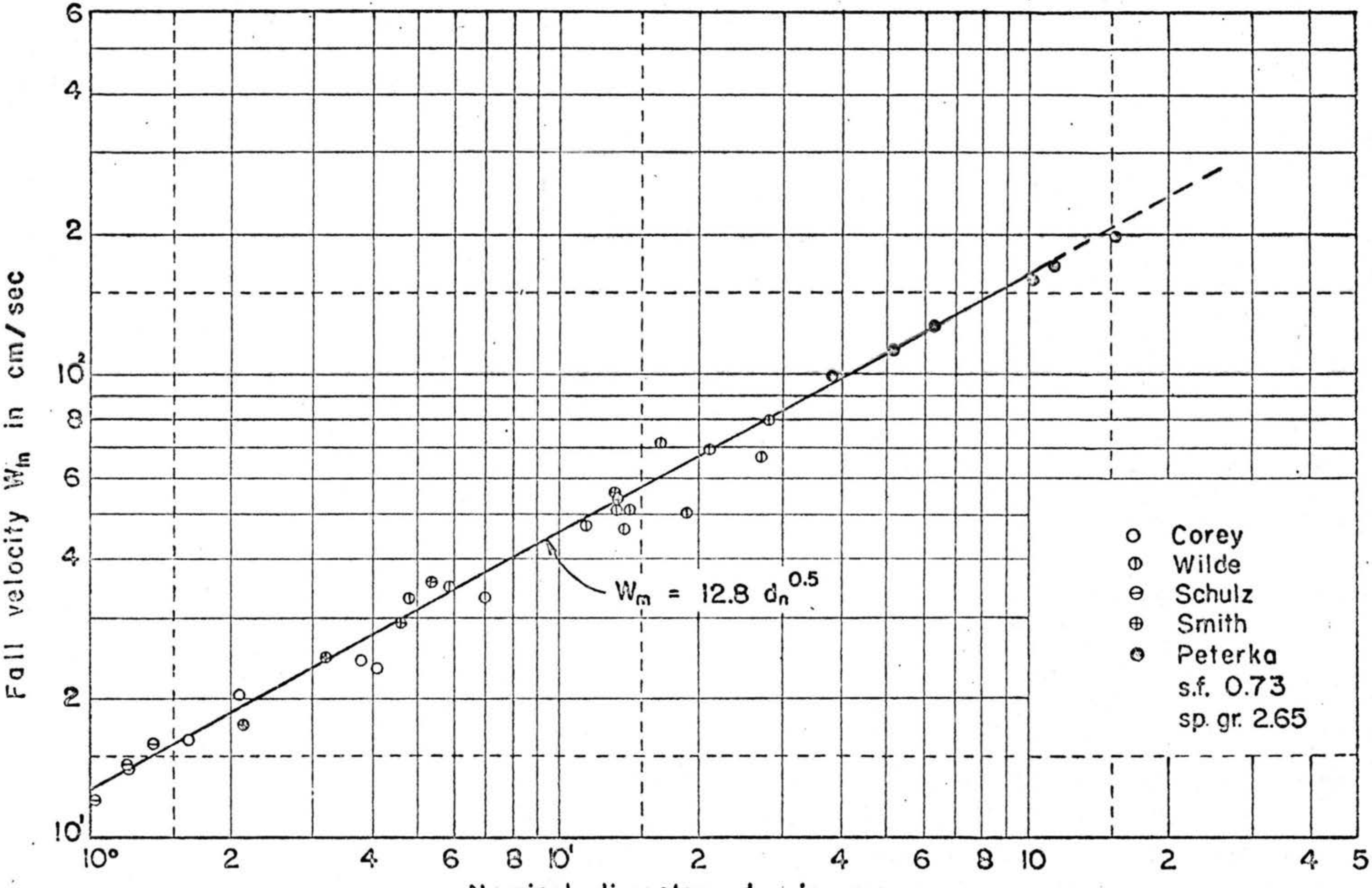

Nominal diameter d_n in mm.

Fig. 32 Terminal fall velocity of sediment particles having a shape factor of 0.73 and a specific gravity of 2.65.

APPENDIX

B. DESIGN CRITERIA FOR A PRE-SHAPED ARMORPLATED STILLING BASIN

A design criteria for a pre-shaped armorplated stilling basin was developed.

a. By relating different profiles of the scour hole to the geometry of a right truncated cone,

b. By giving the geometry of the pre-shaped basin and its orientation relative to the end of the culvert in terms of the cube root of the volume of scour at time t $h_t^* = (V_{s_t})^{1/3}$,

c. By verifying the criteria of item 2 by means of experimental data,

d. By assuming that the armorplate would cover completely the surface of the scour hole and then developing criteria for its thickness and quantity using a procedure similar to that of item 1, and

e. By determining a relationship between thickness, quantity of armorplate and h_t^* .

Theoretical analysis: Pre-shaped basin

It was assumed that the volume V_s of the scour hole could be approximated by the volume of a right truncated cone for the following reasons:

a. The contoured lines indicating water surface in a scour hole (see Fig. 7) approximated concentric circles, and

b. The profile of the hole caused by localized scour at the culvert outlet (see Fig. 33) was of a conical shape.

The equation for a right truncated cone is given by

$$V = \frac{\pi h}{3} (r_1^2 + r_1 r_2 + r_2^2) \tag{20}$$

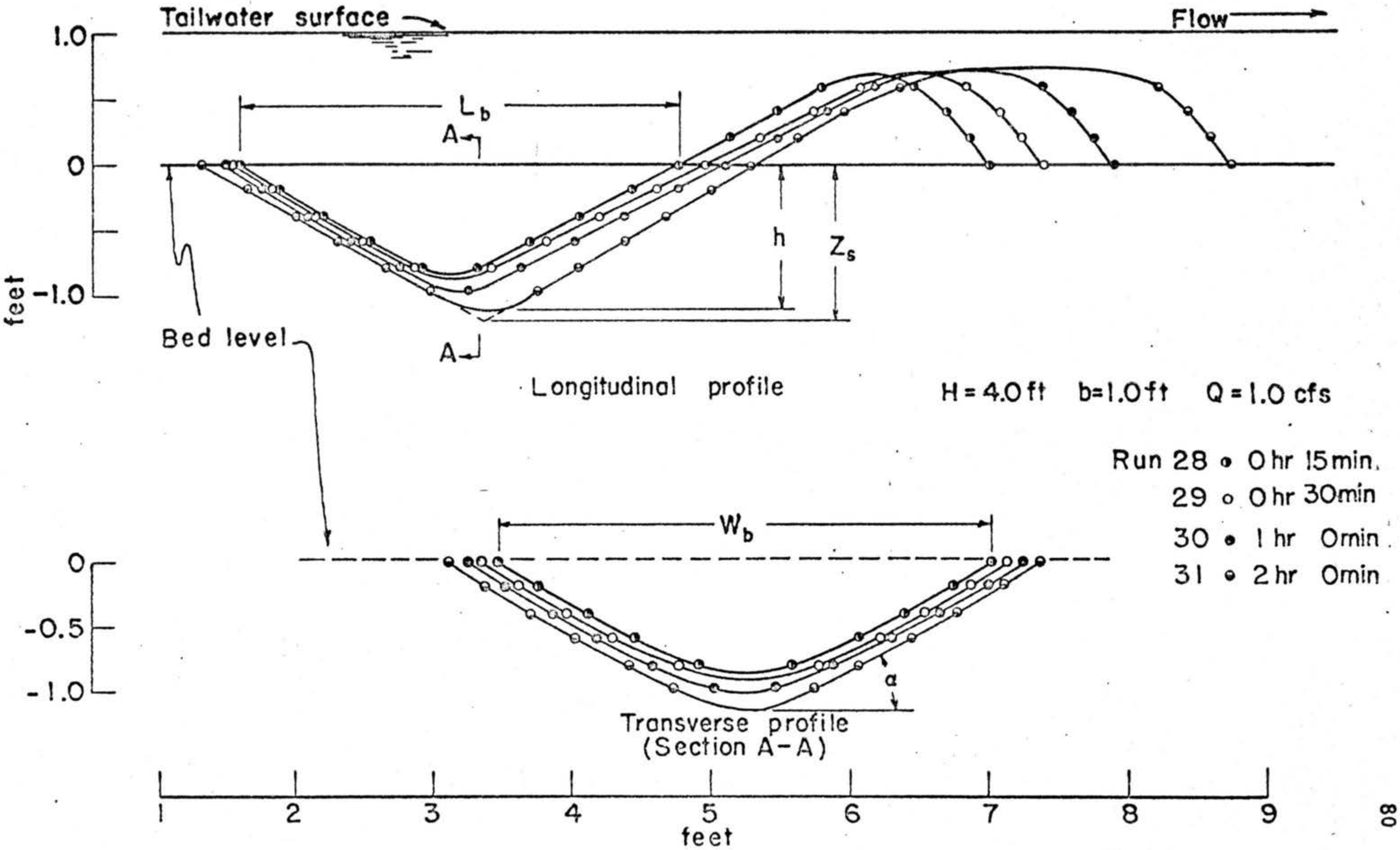

Fig. 33 Typical cross-section of scour hole developed in a simulated stream bed by localized scour showing significant dimensions.

That Eq. 20 is applicable for determining the geometry of a pre-shaped basin was demonstrated by expressing h, r_1 and r_2 in terms of various dimensions of the scour hole and then checking the developed criteria by use of the experimental data given in Tables 5 and 8 .

We can write

$$(r_1^2 + r_1 r_2 + r_2^2)$$

as

$$(r_1 + r_2)^2 - r_1 r_2$$

If we let

$r_1 = \frac{d_T}{2}$ (radius of scour hole at original bed level)

$r_2 = \frac{d_B}{2}$ (radius of scour hole at depth h)

$V = V_{s_t}$ (volume of scour hole at time t)

$h = h_{max}$ = depth of pre-shaped scour hole measured from original bed level.

Then

$$V_{s_t} = \frac{\pi h_{max}}{12} \left[(d_T + d_B)^2 - d_T d_B \right] \qquad (21)$$

Since

$$\tan \alpha = \frac{2 h_{max}}{d_T - d_B}$$

and letting

$$\psi = \frac{h_{max}}{d_T}$$

obtain

$$V_{s_t} = \frac{\pi h_{max}}{12}\left[(2 d_T - \frac{2 h_{max}}{\tan \alpha})^2 - (d_T^2 - \frac{2 d_T h_{max}}{\tan \alpha})\right]$$

$$= d_T^3 \left\{ \frac{\pi \psi}{3} \left[(1 - \frac{\psi}{\tan \alpha})^2 - 1/4 (1 - \frac{2\psi}{\tan \alpha}) \right] \right\} \quad (22)$$

or

$$V_{s_t} = d_T^3 K \quad (23)$$

in which

$$K = \left\{ \frac{\pi \psi}{3} \left[(1 - \frac{\psi}{\tan \alpha})^2 - 1/4 (1 - \frac{2\psi}{\tan \alpha}) \right] \right\} \quad (24)$$

Design criteria for pre-shaped basin -- From Table 5 and Table 8 obtain

$$\psi \approx 0.21$$

$$\alpha \approx 30^0$$

Substituting for ψ and α in Eq. 24 gives $K = 0.074$.

Eq. 23 is now written

$$V_{s_t} = 0.074\, d_T^3$$

Since

$$h_t^* = (V_{s_t})^{1/3}$$

Eq. 23 can now be written

$$h_t^* = 0.42\, d_T \quad (25)$$

or

$$d_T = \frac{h_t^*}{0.42} = 2.38\, h_t^* \quad (26)$$

also

$$h_{max} = 0.21\, d_T = 0.50\, h_t^* \tag{27}$$

and

$$d_B = 2.38\, h_t^* - \frac{(2)(0.50)\, h_t^*}{0.57736}$$

$$= 0.65\, h_t^* \tag{28}$$

To determine the position of the maximum depth h_{max} of the pre-shaped stilling basin relative to the pipe outlet, an analysis of the jet trajectory was first considered. If V_a is the velocity of the jet of water at the pipe outlet, then since the x - component of velocity is constant, obtain $V_a t = X_B$. The time for a particle to drop a distance y_o under the action of gravity when it has no initial velocity in that direction is expressed by $y_o = gt^2/2$. If y_o is equal to H, then after eliminating t in the two foregoing relations, obtain

$$V_a \doteq \frac{X_B}{(2H/g)^{1/2}}$$

in which X_B is the point of jet impingement on the alluvial bed when

$$y_o = H$$

or

$$X_B = V_a \left(\frac{2H}{g}\right)^{1/2}$$

From an analysis of experimental data, the point of maximum depth h_{max} relative to the pipe outlet is equal to

$$X = X_B + C \tag{29}$$

in which C in terms of h_t^*, from Table 5 and Table 8, is equal to

$$C \approx 0.6\, h_t^*$$

Thus, Eq. 29 can be written as

$$X = X_B + 0.6\, h_t^* \qquad (30)$$

<u>Experimental verification of design criteria</u> -- The design criteria given by Eqs. 26, 27, 28, and 30, will be examined by making a comparison between computed and experimental values as follows:

Table 5, for Q = 1 cfs, b = 1 ft, gives a value for h_t^* of 2.30 ft. Substituting this value into Eqs. 26, 27, 28 gives

$$d_T = 5.90 \text{ ft}$$

$$d_B = 1.56 \text{ ft}$$

$$h_{max} = 1.40 \text{ ft}$$

Table 5 shows the experimental values for d_T, d_B and h_{max} to be

$$d_T = 5.46 \text{ ft}$$

$$d_B = 1.50 \text{ ft}$$

$$h_{max} = 1.15 \text{ ft}$$

or

$$\frac{d_T\ (\text{comp.}) - d_T\ (\text{exp.})}{d_T(\text{comp.})} = \frac{5.46 - 5.90}{5.46} \times 100 \approx -8\ \%$$

$$\frac{d_T\ (\text{comp.}) - d_B\ (\text{exp.})}{d_B(\text{comp.})} = \frac{1.50 - 1.56}{1.50} \times 100 \approx + - 4\ \%$$

$$\frac{h_{max}\ (\text{comp.}) - h_{max}\ (\text{exp.})}{h_{max}(\text{comp.})} = \frac{1.15 - 1.40}{1.15} \times 100 \approx -22\ \%$$

Since it was possible to have a variation of $\pm$ 10 % in the determination of d_T, d_B or h_{max} from the original experimental data, it was assumed that Eqs. 26, 27, and 28 are acceptable design criteria for a pre-shaped stilling basin for limited conditions of flow and sediment characteristics and boundary geometry.

Likewise, by substituting the value for X_B into Eq. 30 gives

$$X = 2.52 + 1.34 = 3.86$$

The experimental value for X is 3.70, which is only 4 % less than the computed value. Eq. 30 is applicable, under similar hydraulic conditions as Eqs. 26, 27, and 28, for locating the pre-shaped stilling basin relative to the culvert outlet.

Theoretical analysis: armorplate - - To determine the measure of quantity of graded gravel for armorplating the pre-shaped stilling basin, it was assumed that the gravel, when placed would cover the entire surface of the basin, as illustrated in Fig. 34, and that the thickness would be varied in discrete increments of $\epsilon = nD$, in which D is the maximum diameter of armorplate. If we let V_{ar} equal volume of armorplate, then its equation in terms of h_t^* is determined as follows:

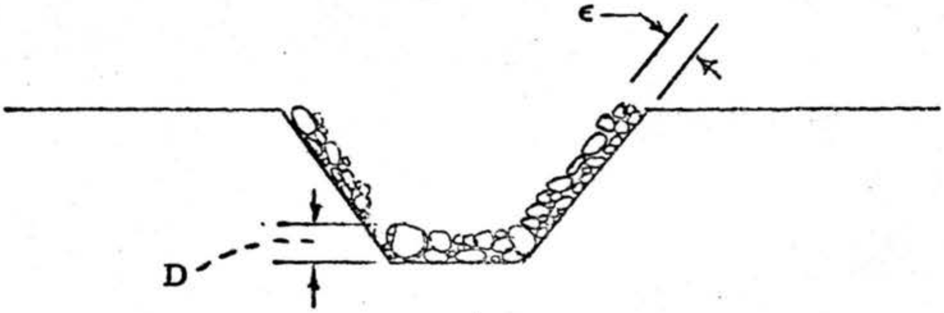

Fig. 34. Schematic diagram showing assumed distribution of armorplate over the surface of the pre-shaped basin.

For a frustum of a cone, the area of the surface of the sides is given by

$$A_s = \pi s (r_1 + r_2)$$

in which

$$s = \left[h_{max}^2 + (r_1 - r_2)^2\right]^{1/2}$$

From Eq. 26 and 28 obtain

$$r_1 = \frac{d_T}{2} = 1.19 h_t^*$$

$$r_2 = \frac{d_B}{2} = 0.33 h_t^*$$

Also,

$$h_{max} = 0.50 h_t^*$$

then

$$s = \left[(0.50 h_t^*)^2 + (1.19 h_t^* - 0.33 h_t^*)^2\right]^{1/2}$$

$$= 0.99 h_t^*$$

and

$$A_s = \pi (0.99 h_t^*)(1.19 h_t^* + 0.33 h_t^*)$$

$$= 4.75 h_t^{*2}$$

Since the bottom will be armorplated also, the surface of the bottom is given by

$$A_b = \frac{\pi d_B^2}{4}$$

$$= (0.7854)(0.65\, h_t^*)^2 = 0.33\, h_t^*$$

The total area is

$$A_t = A_s + A_b = (4.75 + 0.33)\, h_t^{*2} = 5.08\, h_t^{*2}$$

If ϵ equals the assumed thickness of the armorplate in inches covering the surface of the basin, then V_{ar} in cubic feet is given by

$$V_{ar} = \frac{5.08\, h_t^{*2}\, \epsilon}{12} = 0.423\, h_t^{*2}\, \epsilon \qquad (31)$$

APPENDIX

C. EXPERIMENTAL DATA

In this section are reported in tabular form the experimental results of the study. A description of the tables is as follows:

Tables 1, 2, 3, and 4 give the results of the investigation on the physical and hydraulic properties of the alluvial material and armorplate used in the study.

Table 5 gives the experimental values of boundary geometry of the scour hole used in determining design criteria for the pre-shaped stilling basin.

Tables 6 and 7 give the results of armorplate studies of effect of quantity and point of placement of armorplate on the rate of scour.

Table 8 gives the results of the study on the effect of channel width on the rate of scour in an alluvial bed.

Table 9 gives values for use in Eq. 1, that is, values of $\frac{Z_s}{\sqrt{A}\ \sin\theta\ b}$ for given discharge, tailwater depth and B = 10 ft.

Table 10 gives values for use in Eq. 7, that is, values of h^*/H and $\frac{\rho\ Q\ V}{\rho_s\ W_m^{\ 2}\ \sigma_d\ b}$ for given discharge, tailwater depth, and different widths of rectangular channel.

TABLE 1 A. Sieve Analysis of Original Sediment Used in Experimental Flume

Sample No.	Sieve Opening mm	Percent Retained	Percent Passing	Sample No.	Sieve Opening mm	Percent Retained	Percent Passing
A	4.699	3.18	96.82	A	0.833	96.23	3.77
B	"	6.50	93.50	B	"	94.60	5.50
C	"	11.00	89.00	C	"	94.40	5.60
D	"	3.61	96.39	D	"	92.27	7.73
E	"	8.65	91.35	E	"	96.80	3.20
Average		6.59	93.41	Average		94.84	5.16
A	3.327	28.82	71.18	A	0.589	98.73	1.27
B	"	30.30	69.70	B	"	97.00	3.00
C	"	41.50	58.50	C	"	96.60	3.40
D	"	20.39	79.61	D	"	95.88	4.12
E	"	34.10	65.90	E	"	98.25	1.75
Average		31.02	68.98	Average		97.29	2.71
A	2.362	56.84	43.16	A	0.417	99.11	0.89
B	"	56.50	43.50	B	"	98.60	1.40
C	"	70.00	30.00	C	"	98.40	1.60
D	"	44.84	55.16	D	"	98.11	1.89
E	"	63.50	36.50	E	"	99.20	0.80
Average		58.34	41.66	Average		98.68	1.32
A	1.651	79.04	20.96	A	0.295	99.72	0.28
B	"	79.20	20.80	B	"	99.50	0.50
C	"	85.20	14.80	C	"	99.20	0.80
D	"	70.41	29.59	D	"	98.99	1.01
E	"	85.10	14.90	E	"	99.50	0.50
Average		79.79	20.21	Average		99.38	0.62
A	1.168	83.09	16.91	A	0.208	99.88	0.12
B	"	84.70	15.30	B	"	99.80	0.20
C	"	87.40	12.60	C	"	99.70	0.30
D	"	77.08	22.92	D	"	99.53	0.47
E	"	90.10	9.90	E	"	99.75	0.25
Average		84.47	15.53	Average		99.73	0.27

TABLE 1 C. Sieve Analysis of Original Sediment Used in Experimental Basin

Sample No.	Sieve Opening mm	Percent Retained	Percent Passing	Sample No.	Sieve Opening mm	Percent Retained	Percent Passing
A	4.699	2.5	97.5	A	0.833	84.7	15.3
B	"	0.8	99.2	B	"	83.7	16.3
C	"	0.8	99.2	C	"	74.9	25.1
Average		1.4	98.6	Average		81.1	18.9
A	3.327	15.3	84.7	A	0.589	91.5	8.5
B	"	10.5	89.5	B	"	91.4	8.6
C	"	10.6	89.4	C	"	84.2	15.8
Average		12.1	87.9	Average		89.0	11.0
A	2.362	37.1	62.9	A	0.417	95.7	4.3
B	"	31.7	68.3	B	"	96.3	3.7
C	"	28.9	71.1	C	"	90.7	9.3
Average		32.6	67.4	Average		94.2	5.8
A	1.651	58.3	41.7	A	0.295	98.0	2.0
B	"	53.4	46.6	B	"	98.9	1.1
C	"	47.5	52.5	C	"	94.6	5.4
Average		53.1	46.9	Average		97.2	2.8
A	1.168	73.9	26.1	A	0.208	99.3	0.7
B	"	71.6	28.4	B	"	99.2	0.8
C	"	62.7	37.3	C	"	97.2	2.8
Average		69.4	30.6	Average		98.6	1.4

TABLE 1 D. Sieve Analysis of Armorplate

Sample No.	Sieve Opening mm	Percent Retained	Percent Passing	Sample No.	Sieve Opening mm	Percent Retained	Percent Passing
A	26.67	0.00	100.00	A	4.699	97.39	2.61
B	"	0.00	100.00	B	"	97.47	2.53
C	"	3.44	96.56	C	"	96.97	3.03
Average		1.15	98.85	Average		97.28	2.72
A	18.85	40.73	59.27	A	3.327	98.61	1.39
B	"	34.61	65.39	B	"	98.81	1.19
C	"	27.05	72.95	C	"	98.61	1.39
Average		34.13	65.87	Average		98.68	1.32
A	13.33	66.01	33.99	A	2.362	98.95	1.05
B	"	60.05	39.95	B	"	99.21	0.79
C	"	60.52	39.48	C	"	99.02	0.98
Average		62.19	37.81	Average		99.06	0.94
A	9.423	84.80	15.20	A	1.651	99.11	0.89
B	"	81.82	18.18	B	"	99.37	0.63
C	"	80.83	19.17	C	"	99.22	0.78
Average		82.48	17.52	Average		99.23	0.77
A	6.680	94.09	5.91	A	1.168	99.22	0.78
B	"	92.72	7.28	B	"	99.47	0.53
C	"	92.22	7.78	C	"	99.33	0.67
Average		93.01	6.99	Average		99.34	0.66

Particle No.	Sieve Opening mm	W mg	d_n[1] mm	F[2] mg	Particle Dimensions a mm	b mm	c mm	$\frac{c}{\sqrt{ab}}$	W_s cm/sec	W_s fps
1	4.699	176.2	5.02	110.0	7.52	5.68	3.30	0.505	25.2	0.826
2	"	251.0	5.66	157.5	10.41	6.60	2.64	0.320	26.8	0.879
3	"	188.2	5.14	118.0	5.94	5.81	3.70	0.628	----	-----
4	"	183.5	5.10	115.0	6.60	4.62	4.49	0.810	29.6	0.971
5	"	205.1	(lost in testing)							
6	"	161.8	4.88	101.0	6.07	5.28	4.62	0.813	30.6	1.004
7	"	220.1	5.41	137.8	6.60	5.55	4.49	0.741	35.2	1.157
8	"	200.1	5.24	125.0	6.86	5.15	4.88	0.819	32.6	1.070
9	"	166.1	4.93	104.0	6.60	5.42	3.44	0.574	34.4	1.130
Average Values								0.659	30.62	1.004
1	3.327	140.8	4.65	87.6	5.41	4.88	3.70	0.715	28.2	0.924
2	"	73.6	3.76	45.9	5.41	4.48	2.38	0.484	26.2	0.858
3	"	82.6	3.90	51.5	5.15	4.36	2.78	0.582	26.0	0.852
4	"	101.2	4.18	63.2	5.68	4.36	2.78	0.557	----	-----
5	"	127.4	4.50	79.4	6.60	4.62	3.30	0.595	29.8	0.976
6	"	72.2	3.74	45.0	4.62	3.96	3.96	0.926	24.8	0.813
7	"	58.4	3.48	36.4	5.68	3.70	2.24	0.490	23.4	0.766
8	"	102.6	4.19	63.9	5.41	4.22	3.56	0.745	31.2	1.024
9	"	101.3	4.18	63.2	5.80	3.96	3.96	0.828	26.0	0.853
10	"	68.3	3.66	42.5	5.02	3.30	3.17	0.776	27.4	0.898
11	"	130.9	4.55	81.5	7.00	5.15	3.17	0.525	26.8	0.879
Average Values								0.667	26.98	0.885
1	2.362	28.9	2.75	18.0	4.48	3.17	1.98	0.526	----	-----
2	"	40.7	3.08	25.4	4.62	3.04	2.64	0.702	----	-----
3	"	25.5	2.64	15.9	4.10	3.17	1.85	0.514	18.4	0.604
4	"	47.8	3.24	29.8	4.35	3.70	2.90	0.723	24.7	0.810
5	"	28.0	2.72	17.5	3.96	3.17	2.24	0.633	22.8	0.748
6	"	43.2	3.15	27.0	4.36	3.30	2.90	0.763	----	-----
7	"	62.4	3.56	38.9	5.15	3.30	2.78	0.673	27.5	0.901
8	"	18.7	2.38	11.65	3.04	2.78	1.59	0.545	19.3	0.633
9	"	26.2	2.66	16.35	4.35	2.90	1.59	0.444	23.2	0.761
10	"	44.1	3.16	27.50	5.55	3.44	1.85	0.424	----	-----
Average Values								0.565	22.6	0.740
1	1.651	21.1	2.48	13.14	2.78	2.32	2.24	0.883	23.5	0.771
2	"	13.5	2.14	8.40	3.04	2.64	1.45	0.511	16.6	0.545
3	"	12.5	2.08	7.78	2.96	2.24	1.91	0.745	17.0	0.558
4	"	16.2	2.26	10.10	3.10	2.18	2.11	0.812	22.8	0.748
5	"	11.5	2.02	7.16	2.50	2.37	1.52	0.623	20.5	0.673
6	"	13.1	2.12	8.15	3.16	2.24	1.91	0.722	17.1	0.561
7	"	9.3	1.88	5.79	3.10	1.85	1.45	0.604	17.5	0.574
8	"	10.1	1.94	6.28	2.96	2.18	1.98	0.767	16.6	0.545
9	"	12.1	2.06	7.52	2.84	2.44	1.58	0.602	18.9	0.620
10	"	12.4	2.08	7.72	2.70	2.44	1.78	0.690	23.1	0.757
Average Values								0.696	19.36	0.634
1	1.168	8.6	1.84	5.37	2.38	2.04	1.98	0.895	17.8	0.584
2	"	8.8	1.85	5.45	3.16	1.98	1.25	0.496	17.2	0.564
3	"	6.9	1.70	4.27	2.30	1.65	1.58	0.780	20.3	0.666
4	"	10.2	1.94	6.32	3.89	1.65	1.52	0.599	14.0	0.459
5	"	14.1	2.16	8.74	3.76	1.52	1.58	0.665	16.1	0.528
6	"	5.6	1.59	3.46	2.18	1.91	1.19	0.567	15.7	0.515
7	"	7.8	1.77	4.83	2.96	1.78	1.39	0.604	16.5	0.561
8	"	5.2	1.55	3.22	2.44	1.85	1.39	0.656	13.9	0.456
9	"	6.4	1.67	4.00	2.50	1.72	1.19	0.578	15.7	0.515
10	"	5.3	1.56	3.29	2.38	1.98	0.99	0.424	14.4	0.472
Average Values								0.626	16.16	0.528
1	0.833	3.5	1.36	2.16	[3]	[3]	[3]	[3]	16.3	0.537
2	"	1.4	1.00	0.87	[3]	[3]	[3]	[3]	12.1	0.398
3	"	2.2	1.17	1.37	[3]	[3]	[3]	[3]	14.5	0.477
4	"	3.3	1.33	2.04	[3]	[3]	[3]	[3]	13.7	0.450
5	"	1.2	0.95	0.75	[3]	[3]	[3]	[3]	10.6	0.348
6	"	5.2	1.55	3.22	[3]	[3]	[3]	[3]	13.6	0.448
7	"	2.6	1.23	1.61	[3]	[3]	[3]	[3]	11.6	0.382
8	"	4.7	1.50	2.92	[3]	[3]	[3]	[3]	14.7	0.483
9	"	1.0	0.90	0.62	[3]	[3]	[3]	[3]	11.9	0.392
10	"	4.2	1.45	2.62	[3]	[3]	[3]	[3]	14.6	0.480
Average Values									13.36	
1	0.589	1.05	0.91	0.66	[3]	[3]	[3]	[3]	9.00	0.295
2	"	0.80	0.83	0.50	[3]	[3]	[3]	[3]	9.45	0.310
3	"	1.15	0.94	0.72	[3]	[3]	[3]	[3]	9.55	0.313
4	"	(lost in testing)								
5	"	0.85	0.85	0.53	[3]	[3]	[3]	[3]	10.23	0.335
6	"	0.80	0.83	0.50	[3]	[3]	[3]	[3]	10.72	0.351
7	"	0.57	0.74	0.35	[3]	[3]	[3]	[3]	9.19	0.301
8	"	0.60	0.76	0.37	[3]	[3]	[3]	[3]	9.22	0.302
9	"	0.55	0.74	0.35	[3]	[3]	[3]	[3]	8.13	0.267
10	"	(lost in testing)								
Average Values									9.42	0.308

[1] $d_n = 0.897\,(W)^{1/3}$
[2] $F = 0.865\,d_n^3$
[3] No measurements were made of the particle dimensions on particles whose diameters were less than 1.168 mm.

TABLE 2. Physical and Hydraulic Properties of Sediment Particles

TABLE 3. Values Used in Determining Geometric Mean Fall Velocity W_m

Sieve Opening mm	Σ Retained	Δ Retained	W_{ave} cm/sec	$\%W_{ave}$[1] cm/sec	Sieve Opening mm	Percent[2] passing	Percent[3] passing	W_{ave} cm/sec
Method 1 - Measured values of W_m					Method 2 - Arithmetic probability graph[4]			
4.699	0.066	0.066	30.62	2.02	4.699	93.41	93.44	30.62
3.327	0.296	0.230	26.98	6.19	3.327	68.98	72.10	26.98
2.362	0.569	0.273	22.60	6.14	2.362	41.66	45.00	22.60
1.651	0.789	0.220	19.36	4.28	1.651	20.21	22.35	19.36
1.168	0.840	0.051	16.16	0.83	1.168	15.53	16.75	16.16
0.833	0.949	0.109	13.36	1.46	0.833	5.16	5.40	13.36
0.589	0.974	0.026	9.42	0.25	0.589	2.71	2.70	9.42
0.417	0.990	0.016	5.90[5]	0.09	0.417	1.32	0.94	5.90[5]
0.295	0.996	0.006	3.90[5]	0.03	0.295	0.62	0.36	3.90[5]
0.208	0.999	0.003	2.00[5]	0.01	0.208	0.27	0.08	2.00[5]
		1.000	W_m =	21.30				

[1] Weighted average value

[2] Original sediment

[3] Sediment after 100 hours of scouring action

[4] W_m determined by plotting percent passing values against W_{ave} on arithmetic probability graph paper. (See Fig. 30.)

[5] Obtained from Fig. 25 reference (18).

TABLE 4 - Values of d_n and W_s Determined from The Results of Investigations Of The Influence of Shape On The Fall Velocity of Sedimentary Particles.

d_n mm	W_s cm/sec	$\frac{c}{\sqrt{ab_s}}$	s.g.	d_n mm	W_s cm/sec	$\frac{c}{\sqrt{ab_s}}$	s.g.	d_n mm	W_s cm/sec	$\frac{c}{\sqrt{ab_s}}$	s.g.
Schulz				**Wilde**				**Peterka**			
1.03	11.72	0.73	2.65	27.3	65.5	0.72	2.60	6.35	48.8	0.73[1]	2.65[1]
0.24	2.37	0.73	2.65	13.3	50.3	0.73	2.58	12.70	61.0	0.73	2.65
1.38	15.96	0.74	2.65	13.2	55.1	0.72	2.63	19.05	73.2	0.73	2.65
1.22	13.95	0.74	2.65	21.0	68.5	0.72	2.62	25.40	82.4	0.73	2.65
1.20	13.98	0.72	2.65	16.7	70.5	0.74	2.65	38.10	99.0	0.73	2.65
0.76	8.65	0.74	2.65	14.3	50.4	0.72	2.67	50.80	112.8	0.73	2.65
0.77	9.87	0.73	2.57	4.8	32.1	0.73	2.62	63.50	128.0	0.73	2.65
0.69	9.15	0.73	2.65	19.0	50.3	0.74	2.62	76.20	140.0	0.73	2.65
0.64	8.52	0.73	2.65	28.2	80.0	0.73	2.78	88.90	149.4	0.73	2.65
0.48	6.20	0.73	2.65	13.3	54.0	0.73	2.70	101.60	160.0	0.73	2.65
0.32	4.07	0.74	2.65	13.9	45.5	0.73	2.64	114.20	170.8	0.73	2.65
				6.9	34.3	0.72	2.65	127.00	177.0	0.73	2.65
				11.5	46.3	0.72	2.65	139.75	187.5	0.73	2.65
								152.40	193.8	0.73	2.65
								177.80	207.5	0.73	2.65
								203.20	226.0	0.73	2.65
								228.60	238.0	0.73	2.65
Smith				**Corey**							
5.41	35.2	0.74	2.65	7.00	32.6	0.73	2.65				
4.65	28.2	0.72	2.65	3.82	23.9	0.74	2.65				
3.24	24.7	0.72	2.65	4.10	23.0	0.72	2.65				
2.12	17.1	0.72	2.65	2.08	20.4	0.73	2.65				
				1.64	16.2	0.73	2.65				

[1] Assumed values

TABLE 5. Experimental Values[1] of Boundary Geometry of Scour Hole Used In Determining Design Criteria For Pre-shaped Stilling Basin.

Series No.	Run No.	Q cfs	b ft	t hrs	d_T[2] ft	d_B ft	h_{max} ft	$\psi = \frac{h_{max}}{d_t}$	α deg.	X ft	X_B ft	$\sqrt[3]{V_{s_t}} = h_t^*$ ft	$C = \frac{X-X_B}{h_t^*}$
I	5	0.5	0.5	6.0	5.00	1.04	1.06	0.212	28.69	2.90	2.16	1.90	0.39
II	11	1.0	0.5	8.0	4.60	0.80	1.15	0.250	25.45	3.00	2.55	2.08	0.22
III	15	2.0	0.5	2.0	7.90	1.00	1.40	0.177	30.45	5.00	2.66	2.68	0.87
IV	20	1.5	0.5	4.0	7.05	1.06	1.40	0.198	26.37	4.30	2.84	2.56	0.57
V	27	0.5	1.0	16.0	4.00	1.34	0.95	0.238	24.80	2.80	2.06	1.73	0.43
VI	33	1.0	1.0	8.0	5.90	1.56	1.40	0.238	32.50	3.70	2.52	2.30	0.51
VII	37	1.5	1.0	4.0	7.20	2.40	1.40	0.195	30.18	4.70	2.64	2.60	0.79
VIII	41	2.0	1.0	2.0	[3]	2.60	----	----	30.97	----	----	----	----
IX	47	1.0	1.5	16.0	4.90	1.10	1.15	0.234	34.00	3.90	2.50	2.01	0.70
X	54	1.5	1.5	32.0	5.60	1.06	1.30	0.232	35.93	4.40	2.71	2.23	0.76
XI	60	2.0	1.5	8.0	6.30	1.00	1.30	0.206	35.20	5.00	2.91	2.55	0.82
XII	66	0.5	1.5	223.0	3.50	0.66	0.60	0.172	26.57	2.95	2.12	1.37	0.61
	Average							0.210	30^0	3.88	2.52	2.19	0.61

[1] Values obtained from study of reference (12).

[2] $d_T \approx \frac{L_b + W_b}{2}$ (This relation holds also for data given in Table 8.)

[3] Indeterminate because of boundary effects.

TABLE 6 - Volume of Scour as a Function of Quantity of Armorplate, Discharge, and Tailwater Depth in Pre-shaped Basins of Varied Volume. Series I - XVI: B = 10 ft and Series XVII - XXII: B = 20 ft.

Run Series [1]	Run No.	Q cfs	b ft	h_t^* [2] %	ϵ in.	Time Hrs.	Time Min.	V_{s_t} ft^3	$h_t^* = \sqrt[3]{V_{s_t}}$ ft
		1	1	50	0	0	00	1.81	1.22
	1					0	30	7.30	1.94
	2					1	00	8.35	2.03
I [3]	3					2	00	10.30	2.18
	4					4	00	11.78	2.27
		1	1	50	0.25	0	00	1.81	1.22
	5					0	30	6.10	1.83
	6					1	00	7.20	1.93
II	7					2	00	9.23	2.10
	8					4	00	10.70	2.20
		1	1	50	0.50	0	00	1.81	1.22
	9					0	30	5.38	1.75
III	10					2	00	7.40	1.95
	11					4	00	8.40	2.03
		1	1	50	1.00	0	00	1.81	1.22
	12					0	30	4.46	1.64
IV	13					1	00	4.75	1.68
	14					2	00	5.00	1.71
	15					4	00	5.40	1.75
	16					8	00	5.80	1.80
		1	1	50	2.00	0	00	1.81	1.22
	17					0	15	3.95	1.58
V	18					4	00	4.96	1.70
	19					8	00	5.12	1.72

[1] The number of series of runs are not given in the sequence in which they were performed, but are listed here in a more systematic order to provide for better efficiency in data analysis.

[2] In percent of h_t^* for t = 100. Values for h^*_{100} are given in Table 8.

[3] Series I to XVI for B = 10 ft.

TABLE 6 - Continued.

Run[1] Series	Run No.	Q cfs	b ft	h_t^*[2] %	ϵ in.	Time Hrs.	Min.	V_{s_t} ft^3	$h_t^* = \sqrt[3]{V_{s_t}}$ ft
		1	1	50	3	0	00	1.81	1.22
	20					0	30	3.10	1.46
VI	21					4	30	3.64	1.54
	22					8	00	4.03	1.60
		1	1	63	0	0	00	3.59	1.53
	23					0	30	11.50	2.25
VII	24					1	00	13.21	2.36
	25					2	00	14.34	2.43
	26					4	00	15.68	2.50
		1	1	63	0.25	0	00	3.59	1.53
	27					0	30	7.37	1.97
VIII	28					1	00	8.55	2.04
	29					2	00	9.53	2.12
	30					4	00	10.76	2.21
		1	1	63	0.50	0	00	3.59	1.53
	31					0	30	7.20	1.93
IX	32					1	00	7.48	1.96
	33					2	00	8.00	2.00
	34					4	00	8.75	2.06
		1	1	63	1.00	0	00	3.59	1.53
	35					0	30	6.15	1.83
X	36					1	00	6.38	1.85
	37					4	00	6.50	1.87
		1	1	63	2.0	0	00	3.59	1.53
	38					0	30	5.45	1.76
XI	39					1	00	5.55	1.77
	40					2	00	5.62	1.78
	41					4	00	5.68	1.79

TABLE 6 - Continued.

Run[1] Series	Run No.	Q cfs	b ft	h_t^*[2] %	ϵ in.	Time Hrs.	Time Min.	V_{s_t} ft^3	$h_t^* = \sqrt[3]{V_{s_t}}$ ft
		1	1	79	0	0	00	7.06	1.92
	42					0	30	10.95	2.22
XII	43					1	00	11.90	2.28
	44					2	00	12.92	2.34
	45					4	00	13.65	2.39
		1	1	79	0.25	0	00	7.06	1.92
	46					0	30	10.30	2.17
XIII	47					1	00	10.45	2.18
	48					2	00	10.60	2.20
	49					4	00	10.90	2.22
		2	2	79	0.125	0	00	7.06	1.92
	50					0	30	11.03	2.22
	51					1	00	11.55	2.26
XIV	52					2	00	12.05	2.30
	53					4	00	12.85	2.34
	54					8	00	13.80	2.40
	55					16	00	14.95	2.46
		2	2	79	0.25	0	00	7.06	1.92
	56					0	30	9.40	2.11
XV	57					1	00	9.74	2.14
	58					2	00	10.10	2.16
	59					4	00	10.35	2.17
	60					8	00	10.42	2.18
		2	2	79	0.50	0	00	7.06	1.92
	61					0	30	7.20	1.93
	62					1	00	7.41	1.95
XVI	63					2	00	7.80	1.98
	64					4	00	8.00	2.00
	65					8	00	8.11	2.01

TABLE 6 - Continued.

Run Series [1]	Run No.	Q cfs	b ft	h_t^* [2] %	ϵ in.	Time Hrs.	Time Min.	V_{s_t} ft^3	$h_t^* = 3\sqrt{V_{s_t}}$ ft
	66	1	1	63	0.25	0	15	8.09	2.01
	67					0	30	8.90	2.07
XVII [4]	68					1	00	11.61	2.23
	69					2	00	13.14	2.36
	70					4	00	17.39	2.59
	71	1	1	63	0.50	0	15	5.57	1.77
	72					0	30	5.99	1.82
	73					1	00	6.48	1.87
XVIII	74					2	00	7.20	1.93
	75					4	00	8.43	2.04
	76					8	00	9.63	2.13
	77	1	1	63	1.00	0	15	5.61	1.78
	78					0	30	5.85	1.80
XIX	79					1	00	6.72	1.89
	80					2	00	7.16	1.92
	81					4	00	7.43	1.95
XX	82	1.88	1	63	0.25	0	15	23.13	2.85
	83					0	30	31.16	3.12
	84	1.88	1	63	0.50	0	15	16.15	2.53
XXI	85					0	30	19.60	2.70
	86					1	00	22.40	2.81
	87	1.88	1	63	1.00	0	15	16.00	2.52
XXII	88					0	30	19.47	2.69
	89					1	00	22.46	2.81
	90					2	00	27.19	3.01

[4] Series XVII to XXII for B = 20 ft.

TABLE 7 - Volume of Scour as a Function of Location of Armor-plate Relative to Cantilevered Culvert Outlet.

Run Series	Run No.	Q cfs	b ft	X^1 ft	h_t^* %	ϵ in.	Time Hrs.	Min.	V_{s_t} ft^3	$h_t^* = \sqrt[3]{V_{s_t}}$ ft
	1	1	1	2.00	63	0.5	0	30	9.60	2.12
	2						1	00	10.52	2.19
I	3						2	00	11.35	2.25
	4						4	00	12.30	2.31
	5						6	00	13.27	2.37
	6	1	1	2.55	63	0.5	0	30	7.20	1.93
	7						1	00	7.48	1.96
II	8						2	00	8.00	2.00
	9						4	00	8.75	2.06
	10	1	1	3.60	63	0.5	0	30	7.30	1.94
	11						1	00	8.02	2.00
III	12						2	00	8.19	2.14
	13						8	00	11.40	2.25
	14						16	00	12.68	2.33
	15	1	1	4.60	63	0.5	0	30	8.12	2.01
	16						1	00	8.19	2.02
	17						2	00	9.24	2.10
IV	18						4	00	10.53	2.19
	19						6	00	11.28	2.24
	20						8	00	11.59	2.26
	21						16	00	13.33	2.37
	22	1	1	5.25	63	0.5	0	30	9.60	2.12
	23						1	00	10.52	2.19
V	24						2	00	11.35	2.25
	25						4	00	12.30	2.31
	26						6	00	13.27	2.37

[1] Distance from culvert outlet.

TABLE 8 - Scour Hole Dimensions for Given Hydraulic Characteristics and Channel of Width 5 ft to 20 ft.

Series No.	Run No.	Q cfs	b ft	H ft	t hrs	W_b ft	L_b ft	h_{max} ft	X ft	V_{s_t} ft^3	$h_t^* = \sqrt[3]{V_{s_t}}$ ft
B = 5 Feet											
	1	2.0	1.0	4.333	0.125	3.72	4.42	1.00	3.58	5.72	1.79
	2				0.25	4.00	5.17	0.90	4.58	6.71	1.89
I	3				0.50	5.00	5.35	0.88	4.75	9.32	2.16
	4				1.00	5.00	5.50	0.94	5.25	10.74	2.21
	5				2.00	5.00	5.75	0.95	5.35	10.88	2.22
	6				4.00	5.00	5.75	1.20	3.68	14.69	2.45
					100.00						2.48 1/
II	7	2.0	0.5	4.333	0.125	5.00	5.50	1.14	3.42	10.07	2.16
	8				0.25	5.00	5.75	1.22	4.35	15.40	2.49
					100.00						2.85
	9	1.5	0.5	4.250	0.125	5.00	5.00	0.98	3.68	5.84	1.80
III	10				0.25	5.00	5.00	1.11	3.50	9.78	2.14
	11				0.50	5.00	5.50	1.17	3.67	11.84	2.28
	12				1.00	5.00	5.50	1.27	3.92	14.97	2.46
					100.00						2.33
	13	1.0	0.5	4.151	0.125	3.83	3.25	0.82	2.83	3.28	1.49
	14				0.25	4.00	3.75	0.92	2.75	4.56	1.66
IV	15				0.50	4.25	4.25	1.00	2.67	6.01	1.79
	16				1.00	5.00	4.40	1.10	2.90	7.61	1.97
	17				2.00	5.00	4.70	1.16	2.99	10.36	2.34
					100.00						2.20
	18	1.0	1.0	4.151	0.25	3.25	3.60	0.77	2.83	1.96	1.25
	19				0.50	3.36	3.60	0.74	2.83	2.74	1.40
V	20				1.00	3.58	3.83	0.87	3.00	3.34	1.50
	21				2.00	3.83	3.95	0.93	3.00	4.01	1.59
	22				4.00	3.93	3.95	0.93	3.04	4.15	1.61
					100.00						1.95
B = 10 Feet											
	1	0.5	0.5	4.044	0.25	---	---	0.73	3.00	1.64	1.18
	2				0.50	3.53	3.27	0.80	2.90	2.75	1.40
I	3				1.00	4.04	3.63	0.95	2.80	3.67	1.54
	4				2.00	3.60	3.25	1.04	2.83	5.10	1.72
	5				6.00	4.67	5.83	1.06	2.92	6.85	1.90
					100.00						1.98

1/ All values for h_t^* = 100 hrs were determined by means of an equation of the form $h^* = \frac{t}{a + bt}$ in which a and b are constants.

TABLE 8 - Continued

Series No.	Run No.	Q cfs	b ft	H ft	t hrs	W_b ft	L_b ft	h_{max} ft	X ft	V_{s_t} ft^3	$h_t^* = \sqrt[3]{V_{s_t}}$ ft
B = 10 Feet continued											
	6	1.0	0.5	4.008	0.25	3.33	3.33	0.55	2.83	2.05	1.27
	7				0.50	3.50	3.00	0.70	2.71	2.80	1.41
II	8				1.00	4.00	3.80	0.65	2.71	3.72	1.55
	9				2.00	4.80	4.33	0.60	2.75	4.59	1.66
	10				4.00	5.67	4.50	0.90	3.00	6.55	1.87
	11				8.00	5.55[1]	4.00[1]	1.15	3.00	9.00	2.08
					100.00						2.23
	12	2.0	0.5	4.049	0.25	5.67	5.67	1.30	4.38	9.80	2.14
III	13				0.50	6.67	6.33	1.30	4.30	12.80	2.34
	14				1.00	7.50	7.33	1.40	4.50	15.25	2.48
	15				2.00	8.75	7.67	1.40	5.00	19.30	2.68
					100.00						2.91
	16	1.5	0.5	3.966	0.25	4.33	4.25	0.90	3.08	4.68	1.67
	17				0.50	5.00	4.92	1.00	3.00	6.62	1.88
IV	18				1.00	6.00	6.25	1.30	3.58	10.70	2.20
	19				2.00	7.00	7.50	1.40	3.92	14.50	2.44
	20				4.00	7.00	7.50	1.40	4.30	16.80	2.56
					100.00						2.70
	21	0.5	1.0	3.683	0.25	2.83	2.91	0.70	2.17	1.82	1.22
	22				0.50	3.00	3.33	0.75	2.67	2.25	1.31
	23				1.00	3.00	3.40	0.85	3.00	2.35	1.33
V	24				2.00	3.83	3.90	1.00	2.80	3.89	1.57
	25				4.00	3.90	4.00	1.00	2.80	4.10	1.60
	26				8.00	4.08	4.12	1.00	2.80	4.50	1.65
	27				16.00	4.09	4.25	1.05	2.80	5.12	1.73
					100.00						1.92
	28	1.0	1.0	3.898	0.25	3.67	3.50	0.85	2.83	3.38	1.50
	29				0.50	3.83	3.75	0.90	2.83	4.02	1.59
VI	30				1.00	4.00	3.91	1.00	3.00	4.40	1.64
	31				2.00	4.50	4.33	1.15	3.16	6.28	1.87
	32				4.00	5.25	4.83	1.30	3.33	8.78	2.06
	33				8.00	7.00	5.25	1.40	3.75	12.20	2.30
					100.00						2.43

[1] Measurements taken at the -0.2 ft. contour.

TABLE 8 - Continued

Series No.	Run No.	Q cfs	b ft	H ft	t hrs	W_b ft	L_b ft	h_{max} ft	X ft	V_{s_t} ft^3	$h_t^* = \sqrt[3]{V_{s_t}}$ ft
B = 10 Feet - Continued											
	34	1.5	1.0	3.966	0.50	6.00	5.42	1.20	4.50	10.40	2.18
VII	35				1.00	8.00	5.83	1.30	4.50	12.70	2.33
	36				2.00	8.00	6.00	1.40	4.50	14.50	2.44
	37				4.00	10.00	6.25	1.40	4.67	17.50	2.60
					100.00						2.64
	38	2.0	1.0	4.049	0.25	7.00	5.42	1.20	4.50	12.00	2.29
VIII	39				0.50	5.25[1]	5.63[1]	1.30	4.25	13.00	2.35
	40				1.00	5.50[1]	5.67[1]	1.30	4.33	15.50	2.49
	41				2.00	5.67[1]	5.84[1]	1.40	5.00	18.55	2.65
					100.00						2.73
	42	1.0	1.5	4.008	0.50	3.83	3.60	1.02	3.58	3.80	1.56
	43				1.00	4.08	3.96	1.05	3.42	4.73	1.68
	44				2.00	4.33	4.17	1.08	3.38	5.82	1.80
IX	45				4.00	4.58	4.50	1.05	3.80	6.28	1.85
	46				8.00	4.83	4.67	1.16	3.88	7.30	1.94
	47				16.00	5.00	5.33	1.15	3.88	8.05	2.01
					100.00						2.06
	48	1.5	1.5	4.159	0.50	4.20	4.46	1.00	4.42	5.45	1.76
	49				1.00	4.46	4.75	1.11	4.33	7.00	1.91
	50				2.00	5.00	5.00	1.15	4.45	7.85	1.99
X	51				4.00	5.25	5.17	1.22	4.50	9.18	2.09
	52				8.00	5.67	5.26	1.25	4.75	10.02	2.16
	53				16.00	5.75	5.50	1.20	4.58	10.80	2.21
	54				32.00	6.11	5.53	1.27	4.42	11.20	2.23
					100.00						2.25
	55	2.0	1.5	4.159	0.25	4.83	4.83	1.00	4.83	7.20	1.95
	56				0.50	5.42	5.17	1.15	5.12	8.50	2.04
XI	57				1.00	5.83	5.50	1.00	5.00	10.65	2.20
	58				2.00	6.00	5.67	1.32	5.17	12.00	2.29
	59				4.00	6.25	6.00	1.30	5.00	14.20	2.42
	60				8.00	6.83	6.33	1.30	5.00	16.50	2.55
					100.00						2.58

[1] Measurements taken at the -0.2 ft. contour.

TABLE 8 - Continued

Series No.	Run No.	Q cfs	b ft	H ft	t hrs	W_b ft	L_b ft	h_{max} ft	X ft	V_{s_t} ft^3	$h^*_t = \sqrt[3]{V_{s_t}}$ ft
B = 10 Feet - Continued											
	61	0.5	1.5	3.945	1.00	2.17	2.33	0.47	3.00	0.86	0.95
	62				8.00	2.62	2.75	0.54	2.87	1.15	1.05
XII	63				16.00	2.67	2.92	0.61	2.75	1.48	1.14
	64				64.00	3.17	3.38	0.66	2.67	2.15	1.29
	65				128.00	3.33	3.58	0.60	2.83	2.25	1.31
	66				223.00	3.33	3.75	0.61	2.96	2.56	1.37
					100.00						1.33
B = 20 Feet											
	1	0.92	0.5	4.151	0.50	3.51	3.30	0.59	2.81	3.01	1.45
	2				1.00	3.85	3.50	0.68	---	3.52	1.52
I	3				2.00	4.83	4.08	0.88	2.67	5.00	1.71
	4				4.00	6.16	4.50	1.10	2.92	7.74	1.98
	5				8.00	8.41	7.41	1.80	3.95	27.01	3.00
					100.00						5.66
	6	1.88	1.0	4.333	0.25	6.00	6.67	1.70	5.41	18.48	2.64
	7				0.50	7.05	7.10	1.90	4.83	20.85	2.75
II	8				1.00	7.92	8.75	2.00	5.61	34.69	3.26
	9				2.00	8.08	10.00	1.97	6.54	43.98	3.53
	10				4.00	8.40	10.32	2.00	6.00		
					100.00						3.91
	11	0.50	0.5	4.080	0.25	3.00	3.00	0.60	2.25	1.81	1.22
	12				0.50	3.20	3.20	0.61	2.55	2.20	1.30
III	13				1.00	3.55	3.50	0.62	2.40	2.82	1.41
	14				2.00	4.00	3.74	0.81	2.40	3.22	1.47
	15				4.00	4.00	4.00	0.82	2.50	3.22	1.48
	16				8.00	5.16	4.16	1.10	2.50	6.35	1.85
					100.00						2.39
	17	1.00	1.5	4.182	0.50	4.30	4.30	0.99	3.42	3.79	1.56
	18				1.00	4.08	4.60	1.11	3.56	5.90	1.81
IV	19				2.00	4.64	4.88	1.13	3.60	7.63	1.97
	20				4.00	4.83	5.33	1.25	3.65	9.59	2.12
	21				8.00	4.96	5.58	1.26	3.87	11.31	2.24
					100.00						2.33

TABLE 8 - Continued

Series No.	Run No.	Q cfs	b ft	H ft	t hrs	W_b ft	L_b ft	h_{max} ft	X ft	V_{s_t} ft^3	$h^*_t = \sqrt[3]{V_{s_t}}$ ft
B = 20 Feet - Continued											
	22	2.18	2.0	4.333	0.25	5.1	6.1	1.42	6.3	14.34	2.43
	23				0.50	5.4	6.3	1.40	6.3	15.32	2.48
V	24				1.00	5.8	7.3	1.53	6.3	21.39	2.77
	25				2.00	6.2	7.7	1.67	6.5	27.46	3.02
	26				4.00	7.9	8.6	1.97	6.7	37.72	3.45
					100.00						3.50
	27	3.0	2.0	4.333	0.12	6.2	7.5	1.54	8.5	23.22	2.85
	28				0.25	6.3	8.0	1.60	8.5	24.73	2.91
VI	29				0.50	6.5	8.6	1.60	8.6	28.31	3.05
	30				1.00	6.7	9.0	1.85	8.7		
					100.00						4.00
VII	31	2.69	1.0	4.333	0.12	6.8	7.9	1.89	6.4	29.56	3.09
	32	1.50	1.5	4.182	0.25	4.5	5.3	1.34	4.6	9.74	2.14
	33				0.50	5.2	5.7	1.43	4.7	13.24	2.37
VIII	34				1.00	5.5	6.2	1.52	4.7	15.85	2.68
	35				2.00	5.9	6.9	1.68	4.9	20.58	2.74
	36				4.00	6.6	7.7	1.81	5.2	26.24	2.97
	37				8.00	7.3	8.3	1.97	5.5	33.71	3.22
					100.00						3.36
	38	1.0	1.0	4.182	0.25	5.0	5.2	1.35	3.6	9.78	2.14
	39				0.50	5.4	5.4	1.40	3.8	11.11	2.23
IX	40				1.00	5.6	5.8	1.49	3.9	12.89	2.34
	41				2.00	6.3	6.3	1.57	3.9	17.32	2.59
	42				4.00	6.9	7.4	1.68	3.9	22.20	2.81
					100.00						3.22

TABLE 9 - Values of $Z_s / \sqrt{A} \sin\theta$ and $d_s V t / \sqrt{A} \sin\theta\, b$ for given discharge, tailwater depth and B = 10 ft.

Q cfs	b ft	Z_s ft	$\sqrt{A}$ ft	$\sin\theta$	$\frac{Z_s}{\sqrt{A}\sin\theta}$	d_s ft	V fps	t sec	$\frac{d_s V t}{\sqrt{A}\sin\theta\, b}$
0.5	0.5	0.67	0.178	0.959	3.92	0.0085	15.8	900	1420
		0.87			5.08			1800	2840
		1.13			6.60			3600	5680
		1.18			6.90			7200	11360
		1.20			7.00			21600	34200
1.0	0.5	0.64	0.251	0.947	2.68	0.0085	15.9	900	1022
		0.68			2.86			1800	2044
		0.74			3.10			3600	4088
		0.77			3.23			7200	8176
		1.00			4.20			14400	16352
		1.12			4.70			28800	32704
1.5	0.5	1.04	0.306	0.943	3.61	0.0085	16.0	900	850
		1.17			4.06			1800	1700
		1.30			4.52			3600	3400
		1.49			5.17			7200	6800
		1.56			5.42			14400	13600
2.0	0.5	1.34	0.353	0.935	4.07	0.0085	16.0	900	742
		1.46			4.43			1800	1484
		1.60			4.85			3600	2968
		1.60			4.85			7200	5936
0.5	1.0	0.72	0.190	0.947	4.00	0.0085	13.9	900	591
		0.79			4.39			1800	1182
		0.90			5.00			3600	2364
		1.10			6.11			7200	4728
		1.16			6.45			14400	9456
		1.18			6.55			28800	18912
		1.21			6.72			57600	37824
1.0	1.0	0.89	0.262	0.937	3.62	0.0085	14.6	900	465
		0.96			3.90			1800	930
		1.06			4.30			3600	1860
		1.22			4.95			7200	3720
		1.37			5.56			14400	7440
		1.52			6.17			28800	14880

TABLE 9 - Continued

Q cfs	b ft	Z_s ft	$\sqrt{A}$ ft	sin θ	$\frac{Z_s}{\sqrt{A}\ \sin\theta}$	d_s ft	V fps	t sec	$\frac{d_s\ V\ t}{\sqrt{A}\ \sin\theta\ b}$
1.5	1.0	1.46	0.318	0.933	4.93	0.0085	14.8	1800	765
		1.60			5.40			3600	1530
		1.72			5.80			7200	3060
		1.75			5.91			14400	6120
2.0	1.0	1.52	0.365	0.927	4.50	0.0085	15.1	900	342
		1.61			4.75			1800	684
		1.68			4.96			3600	1368
		1.77			5.24			7200	2736
0.5	1.5	0.52	0.194	0.943	2.84	0.0085	13.3	3600	1480
		0.59			3.22			28800	11840
		0.65			3.56			57600	23680
		0.68			3.72			230400	94720
		0.69			3.78			460800	189440
		0.70			3.83			802800	331000
1.0	1.5	1.05	0.270	0.928	4.20	0.0085	13.7	1800	560
		1.14			4.55			3600	1120
		1.21			4.83			7200	2240
		1.28			5.11			14400	4480
		1.36			5.43			28800	8960
		1.41			5.64			57600	17920
1.5	1.5	1.20	0.326	0.920	4.00	0.0085	14.1	1800	480
		1.33			4.44			3600	960
		1.46			4.87			7200	1920
		1.52			5.07			14400	3840
		1.53			5.10			28800	7680
		1.54			5.13			57600	15360
		1.55			5.16			115200	30720
2.0	1.5	1.33	0.374	0.916	3.88	0.0085	14.3	900	213
		1.42			4.13			1800	426
		1.52			4.43			3600	852
		1.53			4.46			7200	1704
		1.55			4.52			14400	3408
		1.56			4.54			28800	6816

TABLE 10 - Values of h^*/H and $\rho QV/\rho_s\ W_m^2\ b\ \sigma_d$ for given Hydraulic Conditions and Different Widths of Rectangular Channel

B ft	Q cfs	b ft	H ft	h_t^* [1/] ft	$\frac{h^*}{H}$	V fps	Q/b ft^2/sec	$\rho/\rho_s\ W_m^2\sigma_d$ $ft^{-3}\ sec^2$	$\frac{\rho Q V}{\rho_s W_m^2 \sigma_d\ b}$
5	1.0	0.5	4.151	2.20	0.530	16.2	2.0	249	8060
	1.5		4.250	2.33	0.548	16.4	3.0		12250
	2.0		4.333	2.85	0.657	16.7	4.0		16700
5	1.0	1.0	4.151	1.95	0.470	15.1	1.0	249	3760
	2.0		4.333	2.48	0.573	15.7	2.0		7820
10	0.5	1.0	3.683	1.92	0.521	13.9	0.5	249	1730
	1.0		3.898	2.43	0.623	14.6	1.0		3640
	1.5		3.966	2.64	0.666	14.8	1.5		5540
	2.0		4.049	2.73	0.674	15.1	2.0		7525
10	1.0	1.5	4.008	2.06	0.514	13.7	0.7	249	2280
	1.5		4.159	2.25	0.541	14.1	1.0		3510
	2.0		4.159	2.58	0.620	14.3	1.3		4740
20	1.0	1.0	4.182	3.22	0.770	15.2	1.0	249	3880
	1.9		4.333	3.91	0.904	15.7	1.9		7350
20	1.0	1.5	4.182	2.84	0.680	14.1	0.7	249	2340
	1.5		4.250	3.36	0.790	14.3	1.0		3560
20	2.18	2.0	4.333	3.50	0.808	13.8	1.1	249	3740
	3.00		4.333	4.00	0.925	14.9	1.5		5570

1/ Values of h_t^* for t = 100 hrs.